

Impact Factor:	ISRA (India) = 6.317	SIS (USA) = 0.912	ICV (Poland) = 6.630
	ISI (Dubai, UAE) = 1.582	РИНЦ (Russia) = 3.939	PIF (India) = 1.940
	GIF (Australia) = 0.564	ESJI (KZ) = 9.035	IBI (India) = 4.260
	JIF = 1.500	SJIF (Morocco) = 7.184	OAJI (USA) = 0.350

SOI: 1.1/TAS DOI: 10.15863/TAS

International Scientific Journal
Theoretical & Applied Science

p-ISSN: 2308-4944 (print) e-ISSN: 2409-0085 (online)

Year: 2021 Issue: 11 Volume: 103

Published: 30.11.2021 <http://T-Science.org>

QR – Issue



QR – Article



Denis Chemezov

Vladimir Industrial College

M.Sc.Eng., Corresponding Member of International Academy of Theoretical and Applied Sciences, Lecturer,
Russian Federation

<https://orcid.org/0000-0002-2747-552X>

vic-science@yandex.ru

Semyon Galaktionov

Vladimir Industrial College
Student, Russian Federation

Viktoriya Koroleva

Vladimir Industrial College
Student, Russian Federation

Alyona Kozlova

Vladimir Industrial College
Student, Russian Federation

Sergey Lukashov

Vladimir State University named after Alexander & Nikolay Stoletovs
Institute of Mechanical Engineering & Automobile Transport
Student, Russian Federation

Yuriy Mironov

Vladimir Industrial College
Student, Russian Federation

Nikolay Kornev

Vladimir Industrial College
Student, Russian Federation

REFERENCE DATA OF PRESSURE DISTRIBUTION ON THE SURFACES OF AIRFOILS HAVING THE NAMES BEGINNING WITH THE LETTER B

Abstract: The results of the computer calculation of air flow around the airfoils having the names beginning with the letter B are presented in the article. The contours of pressure distribution on the surfaces of the airfoils at the angles of attack of 0, 15 and -15 degrees in conditions of the subsonic airplane flight speed were obtained.

Key words: the airfoil, the angle of attack, pressure, the surface.

Language: English

Citation: Chemezov, D., et al. (2021). Reference data of pressure distribution on the surfaces of airfoils having the names beginning with the letter B. *ISJ Theoretical & Applied Science*, 11 (103), 1001-1076.

Soi: <http://s-o-i.org/1.1/TAS-11-103-120>

Doi:  <https://dx.doi.org/10.15863/TAS.2021.11.103.120>

Scopus ASCC: 1507.

Impact Factor:

ISRA (India) = **6.317**
ISI (Dubai, UAE) = **1.582**
GIF (Australia) = **0.564**
JIF = **1.500**

SIS (USA) = **0.912**
РИНЦ (Russia) = **3.939**
ESJI (KZ) = **9.035**
SJIF (Morocco) = **7.184**

ICV (Poland) = **6.630**
PIF (India) = **1.940**
IBI (India) = **4.260**
OAJI (USA) = **0.350**

Introduction

Creating reference materials that determine the most accurate pressure distribution on the airfoils surfaces is an actual task of the airplane aerodynamics.

Materials and methods

The study of air flow around the airfoils was carried out in a two-dimensional formulation by means of the computer calculation in the *Comsol Multiphysics* program. The airfoils in the cross section were taken as objects of research [1-12]. In this work,

the airfoils having the names beginning with the letter *B* were adopted. Air flow around the airfoils was carried out at the angles of attack (α) of 0, 15 and -15 degrees. The flight speed of the airplane in each case was subsonic. The airplane flight in the atmosphere was carried out under normal weather conditions. The geometric characteristics of the studied airfoils are presented in the Table 1. The studied geometric shapes of the airfoils in the cross section are presented in the Table 2.

Table 1. The geometric characteristics of the airfoils.

Airfoil name	Max. thickness	Max. camber	Leading edge radius	Trailing edge thickness
<i>B-29 ROOT</i>	21.98% at 30.2% of the chord	1.73% at 30.2% of the chord	3.1357%	0.0%
<i>B-29 TIP</i>	9.00% at 30.0% of the chord	2.23% at 30.0% of the chord	0.5306%	0.0%
<i>B-8306-B</i>	8.09% at 20.0% of the chord	6.67% at 30.0% of the chord	0.9045%	0.35%
<i>BA 18</i>	9.5% at 30.0% of the chord	10.85% at 30.0% of the chord	1.5426%	0.0%
<i>BA 19</i>	9.9% at 30.0% of the chord	8.72% at 10.0% of the chord	1.586%	0.0%
<i>BABIC</i>	6.5% at 20.0% of the chord	6.2% at 40.0% of the chord	0.7642%	0.5%
<i>BAMBINO7</i>	6.0% at 30.0% of the chord	3.0% at 30.0% of the chord	1.5544%	0.0%
<i>BE10255B</i>	9.2% at 30.0% of the chord	6.15% at 40.0% of the chord	1.3133%	0.2%
<i>BE10305B</i>	10.01% at 25.0% of the chord	6.44% at 30.0% of the chord	0.6577%	0.25%
<i>BE10307B</i>	9.95% at 25.0% of the chord	7.49% at 30.0% of the chord	0.6546%	0.0%
<i>BE10357B</i>	9.99% at 20.0% of the chord	7.44% at 40.0% of the chord	1.6997%	0.27%
<i>BE12305B</i>	11.98% at 25.0% of the chord	6.31% at 25.0% of the chord	1.4179%	0.23%
<i>BE12307B</i>	11.97% at 25.0% of the chord	7.92% at 30.0% of the chord	1.4749%	0.25%
<i>BE12355D</i>	11.95% at 25.0% of the chord	6.61% at 30.0% of the chord	0.7379%	0.25%
<i>BE12357B</i>	11.97% at 25% of the chord	7.72% at 40.0% of the chord	1.4928%	0.33%
<i>BE3259B</i>	3.04% at 5.0% of the chord	9.12% at 30.0% of the chord	1.9315%	0.0%
<i>BE3307B</i>	2.95% at 20.0% of the chord	7.18% at 30.0% of the chord	1.4507%	0.12%
<i>BE3309B</i>	2.99% at 20.0% of the chord	9.16% at 30.0% of the chord	0.694%	0.1%
<i>BE3357B</i>	2.95% at 15.0% of the chord	7.19% at 50.0% of the chord	0.5073%	0.15%
<i>BE3359B</i>	2.98% at 25.0% of the chord	9.09% at 30.0% of the chord	0.6117%	0.1%
<i>BE50 (original)</i>	7.27% at 25.0% of the chord	4.81% at 45.0% of the chord	0.6484%	0.26%
<i>BE50 (smoothed)</i>	7.32% at 23.8% of the chord	3.96% at 45.4% of the chord	0.5776%	0.259%
<i>BE5456</i>	5.05% at 30.0% of the chord	5.0% at 40.0% of the chord	0.5963%	0.6%
<i>BE6306B</i>	6.0% at 20.0% of the chord	6.25% at 30.0% of the chord	0.6746%	0.3%
<i>BE6308B</i>	6.12% at 20.0% of the chord	8.3% at 30.0% of the chord	0.7181%	0.28%
<i>BE6356</i>	6.1% at 20.0% of the chord	6.27% at 40.0% of the chord	1.292%	0.22%
<i>BE6356B</i>	6.1% at 20.0% of the chord	6.27% at 40.0% of the chord	0.6768%	0.22%
<i>BE6358B</i>	6.1% at 20.0% of the chord	8.18% at 40.0% of the chord	0.6867%	0.25%
<i>BE6407E</i>	6.05% at 15.0% of the chord	6.93% at 40.0% of the chord	0.765%	0.0%
<i>BE6453B</i>	6.45% at 25.0% of the chord	4.25% at 40.0% of the chord	0.7532%	0.45%
<i>BE6455B</i>	6.35% at 25.0% of the chord	5.08% at 40.0% of the chord	0.6177%	0.5%
<i>BE6456F</i>	6.5% at 20.0% of the chord	6.45% at 40.0% of the chord	0.8198%	0.5%
<i>BE6458</i>	6.05% at 40.0% of the chord	7.98% at 40.0% of the chord	0.7174%	0.7%
<i>BE6556</i>	6.1% at 60.0% of the chord	6.05% at 50.0% of the chord	0.665%	0.6%
<i>BE6556B</i>	6.15% at 30.0% of the chord	6.42% at 50.0% of the chord	0.7091%	0.45%
<i>BE6556C</i>	6.25% at 30.0% of the chord	6.55% at 50.0% of the chord	0.6914%	0.4%
<i>BE6557B</i>	6.05% at 30.0% of the chord	7.5% at 50.0% of the chord	0.7345%	0.5%
<i>BE6606</i>	6.01% at 50.0% of the chord	6.0% at 60.0% of the chord	0.6865%	0.6%
<i>BE7404B</i>	7.35% at 20.0% of the chord	4.6% at 30.0% of the chord	0.8691%	0.45%
<i>BE7455E</i>	6.9% at 20.0% of the chord	5.9% at 40.0% of the chord	0.8467%	0.0%
<i>BE7457D</i>	7.15% at 20.0% of the chord	7.08% at 50.0% of the chord	0.7879%	0.5%
<i>BE7457D2</i>	7.15% at 20.0% of the chord	7.08% at 50.0% of the chord	0.7879%	0.5%
<i>BE7505D</i>	7.6% at 20.0% of the chord	6.58% at 40.0% of the chord	0.452%	0.2%
<i>BE7505E</i>	7.2% at 20.0% of the chord	6.15% at 50.0% of the chord	0.8139%	0.0%
<i>BE8258</i>	8.09% at 20.0% of the chord	8.54% at 30.0% of the chord	1.2213%	0.25%
<i>BE8306</i>	8.09% at 20.0% of the chord	6.67% at 40.0% of the chord	0.9045%	0.35%
<i>BE8306B</i>	8.09% at 20.0% of the chord	6.67% at 30.0% of the chord	0.9045%	0.35%
<i>BE8308B</i>	8.17% at 20.0% of the chord	8.4% at 30.0% of the chord	1.6955%	0.3%
<i>BE8353B</i>	7.7% at 25.0% of the chord	4.42% at 30.0% of the chord	0.2877%	0.4%
<i>BE8353B2</i>	7.7% at 25.0% of the chord	4.35% at 25.0% of the chord	0.7862%	0.4%
<i>BE8356</i>	8.1% at 20.0% of the chord	6.54% at 30.0% of the chord	1.5145%	0.33%

Impact Factor:

ISRA (India)	= 6.317	SIS (USA)	= 0.912	ICV (Poland)	= 6.630
ISI (Dubai, UAE)	= 1.582	РИНЦ (Russia)	= 3.939	PIF (India)	= 1.940
GIF (Australia)	= 0.564	ESJI (KZ)	= 9.035	IBI (India)	= 4.260
JIF	= 1.500	SJIF (Morocco)	= 7.184	OAJI (USA)	= 0.350

<i>BE8356B</i>	8.1% at 20.0% of the chord	6.54% at 30.0% of the chord	0.893%	0.33%
<i>BE8356B2</i>	8.02% at 20.0% of the chord	6.8% at 30.0% of the chord	1.238%	0.33%
<i>BE8356B3</i>	7.45% at 20.0% of the chord	6.4% at 40.0% of the chord	0.8385%	0.5%
<i>BE8358B</i>	8.2% at 20.0% of the chord	8.4% at 30.0% of the chord	1.5721%	0.3%
<i>BE8403B</i>	7.95% at 25.0% of the chord	4.58% at 30.0% of the chord	0.8174%	0.35%
<i>BE8405B</i>	7.95% at 25.0% of the chord	6.13% at 40.0% of the chord	0.904%	0.7%
<i>BE8406C</i>	8.0% at 20.0% of the chord	6.72% at 40.0% of the chord	0.8799%	0.4%
<i>BE8452B</i>	7.95% at 25.0% of the chord	4.05% at 30.0% of the chord	0.31%	0.4%
<i>BE8456D</i>	8.0% at 20.0% of the chord	6.68% at 40.0% of the chord	1.0068%	0.3%
<i>BE8457E</i>	8.0% at 20.0% of the chord	7.45% at 40.0% of the chord	1.0527%	0.0%
<i>BE8505E</i>	8.0% at 20.0% of the chord	6.17% at 40.0% of the chord	0.9738%	0.0%
<i>BE8556B</i>	7.7% at 30.0% of the chord	6.97% at 50.0% of the chord	1.505%	0.6%
<i>BE9304B</i>	8.9% at 25.0% of the chord	5.05% at 25.0% of the chord	0.5013%	0.25%
<i>BE9403B</i>	8.95% at 20.0% of the chord	4.63% at 30.0% of the chord	0.6775%	0.45%
<i>BE9404B</i>	9.25% at 25.0% of the chord	5.45% at 30.0% of the chord	0.6768%	0.0%
<i>BELL 540</i>	9.71% at 22.1% of the chord	0.0% at 0.0% of the chord	1.4922%	0.41%
<i>Bell AH-1</i>	9.71% at 22.1% of the chord	0.0% at 0.0% of the chord	1.4922%	0.41%
<i>BELL-WORTMANN FX 69-H-083</i>	8.4% at 33.3% of the chord	2.44% at 33.3% of the chord	0.2895%	0.19%
<i>BELL-WORTMANN FX 69-H-098</i>	9.89% at 28.2% of the chord	1.74% at 22.4% of the chord	0.599%	0.22%
<i>Benedek 10355 B</i>	9.9% at 30.0% of the chord	6.43% at 30.0% of the chord	1.2071%	0.24%
<i>Benedek 1053 B</i>	10.01% at 25.0% of the chord	6.44% at 30.0% of the chord	0.9557%	0.25%
<i>Benedek 12355 B</i>	11.95% at 25.0% of the chord	6.61% at 30.0% of the chord	1.233%	0.25%
<i>Benedek 7406 F</i>	7.25% at 20.0% of the chord	6.35% at 40.0% of the chord	0.9017%	0.95%
<i>Benedek 8353 B-2</i>	7.7% at 25.0% of the chord	4.42% at 30.0% of the chord	0.7862%	0.4%
<i>Benedek 8405 A</i>	8.03% at 25% of the chord	6.89% at 40.0% of the chord	1.2155%	0.28%
<i>Benedek 8406 B</i>	8.06% at 25.0% of the chord	7.13% at 40.0% of the chord	1.3431%	0.33%
<i>Benedek 8406 C</i>	8.0% at 20.0% of the chord	6.72% at 40.0% of the chord	1.0754%	0.4%
<i>Benedek 9304 B</i>	8.9% at 35.0% of the chord	5.05% at 25.0% of the chord	0.9249%	0.25%
<i>Benedek 9403 B</i>	8.95% at 20.0% of the chord	4.63% at 30.0% of the chord	1.0802%	0.45%
<i>Benedek 9404 B</i>	9.25% at 25.0% of the chord	5.45% at 30.0% of the chord	1.0257%	0.0%
<i>Bergey BW-3 (smoothed)</i>	5.02% at 7.4% of the chord	5.79% at 41.6% of the chord	1.1768%	0.6617%
<i>Blanchard WB135/35</i>	13.55% at 25.0% of the chord	3.75% at 50.0% of the chord	1.0142%	0.0%
<i>Blanchard WB140/35/FB</i>	13.93% at 30.0% of the chord	3.7% at 45.0% of the chord	1.096%	0.5%
<i>BO 545-310</i>	10.0% at 30.0% of the chord	4.95% at 40.0% of the chord	1.0094%	0.0%
<i>BO 560-38</i>	8.0% at 30.0% of the chord	5.0% at 60.0% of the chord	0.7486%	0.0%
<i>BOBWHITE</i>	6.3% at 22.2% of the chord	4.95% at 50.0% of the chord	0.713%	1.6%
<i>BOEING</i>	10.07% at 40.0% of the chord	1.73% at 78.0% of the chord	1.4372%	0.136%
<i>BOEING 103</i>	12.72% at 30.0% of the chord	3.6% at 40.0% of the chord	1.5187%	0.12%
<i>BOEING 106</i>	13.06% at 30.0% of the chord	3.34% at 40.0% of the chord	1.3888%	0.04%
<i>BOEING 707,.08 SPAN</i>	11.43% at 24.0% of the chord	0.23% at 6.0% of the chord	2.6475%	0.0%
<i>BOEING 707,.19 SPAN</i>	12.16% at 30.1% of the chord	0.73% at 10.1% of the chord	0.9337%	0.0%
<i>BOEING 707,.40 SPAN</i>	9.58% at 30.0% of the chord	1.9% at 15.0% of the chord	0.9012%	0.0%
<i>BOEING 707,.54 SPAN</i>	8.97% at 40.0% of the chord	2.0% at 30.0% of the chord	0.3861%	0.0%
<i>BOEING 707,.99 SPAN</i>	9.01% at 42.0% of the chord	1.78% at 34.0% of the chord	0.4675%	0.0%
<i>BOEING 707 .08 SPAN AIRFOIL</i>	11.43% at 24.0% of the chord	0.22% at 6.0% of the chord	2.6461%	0.0%
<i>BOEING 707 .19 SPAN AIRFOIL</i>	12.16% at 30.1% of the chord	0.73% at 10.1% of the chord	0.9341%	0.0%
<i>BOEING 707 .54 SPAN AIRFOIL</i>	8.97% at 40.0% of the chord	2.0% at 30.0% of the chord	0.3861%	0.0%
<i>BOEING 707 .99 SPAN AIRFOIL</i>	9.01% at 42.0% of the chord	1.78% at 34.0% of the chord	0.4676%	0.0%
<i>BOEING 737 MIDSPAN</i>	10.0% at 40.0% of the chord	1.45% at 20.4% of the chord	0.3443%	0.1%
<i>BOEING 737 MIDSPAN AIRFOIL</i>	12.54% at 25.0% of the chord	1.54% at 7.2% of the chord	1.7443%	0.08%
<i>BOEING 737 MIDSPAN AIRFOIL-b</i>	10.0% at 40.0% of the chord	1.45% at 20.4% of the chord	0.3443%	0.1%
<i>BOEING 737 OUTBOARD</i>	10.8% at 40.0% of the chord	1.58% at 20.0% of the chord	0.5016%	0.16%
<i>BOEING 737 OUTBOARD AIRFOIL</i>	10.8% at 40.0% of the chord	1.58% at 20.0% of the chord	0.5016%	0.16%
<i>BOEING 737 ROOT</i>	15.37% at 19.5% of the chord	1.91% at 4.9% of the chord	3.8212%	0.06%
<i>BOEING 737 ROOT AIRFOIL</i>	15.37% at 19.5% of the chord	1.91% at 4.9% of the chord	3.8212%	0.06%
<i>Boeing B-29 root airfoil</i>	21.98% at 30.2% of the chord	1.73% at 30.2% of the chord	3.1372%	0.0%
<i>Boeing B-29 tip airfoil</i>	9.0% at 30.0% of the chord	2.23% at 30.0% of the chord	0.5303%	0.0%
<i>BOEING BACXXX</i>	11.31% at 35.0% of the chord	1.4% at 15.0% of the chord	0.5653%	0.08%
<i>Boeing Commercial Airplane Company airfoil J</i>	10.07% at 40.0% of the chord	1.73% at 78.0% of the chord	1.4417%	0.136%

Impact Factor:

ISRA (India)	= 6.317	SIS (USA)	= 0.912	ICV (Poland)	= 6.630
ISI (Dubai, UAE)	= 1.582	РИНЦ (Russia)	= 3.939	PIF (India)	= 1.940
GIF (Australia)	= 0.564	ESJI (KZ)	= 9.035	IBI (India)	= 4.260
JIF	= 1.500	SJIF (Morocco)	= 7.184	OAJI (USA)	= 0.350

<i>Boeing Commercial Airplane Company BACXXX</i>	11.31% at 35.0% of the chord	1.4% at 15.0% of the chord	0.5653%	0.08%
<i>BOEING VERTOL V(1,95)3009-1,25</i>	9.0% at 29.9% of the chord	1.3% at 19.9% of the chord	0.9852%	0.11%
<i>BOEING VERTOL V13006-7</i>	5.98% at 30.1% of the chord	0.91% at 20.1% of the chord	0.4754%	0.12%
<i>BOEING VERTOL V43012-1,58</i>	12.04% at 32.0% of the chord	3.67% at 15.0% of the chord	1.8955%	0.0%
<i>BOEING VERTOL V43015-2,48</i>	15.03% at 30.0% of the chord	3.68% at 15.0% of the chord	2.4422%	0.0%
<i>BOEING10</i>	12.72% at 30.0% of the chord	5.28% at 30.0% of the chord	1.3978%	0.12%
<i>BOEING16</i>	13.06% at 30.0% of the chord	5.35% at 30.0% of the chord	1.379%	0.03%
<i>BOEING-VERTOL V23010-1,58</i>	10.18% at 30.0% of the chord	1.75% at 15.0% of the chord	1.3868%	0.0%
<i>BOEING-VERTOL VR-1</i>	10.97% at 35.3% of the chord	1.53% at 43.3% of the chord	1.3672%	0.0%
<i>BOEING-VERTOL VR-11X</i>	10.97% at 40.0% of the chord	2.42% at 25.0% of the chord	1.1288%	0.3%
<i>BOEING-VERTOL VR-12</i>	10.57% at 35.0% of the chord	2.28% at 20.0% of the chord	0.8713%	0.3%
<i>BOEING-VERTOL VR-13</i>	9.45% at 35.0% of the chord	2.04% at 20.0% of the chord	0.6814%	0.2684%
<i>BOEING-VERTOL VR-14</i>	7.96% at 35.0% of the chord	1.72% at 20.0% of the chord	0.4598%	0.2226%
<i>BOEING-VERTOL VR-15</i>	7.96% at 35.0% of the chord	1.29% at 20.0% of the chord	0.5486%	0.2389%
<i>BOEING-VERTOL VR-5</i>	12.0% at 35.0% of the chord	3.4% at 35.0% of the chord	0.796%	0.08%
<i>BOEING-VERTOL VR-7</i>	12.03% at 33.0% of the chord	3.12% at 33.0% of the chord	1.1055%	0.5%
<i>BOEING-VERTOL VR-8</i>	8.07% at 34.7% of the chord	1.26% at 34.7% of the chord	0.5681%	0.5%
<i>BOEING-VERTOL VR-9</i>	6.06% at 35.0% of the chord	0.33% at 35.0% of the chord	0.4711%	0.0%
<i>Borge' B3</i>	11.7% at 30.0% of the chord	5.85% at 30.0% of the chord	1.2661%	0.0%
<i>BP4D</i>	10.16% at 29.0% of the chord	1.68% at 36.8% of the chord	1.1709%	0.078%
<i>Broggini 55509</i>	9.2% at 20.0% of the chord	5.0% at 25.0% of the chord	1.2236%	0.0%
<i>Brogly</i>	9.1% at 30.0% of the chord	5.8% at 40.0% of the chord	1.2498%	0.0%
<i>BRUXEL33</i>	12.99% at 30.0% of the chord	6.5% at 30.0% of the chord	2.217%	0.0%
<i>BRUXEL36</i>	16.23% at 30.0% of the chord	8.12% at 30.0% of the chord	3.0597%	0.0%
<i>BTP8</i>	7.95% at 19.9% of the chord	0.0% at 0.0% of the chord	0.7248%	0.0%

Note:

Bell AH-1 (operational loads survey, rotor blade airfoil, modified NACA 0012);

Blanchard WB135/35 (R/C sailplane airfoil 13.5% smooth), *Blanchard WB140/35/FB* (R/C sailplane airfoil 14%);

BO 545-310 (W. Bogart (USA));

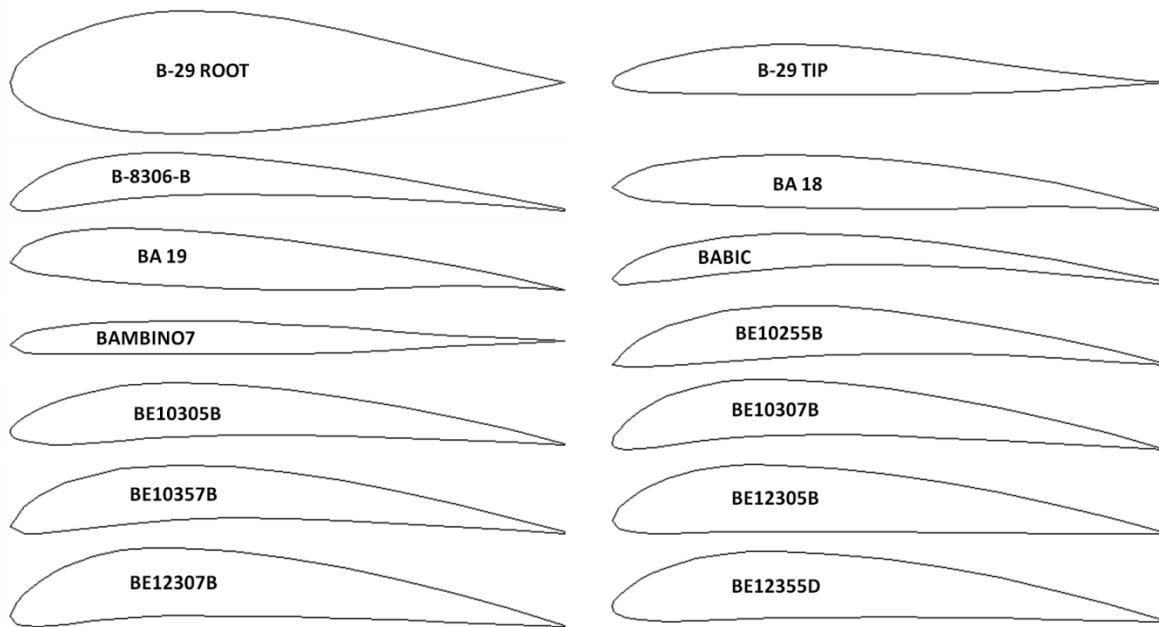
BOEING 707 .08 SPAN AIRFOIL, *BOEING 737 ROOT AIRFOIL* (Boeing Commercial Airplane), *Boeing Commercial Airplane Company BACXXX* (BACXXX Energy Efficient Transport Program Airfoil);

Borge' B3 (C. Borge' (France));

Broggini 55509 (C. Broggini (Italy));

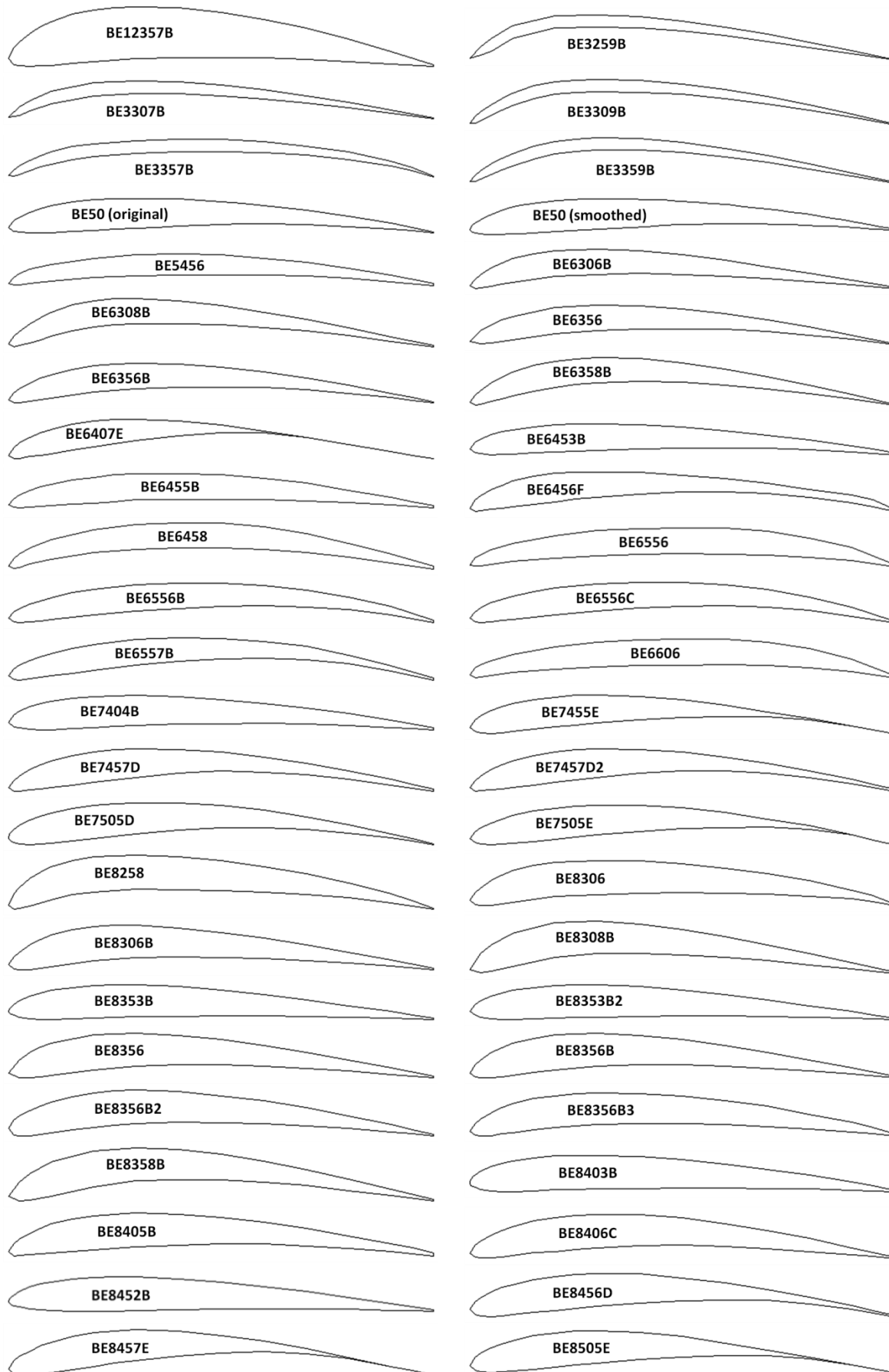
Brogly (R. Brogly (France)).

Table 2. The geometric shapes of the airfoils in the cross section.



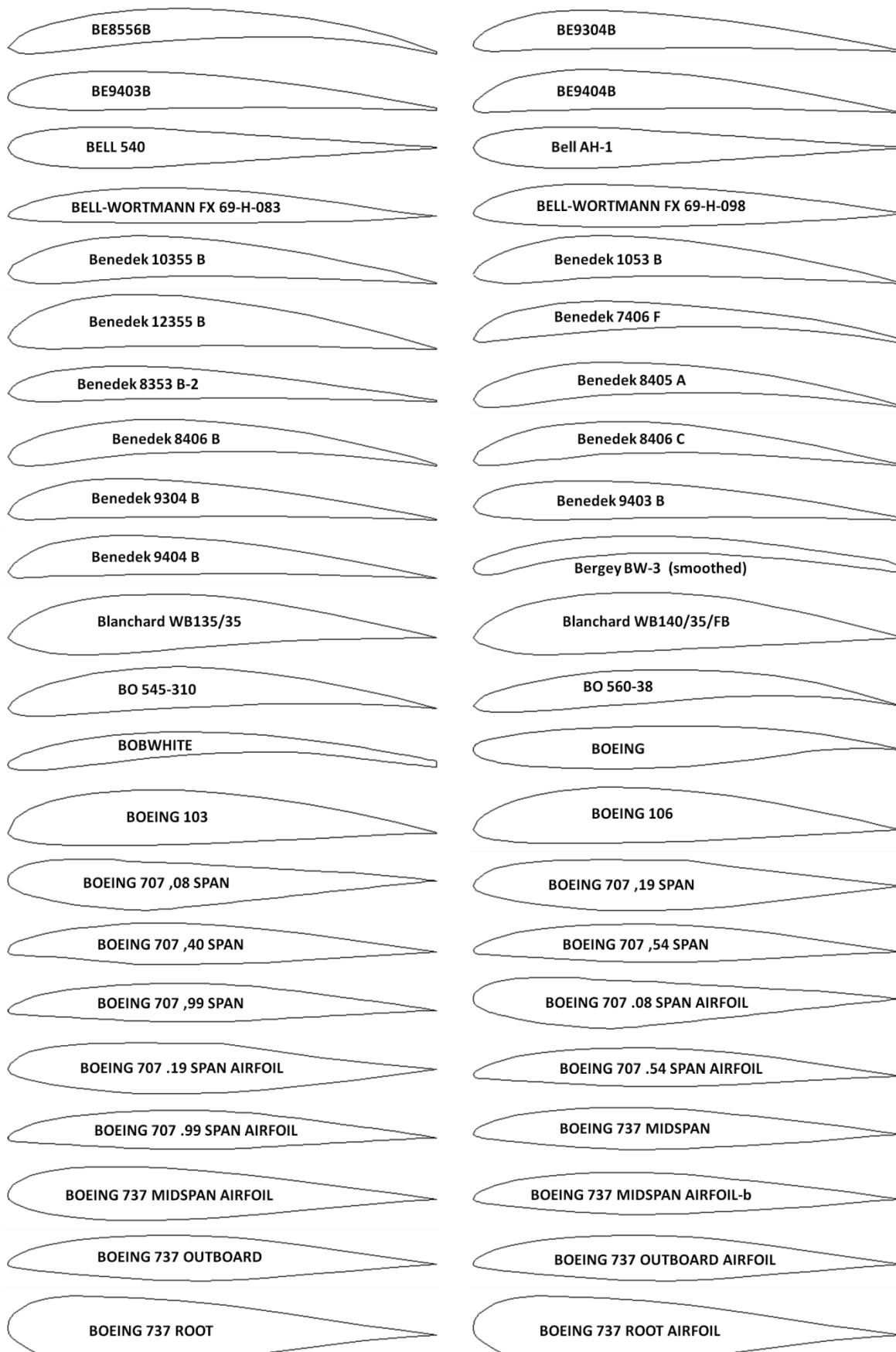
Impact Factor:

ISRA (India)	= 6.317	SIS (USA)	= 0.912	ICV (Poland)	= 6.630
ISI (Dubai, UAE)	= 1.582	РИНЦ (Russia)	= 3.939	PIF (India)	= 1.940
GIF (Australia)	= 0.564	ESJI (KZ)	= 9.035	IBI (India)	= 4.260
JIF	= 1.500	SJIF (Morocco)	= 7.184	OAJI (USA)	= 0.350



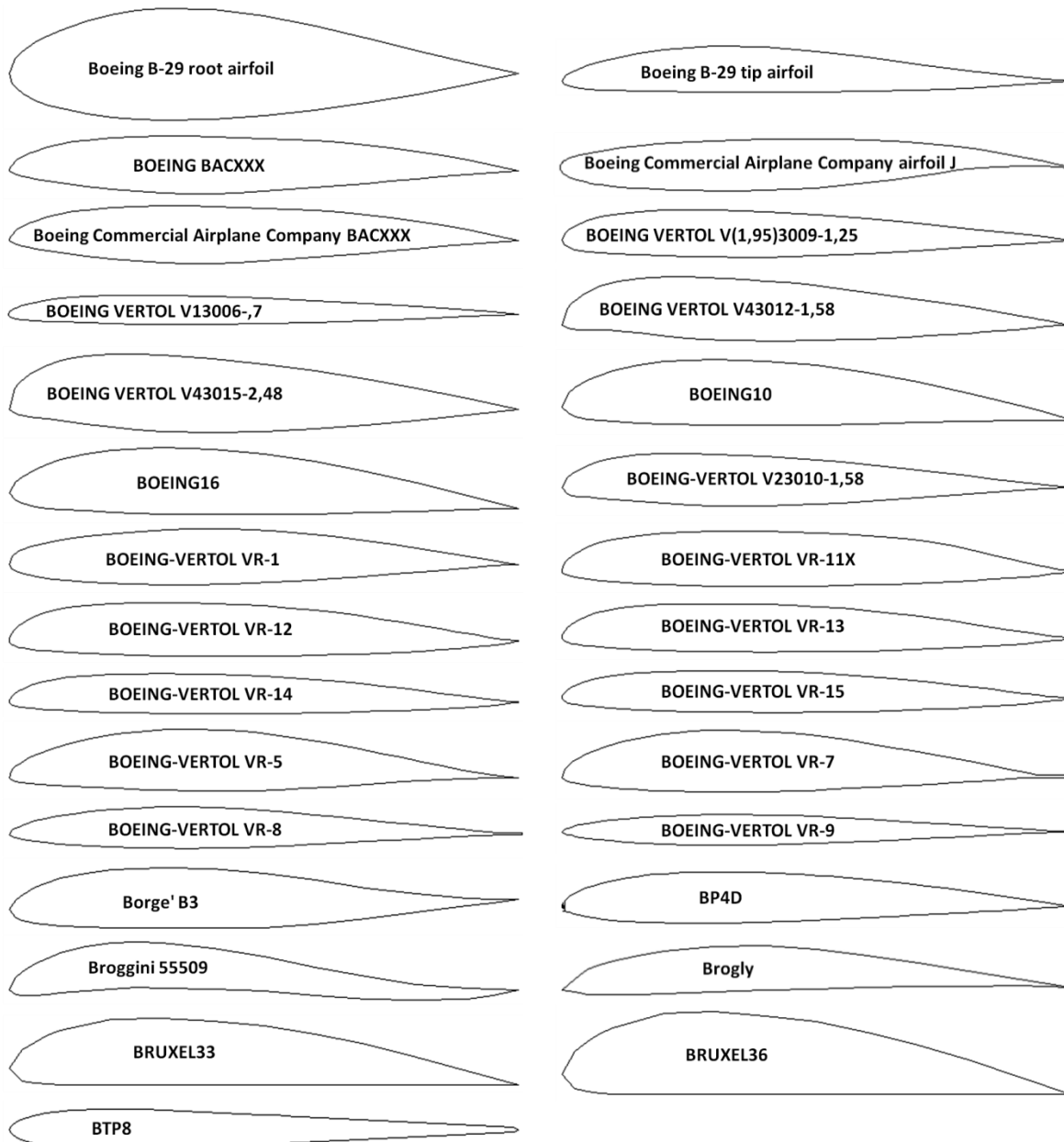
Impact Factor:

ISRA (India) = 6.317	SIS (USA) = 0.912	ICV (Poland) = 6.630
ISI (Dubai, UAE) = 1.582	РИНЦ (Russia) = 3.939	PIF (India) = 1.940
GIF (Australia) = 0.564	ESJI (KZ) = 9.035	IBI (India) = 4.260
JIF = 1.500	SJIF (Morocco) = 7.184	OAJI (USA) = 0.350



Impact Factor:

ISRA (India)	= 6.317	SIS (USA)	= 0.912	ICV (Poland)	= 6.630
ISI (Dubai, UAE)	= 1.582	РИНЦ (Russia)	= 3.939	PIF (India)	= 1.940
GIF (Australia)	= 0.564	ESJI (KZ)	= 9.035	IBI (India)	= 4.260
JIF	= 1.500	SJIF (Morocco)	= 7.184	OAJI (USA)	= 0.350



Results and discussion

The calculated pressure contours on the surfaces of the airfoils at the different angles of attack are presented in the Figs. 1-135. The calculated

magnitudes on the scale can be represented as the basic magnitudes when comparing the pressure drop under conditions of changing the angle of attack of the airfoils.

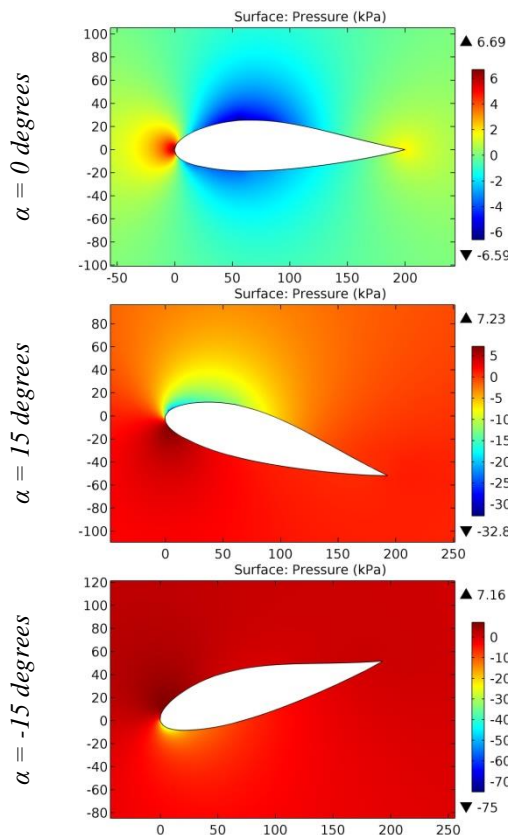


Figure 1. The pressure contours on the surfaces of the B-29 ROOT airfoil.

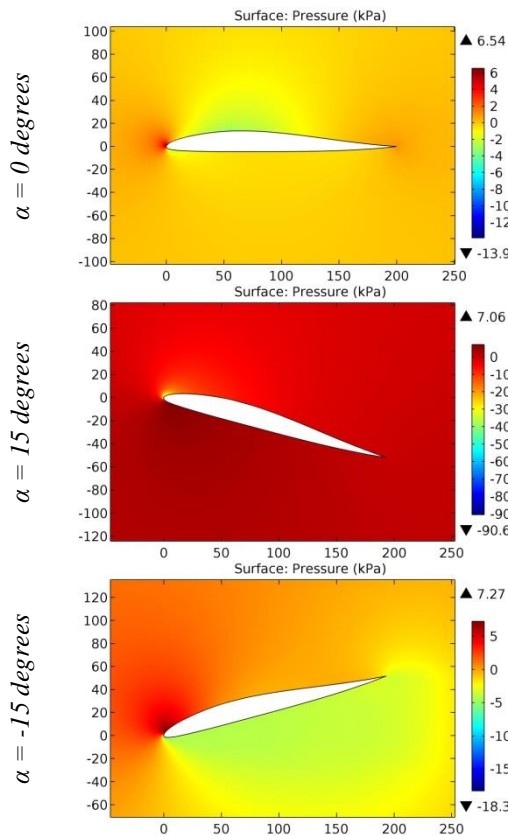


Figure 2. The pressure contours on the surfaces of the B-29 TIP airfoil.

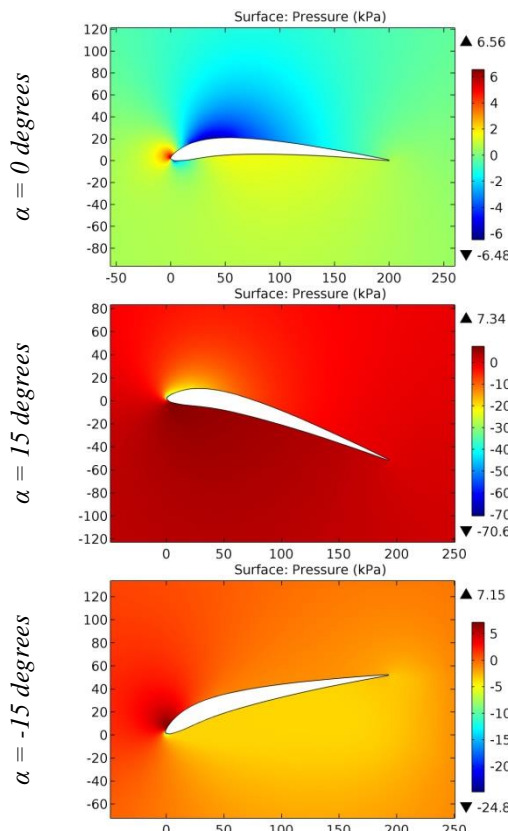


Figure 3. The pressure contours on the surfaces of the B-8306-B airfoil.

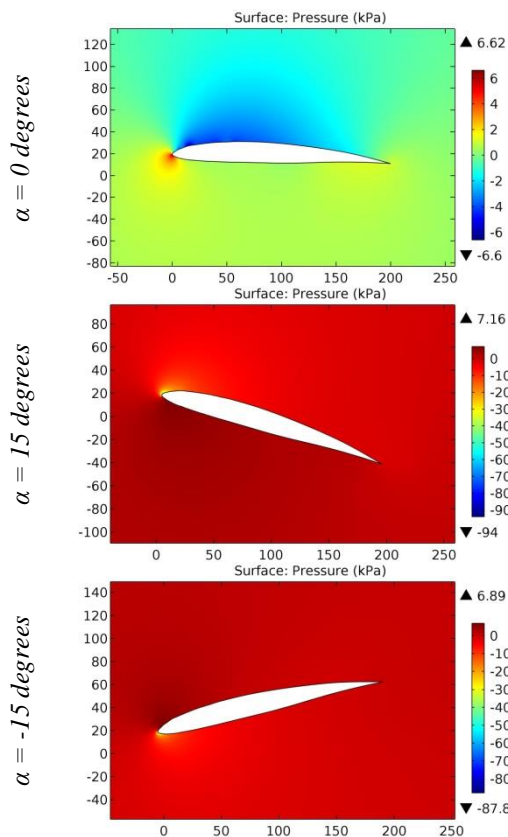


Figure 4. The pressure contours on the surfaces of the BA 18 airfoil.

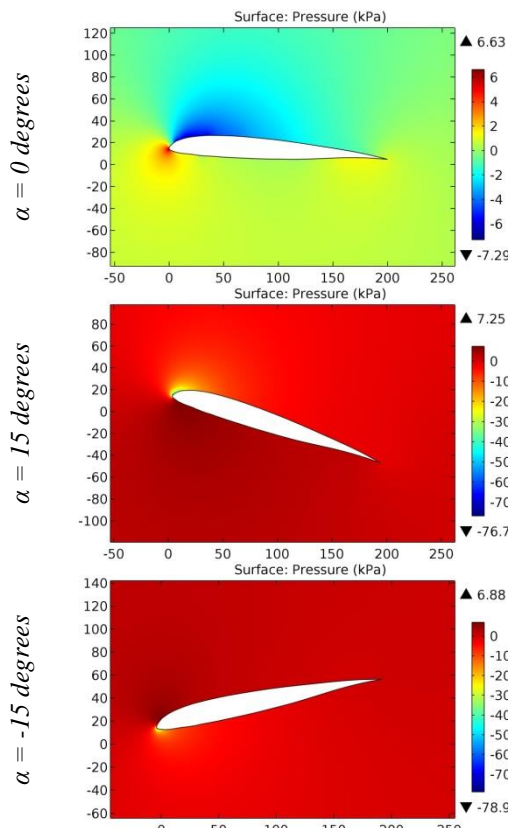


Figure 5. The pressure contours on the surfaces of the BA 19 airfoil.

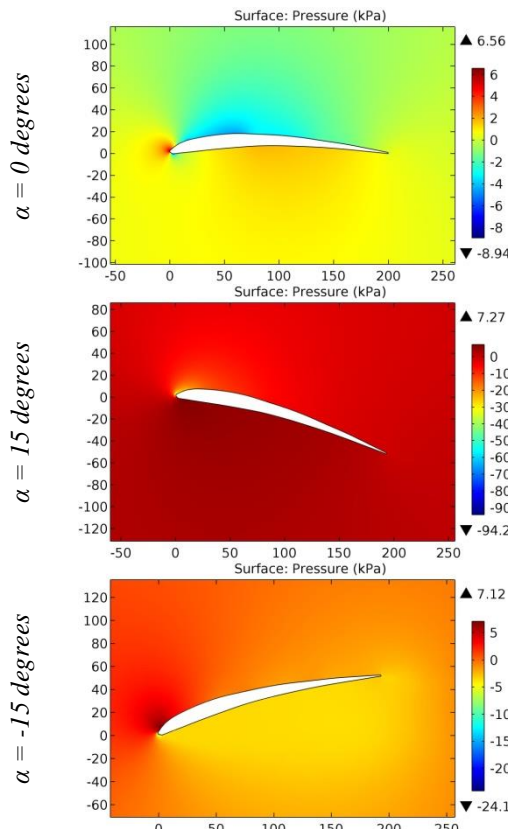


Figure 6. The pressure contours on the surfaces of the BABIC airfoil.

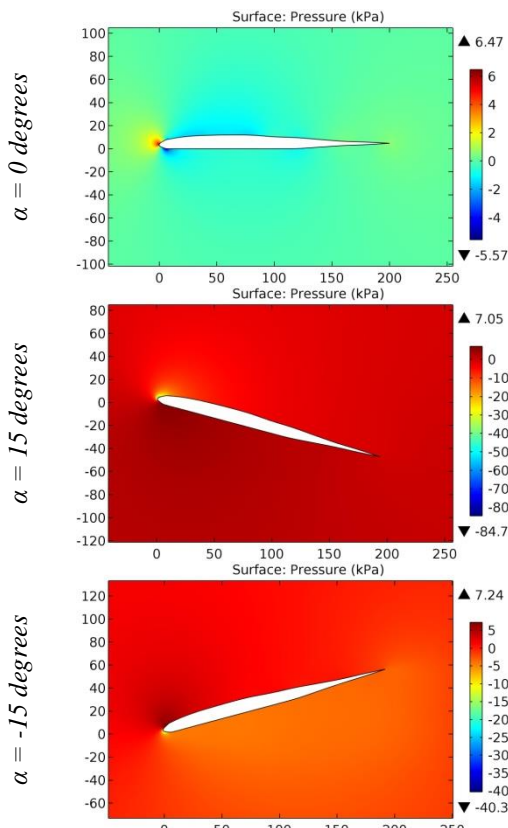


Figure 7. The pressure contours on the surfaces of the BAMBINO7 airfoil.

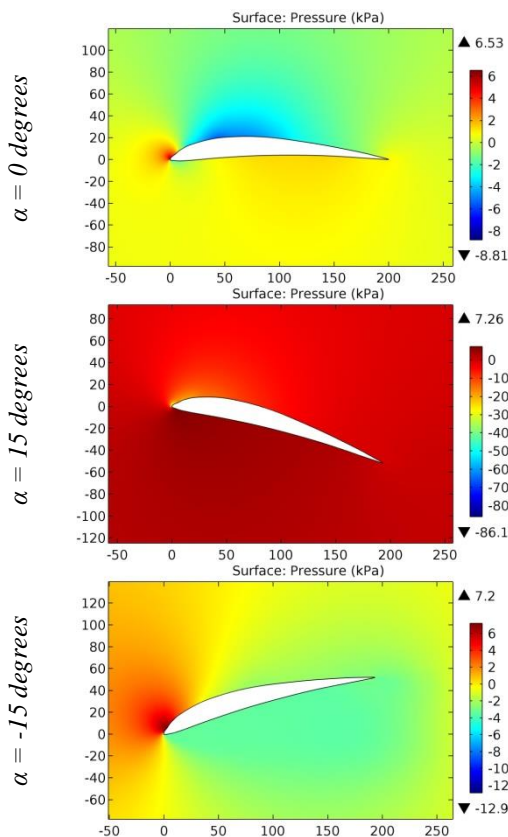


Figure 8. The pressure contours on the surfaces of the BE10255B airfoil.

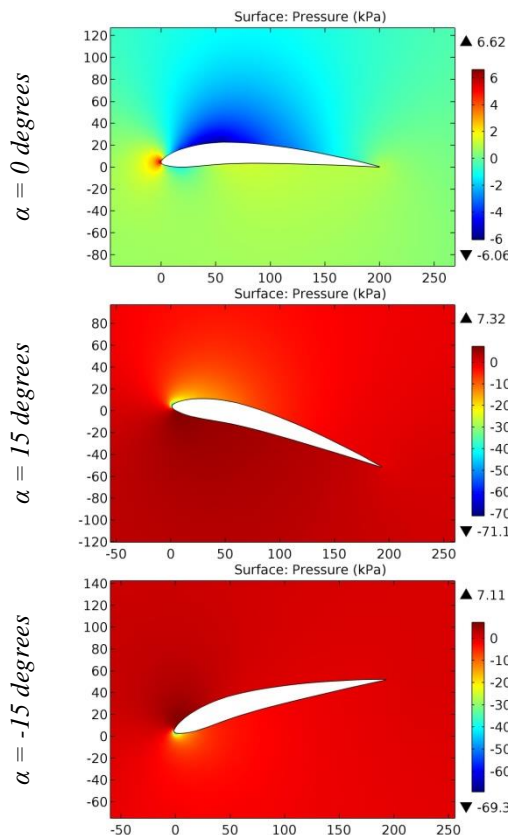


Figure 9. The pressure contours on the surfaces of the BE10305B airfoil.

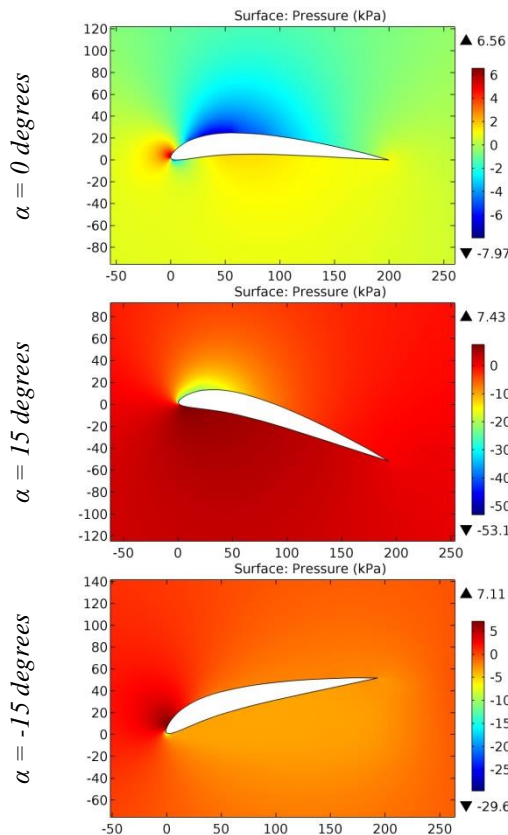


Figure 10. The pressure contours on the surfaces of the BE10307B airfoil.

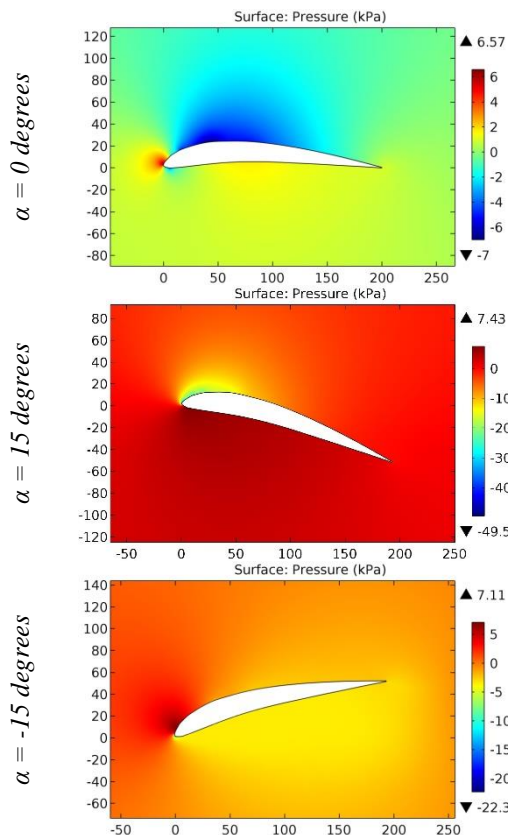


Figure 11. The pressure contours on the surfaces of the BE10357B airfoil.

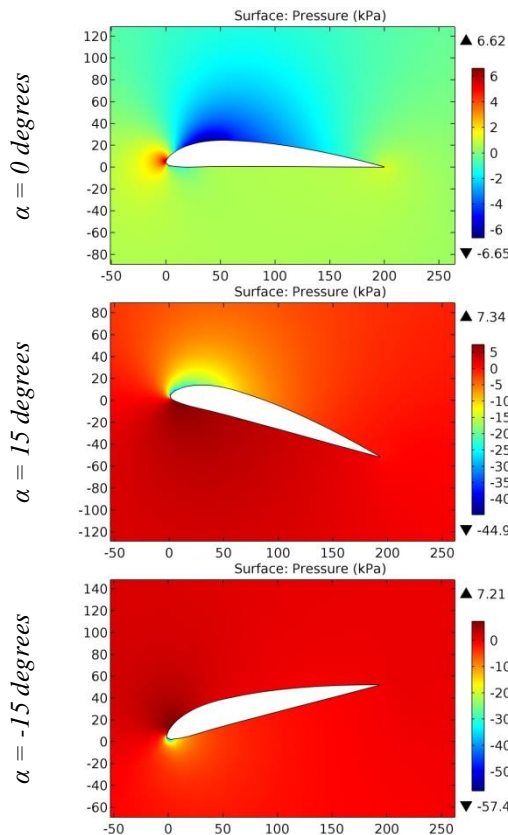


Figure 12. The pressure contours on the surfaces of the BE12305B airfoil.

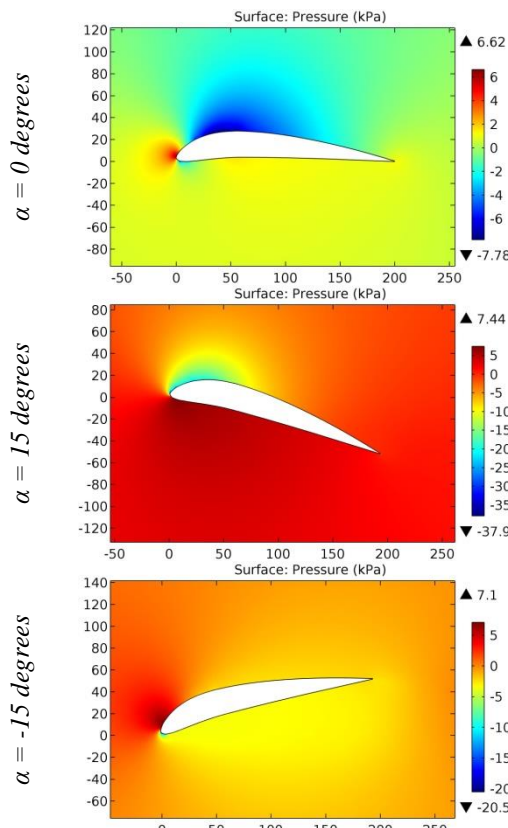


Figure 13. The pressure contours on the surfaces of the BE12307B airfoil.

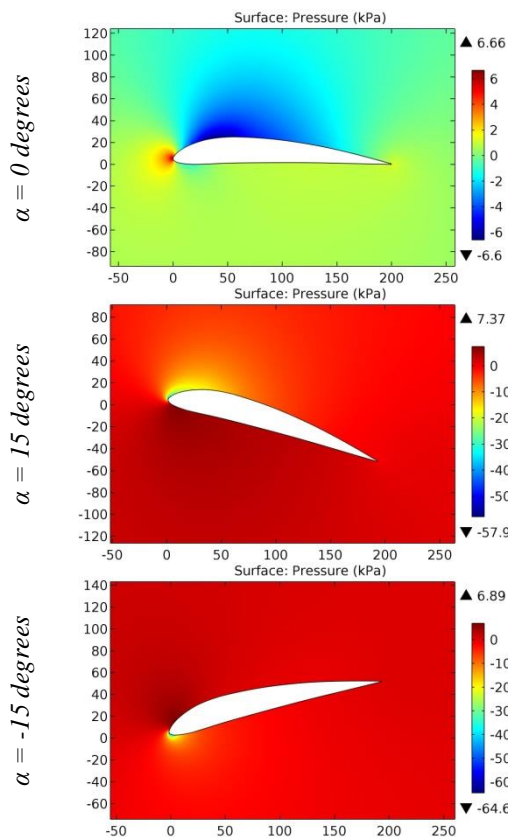


Figure 14. The pressure contours on the surfaces of the BE12355D airfoil.

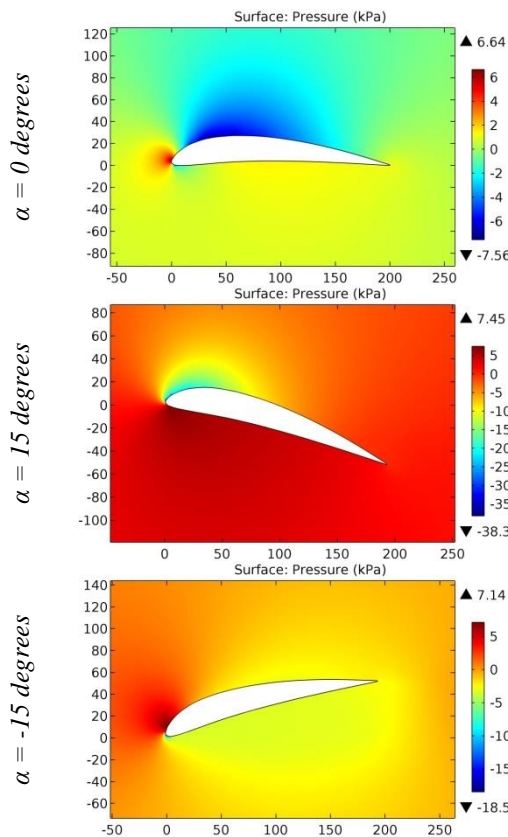


Figure 15. The pressure contours on the surfaces of the BE12357B airfoil.

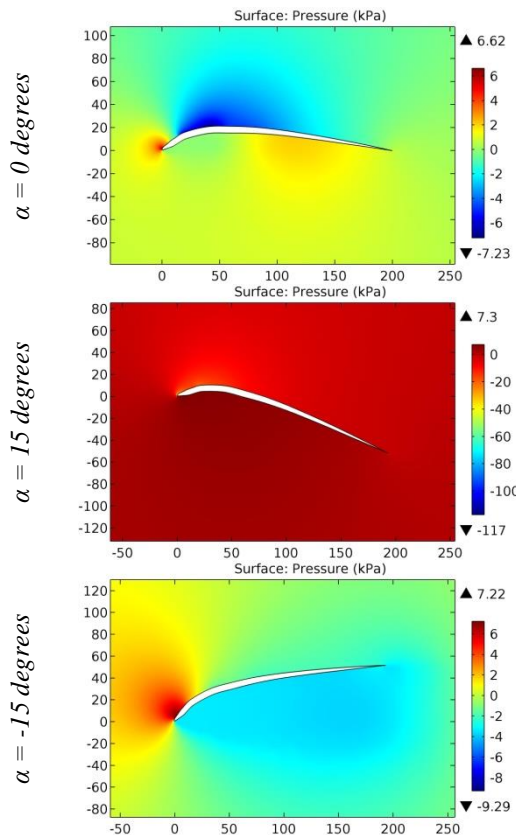


Figure 16. The pressure contours on the surfaces of the BE3259B airfoil.

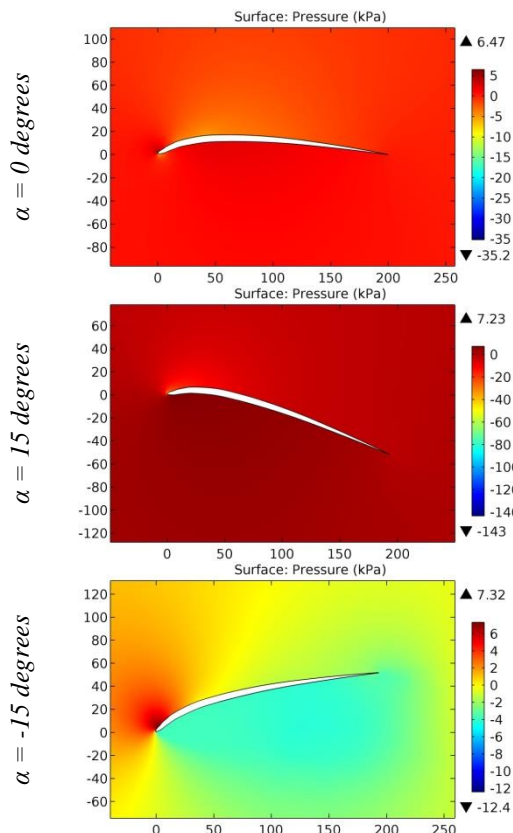


Figure 17. The pressure contours on the surfaces of the BE3307B airfoil.

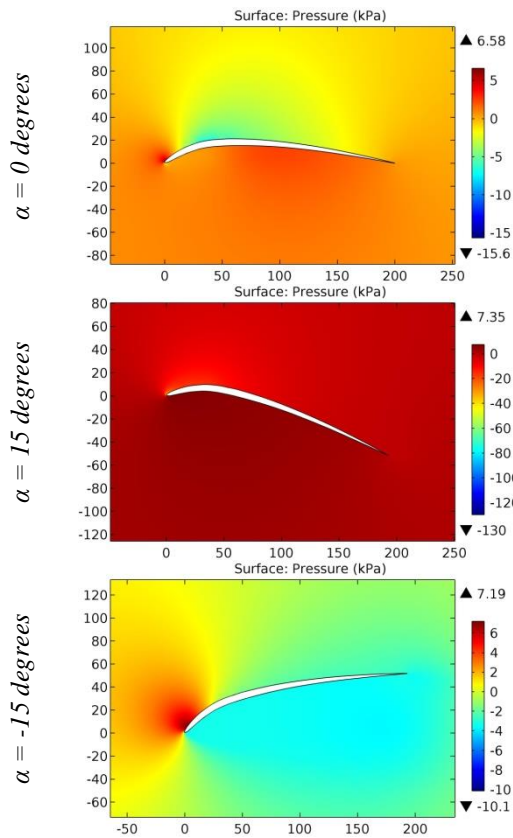


Figure 18. The pressure contours on the surfaces of the BE3309B airfoil.

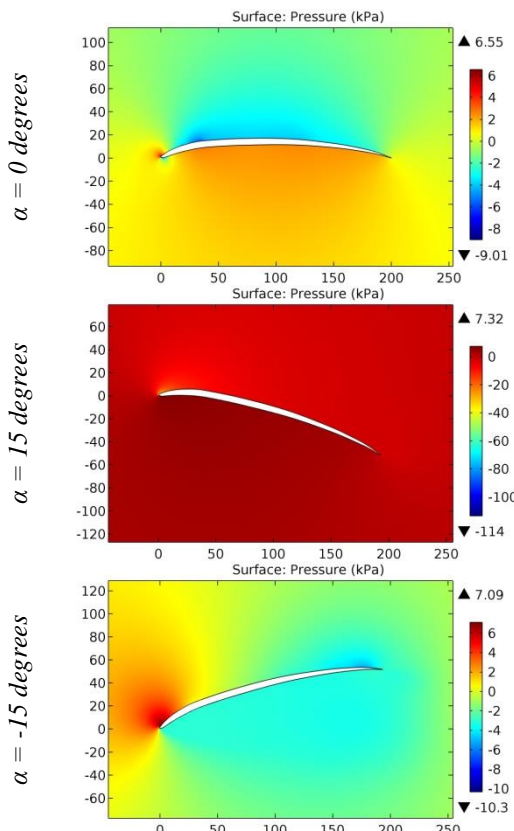


Figure 19. The pressure contours on the surfaces of the BE3357B airfoil.

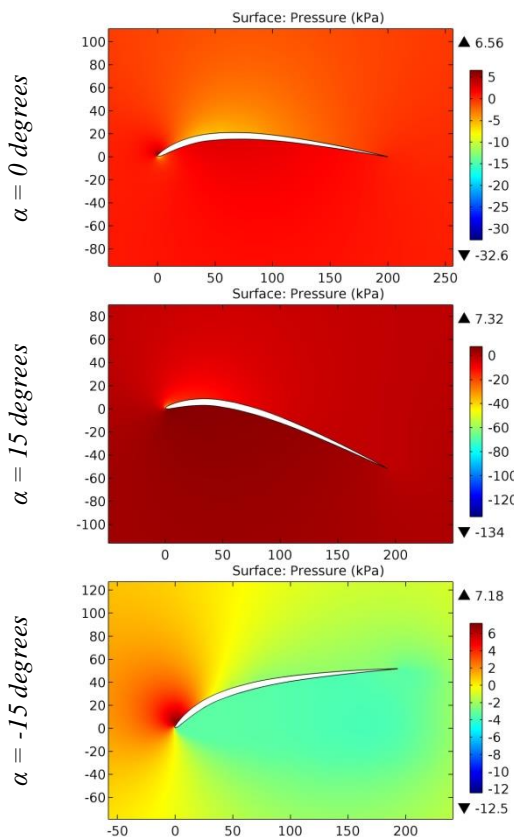


Figure 20. The pressure contours on the surfaces of the BE3359B airfoil.

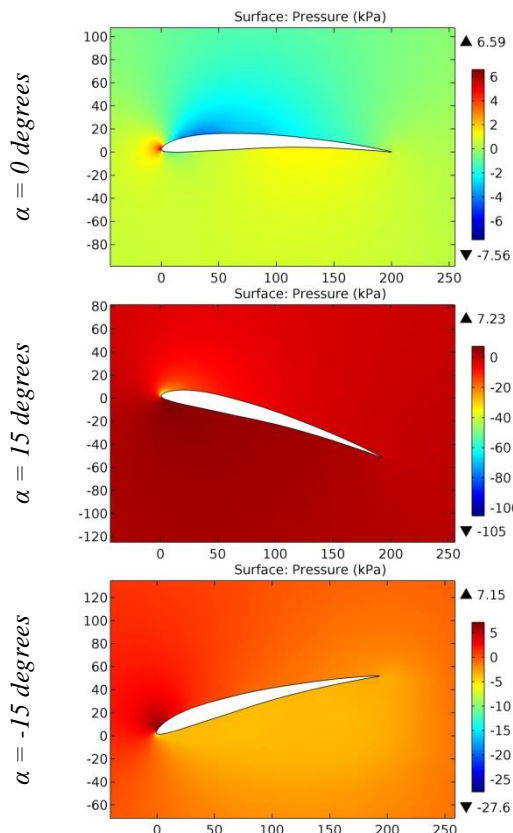


Figure 21. The pressure contours on the surfaces of the BE50 (original) airfoil.

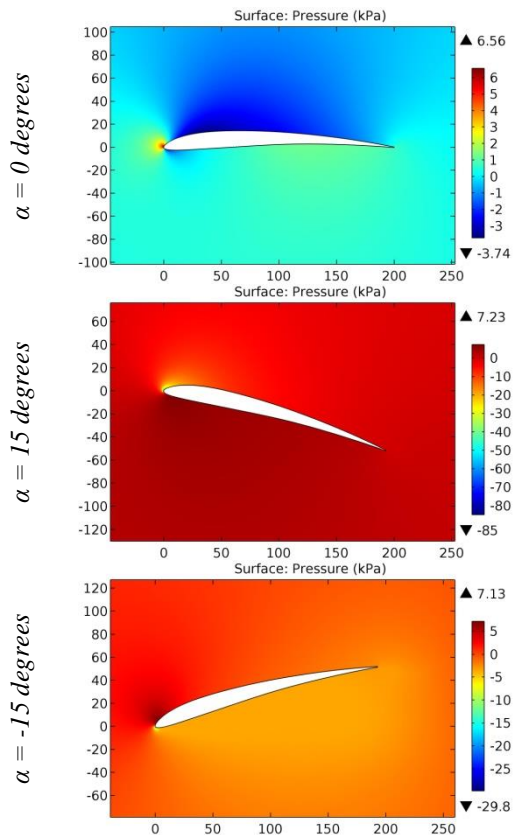


Figure 22. The pressure contours on the surfaces of the BE50 (smoothed) airfoil.

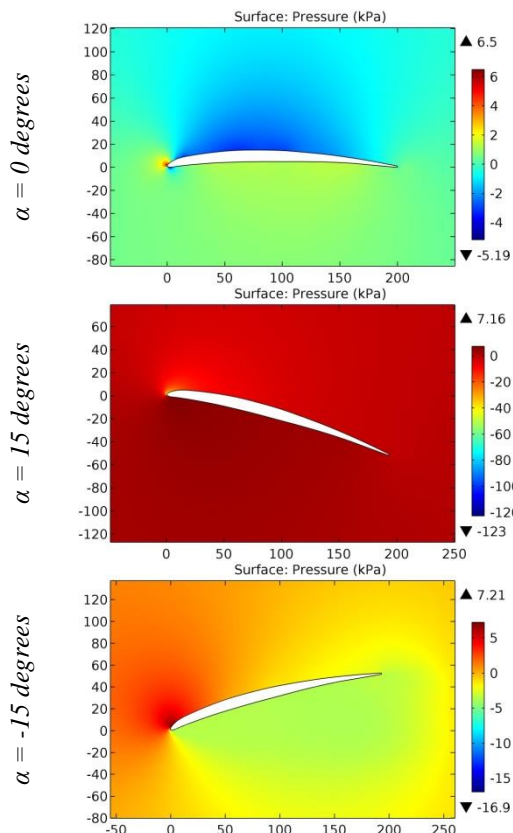


Figure 23. The pressure contours on the surfaces of the BE5456 airfoil.

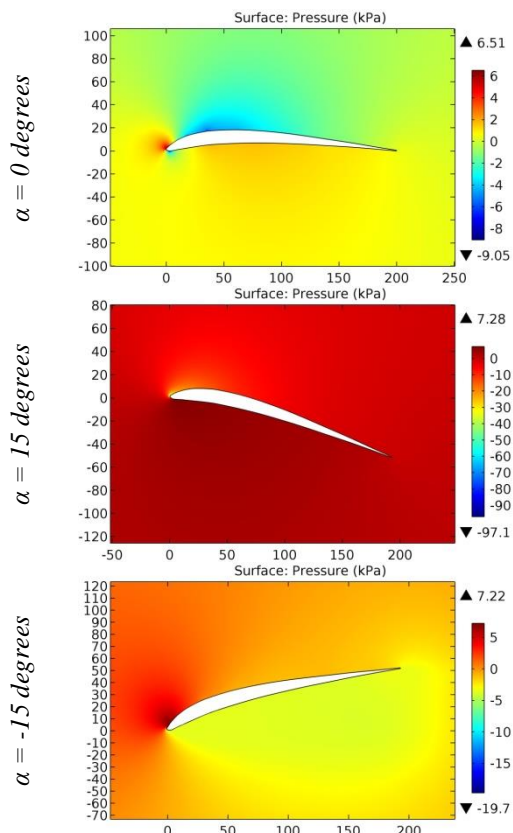


Figure 24. The pressure contours on the surfaces of the BE6306B airfoil.

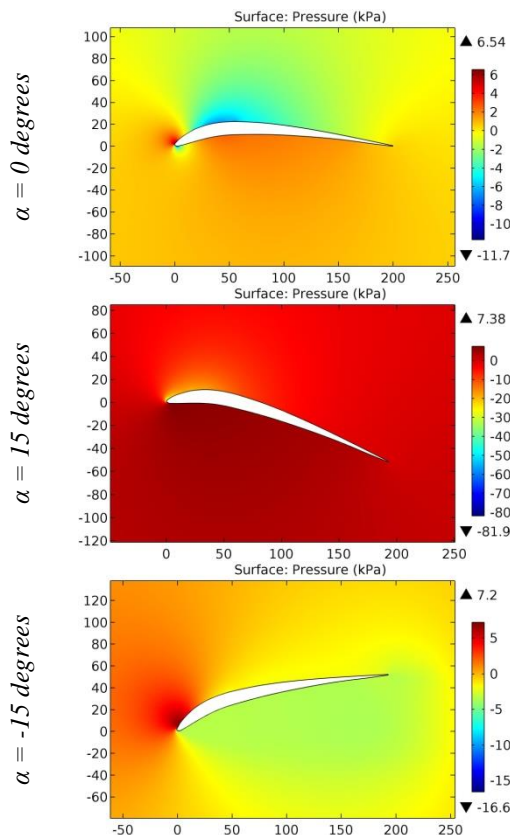


Figure 25. The pressure contours on the surfaces of the BE6308B airfoil.

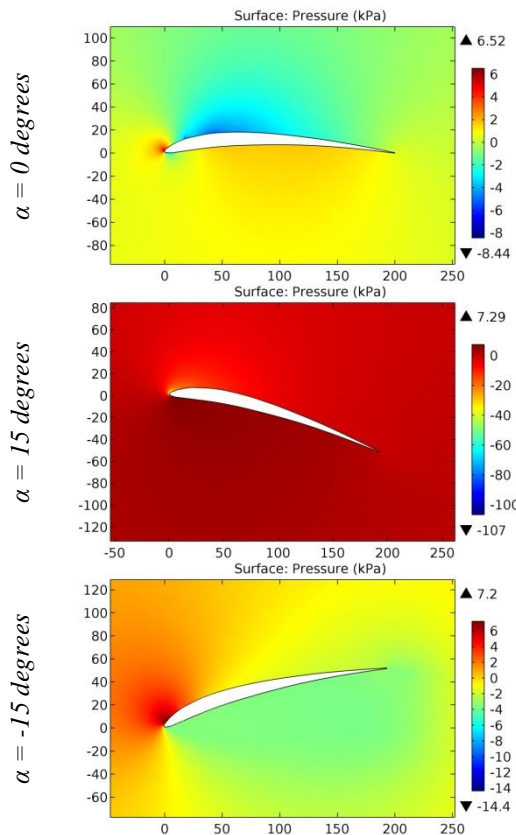


Figure 26. The pressure contours on the surfaces of the BE6356 airfoil.

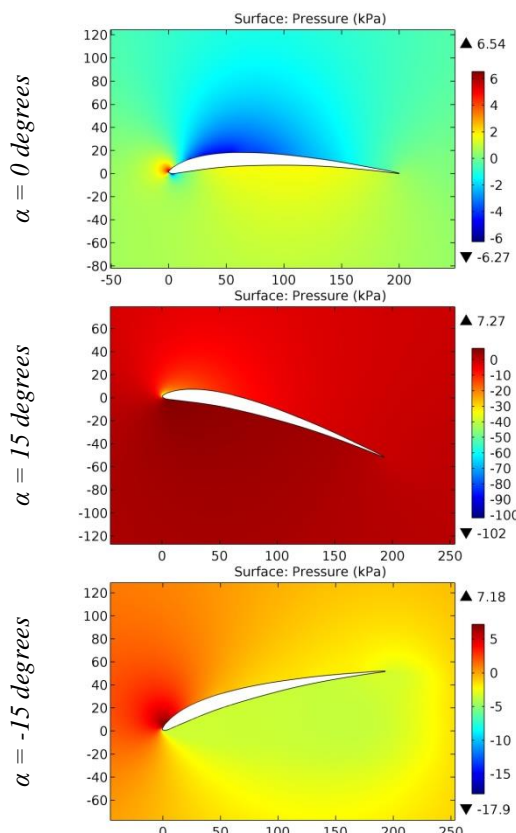


Figure 27. The pressure contours on the surfaces of the BE6356B airfoil.

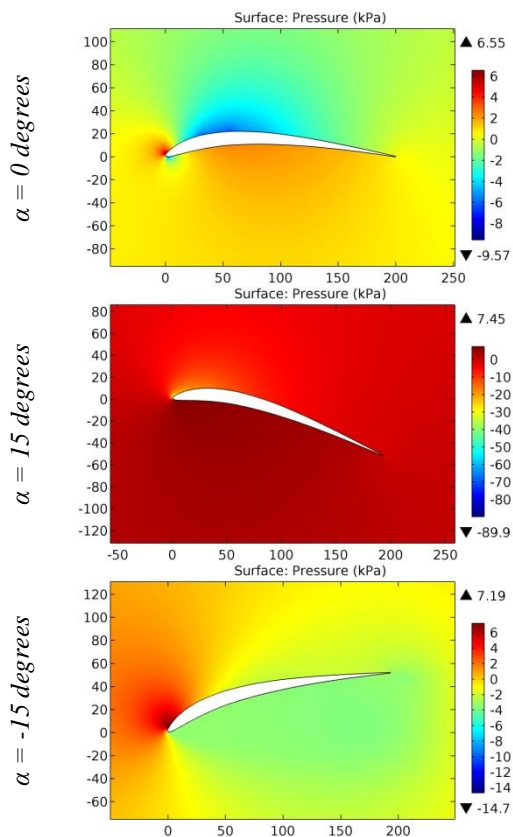


Figure 28. The pressure contours on the surfaces of the BE6358B airfoil.

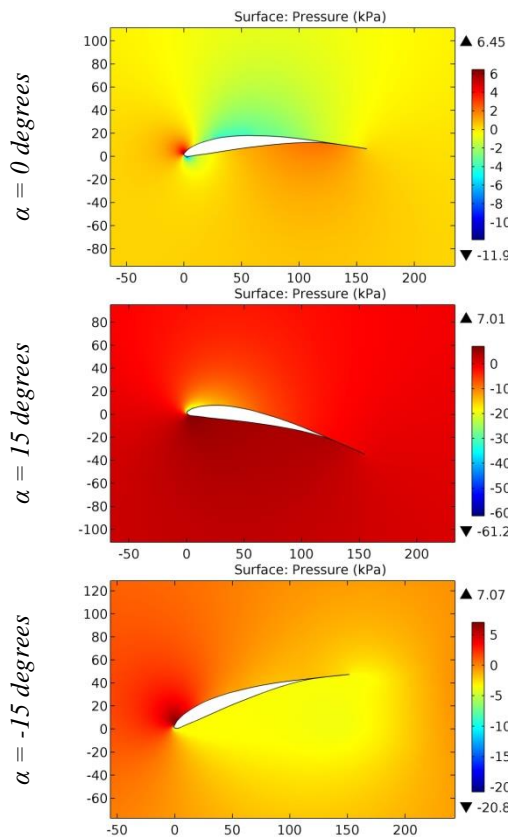


Figure 29. The pressure contours on the surfaces of the BE6407E airfoil.

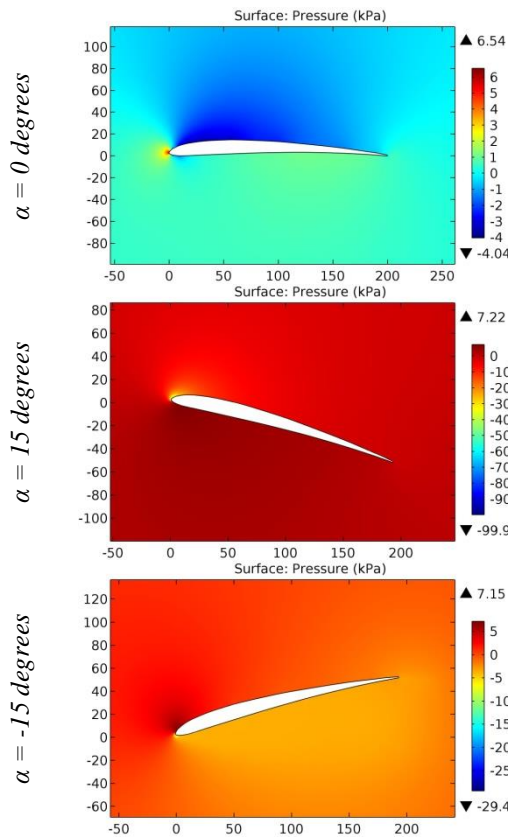


Figure 30. The pressure contours on the surfaces of the BE6453B airfoil.

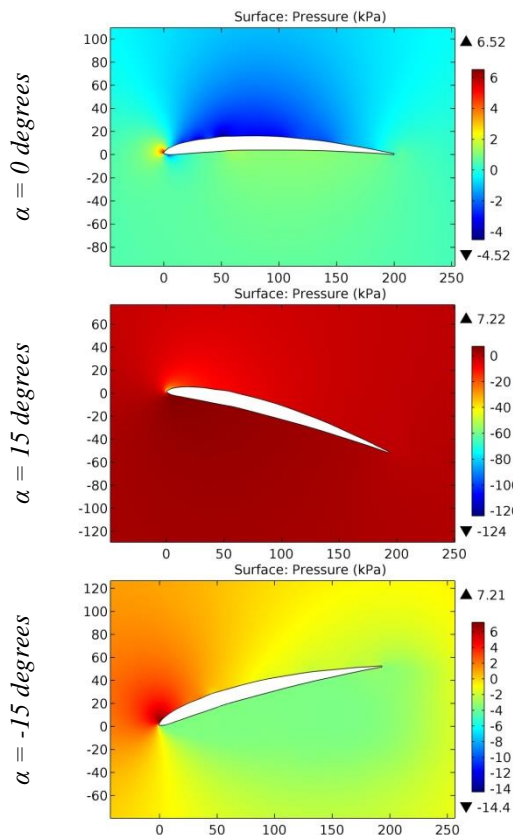


Figure 31. The pressure contours on the surfaces of the BE6455B airfoil.

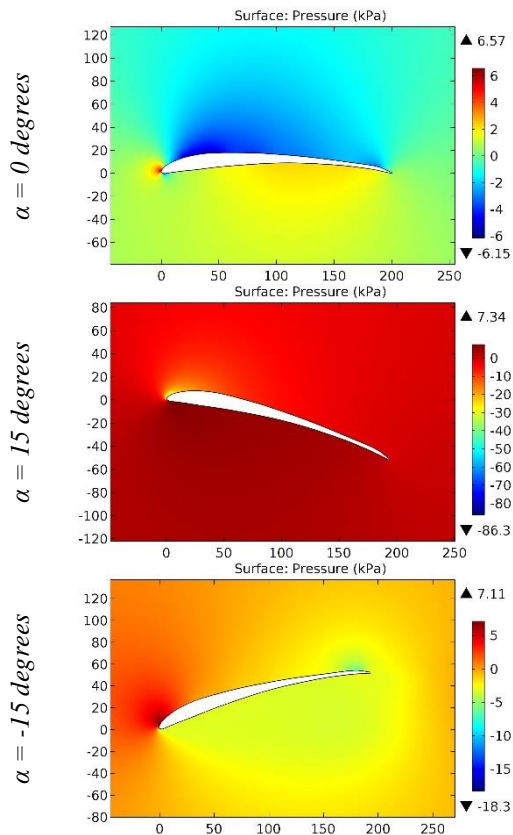


Figure 32. The pressure contours on the surfaces of the BE6456F airfoil.

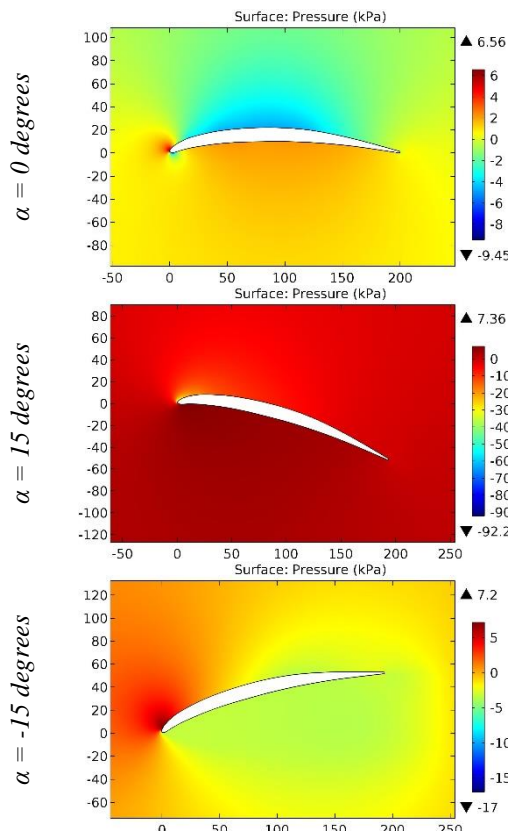


Figure 33. The pressure contours on the surfaces of the BE6458 airfoil.

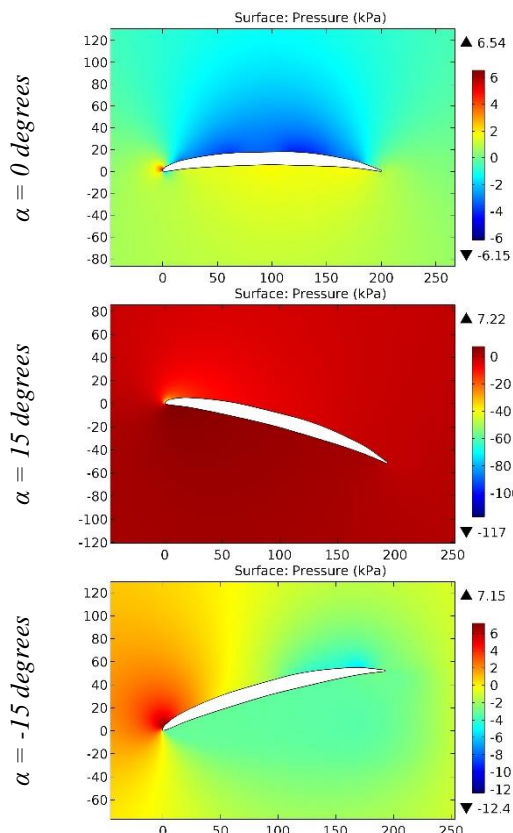


Figure 34. The pressure contours on the surfaces of the BE6556 airfoil.

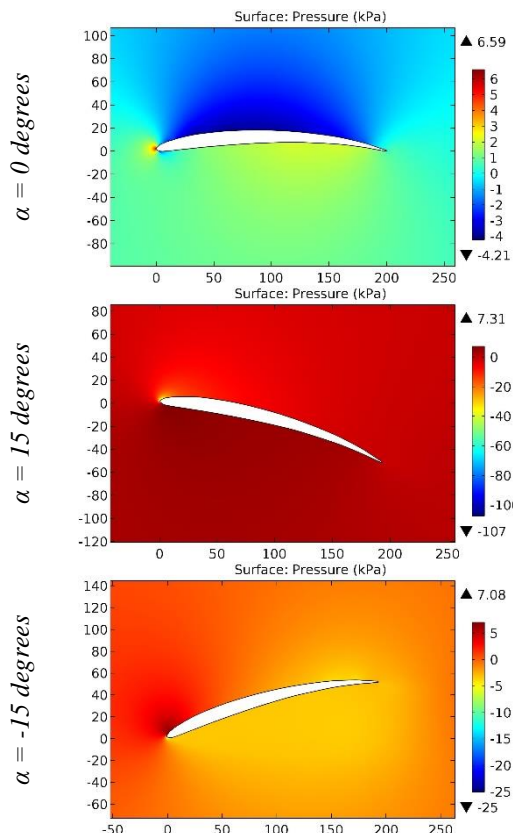


Figure 35. The pressure contours on the surfaces of the BE6556B airfoil.

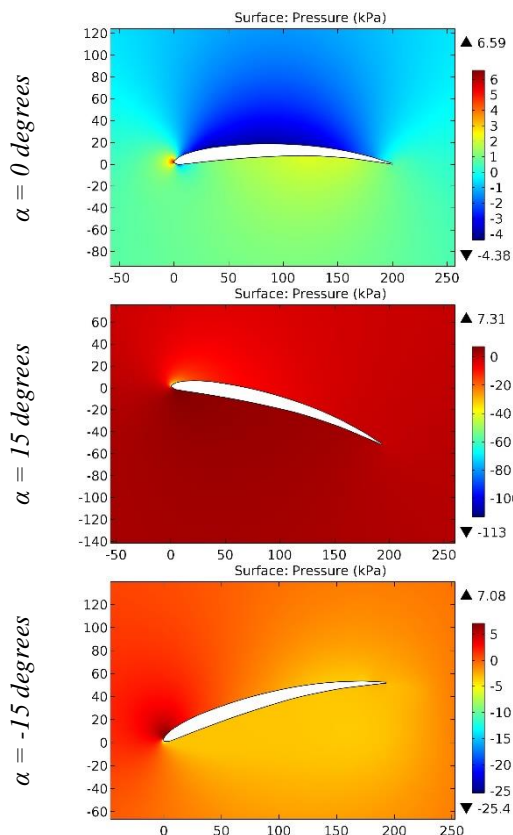


Figure 36. The pressure contours on the surfaces of the BE6556C airfoil.

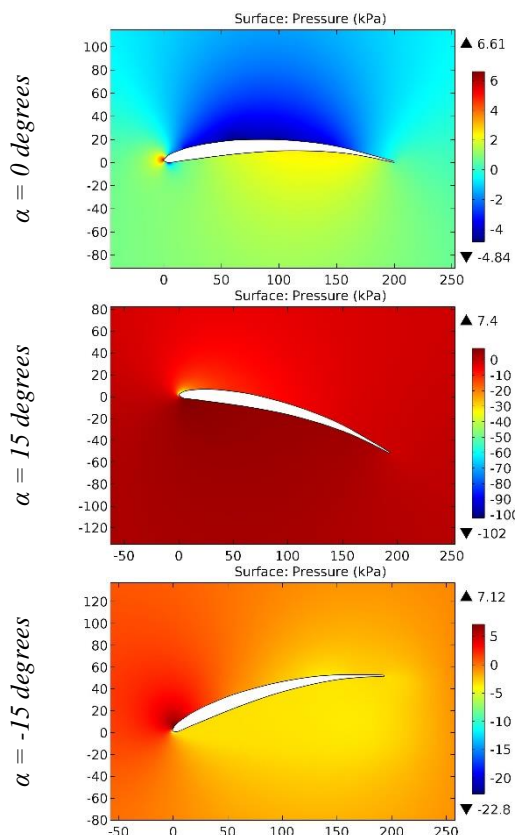


Figure 37. The pressure contours on the surfaces of the BE6557B airfoil.

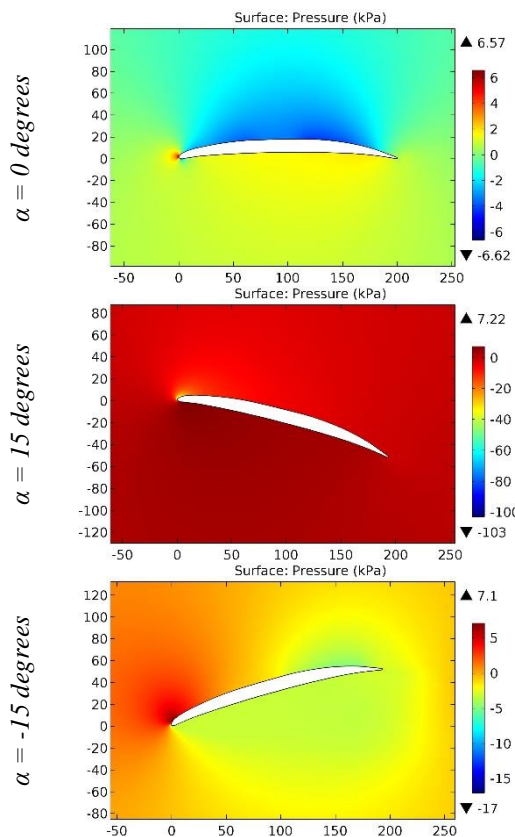


Figure 38. The pressure contours on the surfaces of the BE6606 airfoil.

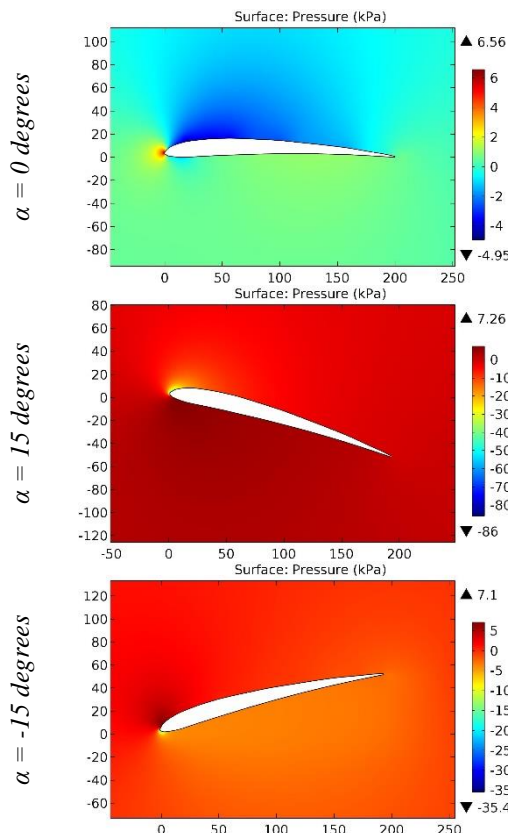


Figure 39. The pressure contours on the surfaces of the BE7404B airfoil.

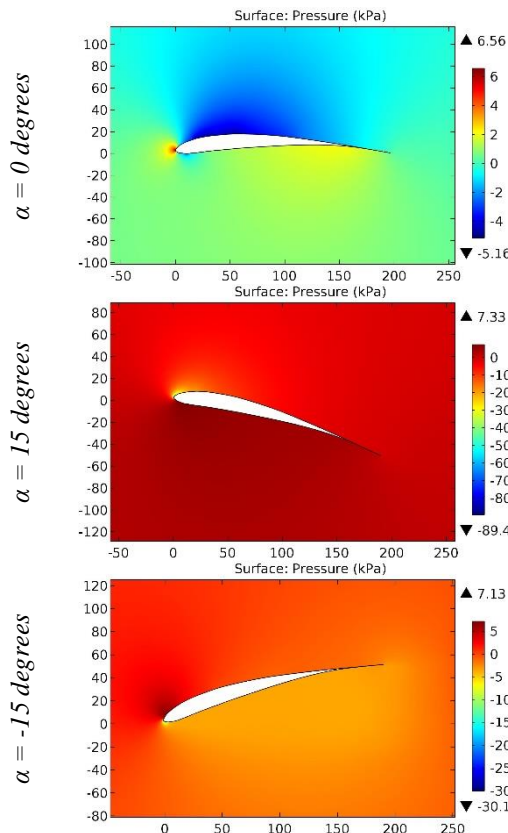


Figure 40. The pressure contours on the surfaces of the BE7455E airfoil.

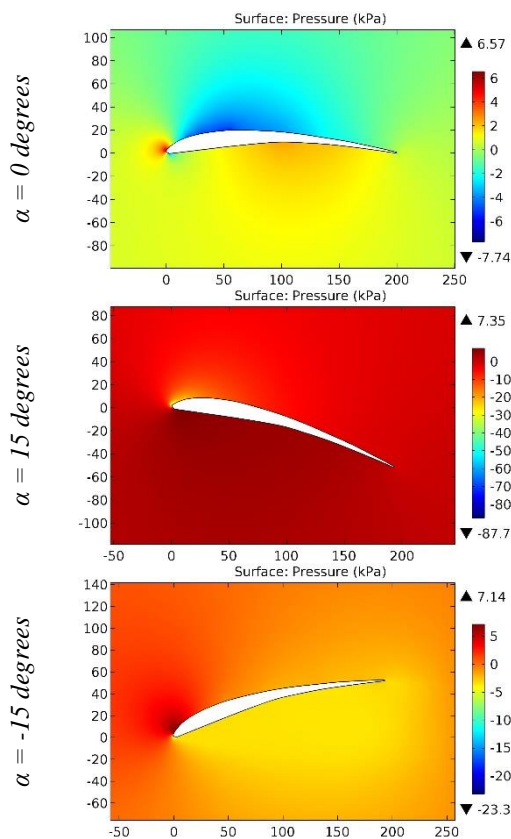


Figure 41. The pressure contours on the surfaces of the BE7457D airfoil.

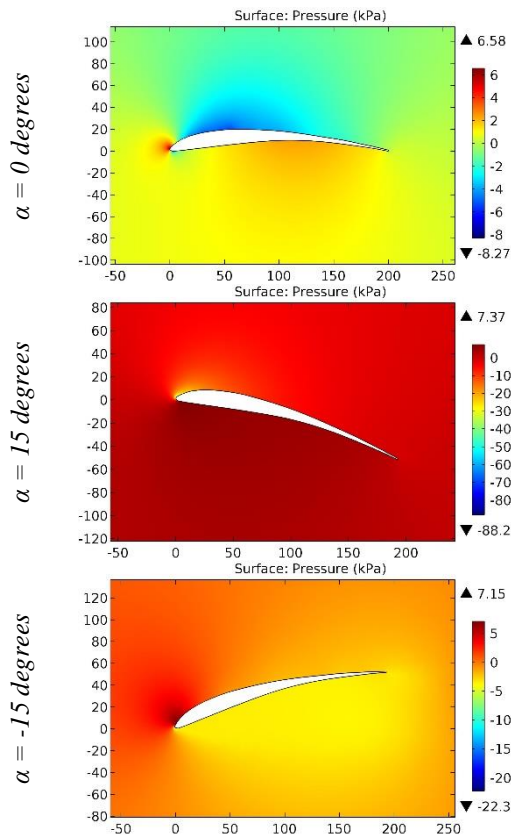


Figure 42. The pressure contours on the surfaces of the BE7457D2 airfoil.

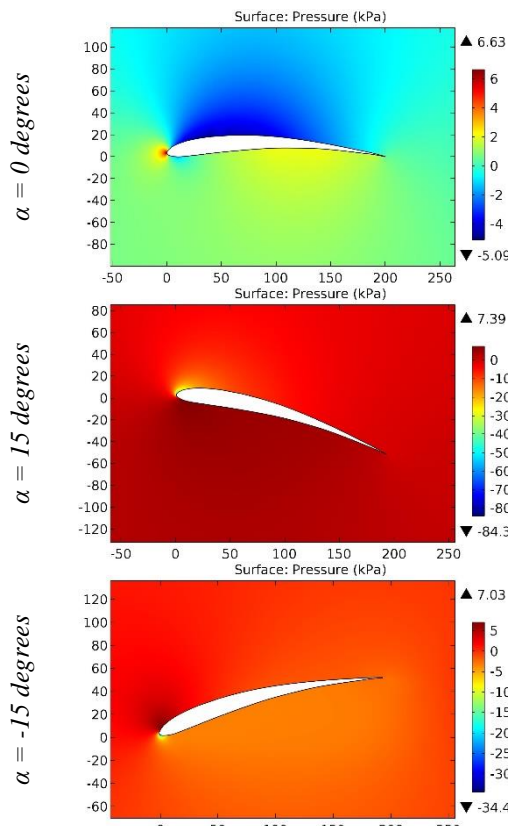


Figure 43. The pressure contours on the surfaces of the BE7505D airfoil.

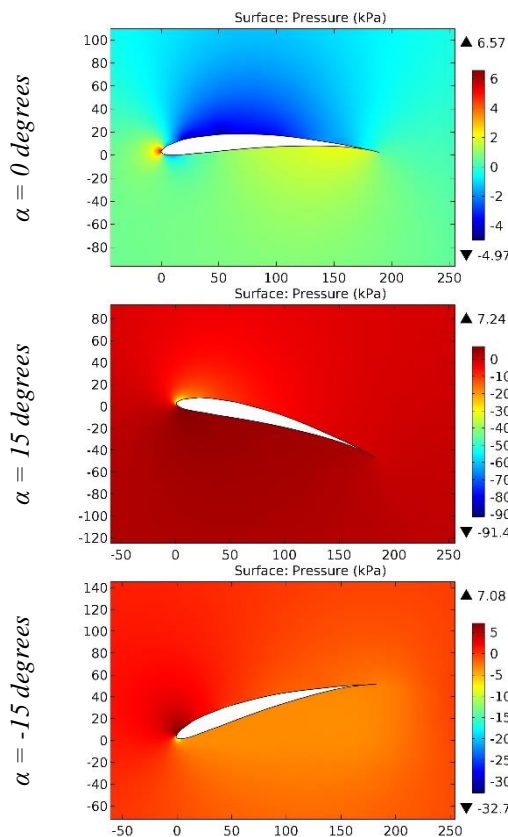


Figure 44. The pressure contours on the surfaces of the BE7505E airfoil.

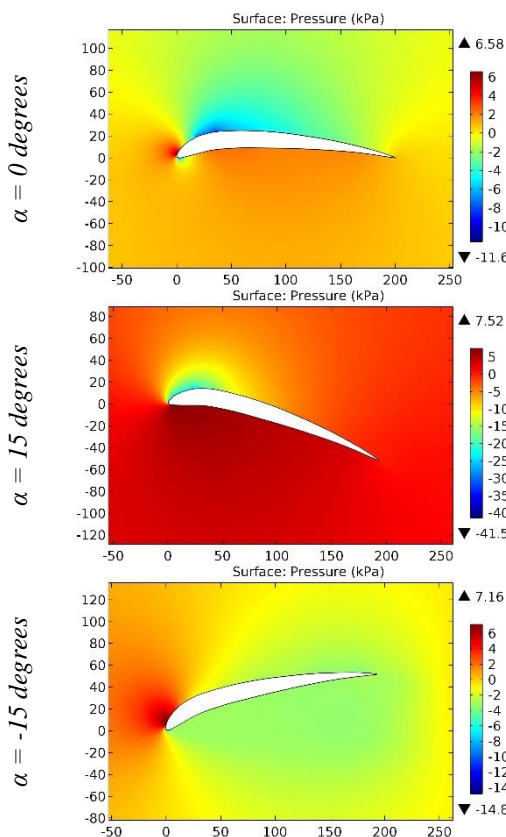


Figure 45. The pressure contours on the surfaces of the BE8258 airfoil.

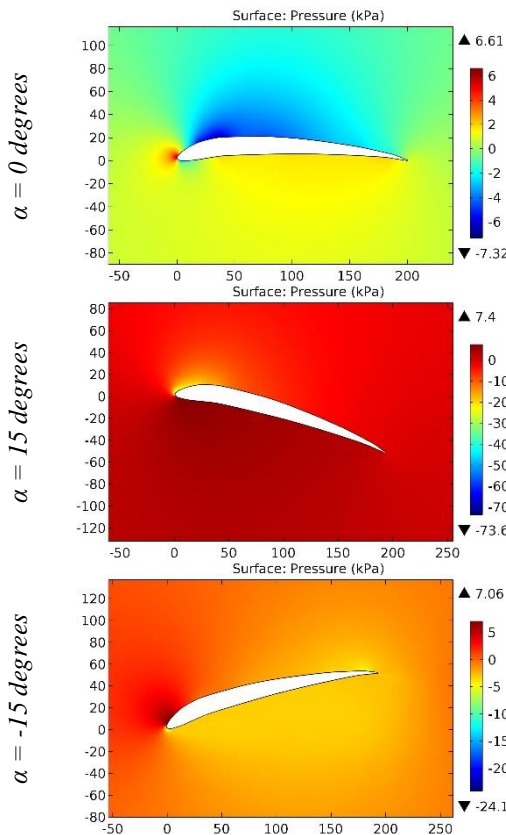


Figure 46. The pressure contours on the surfaces of the BE8306 airfoil.

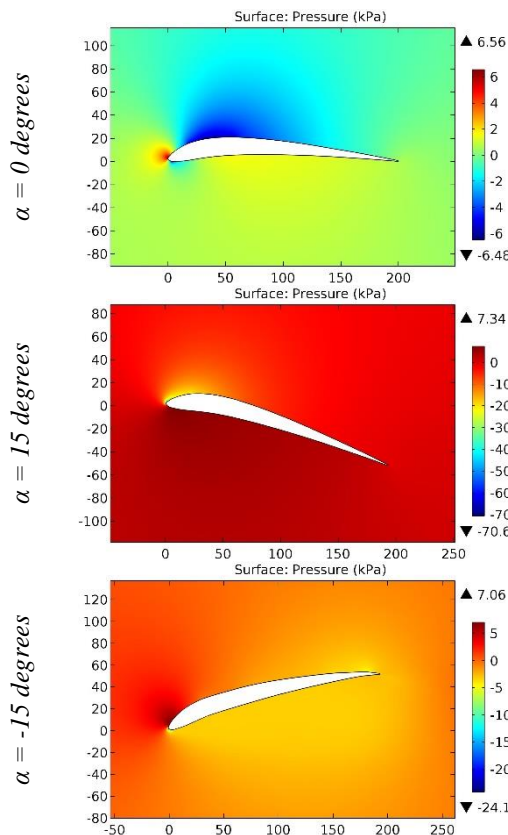


Figure 47. The pressure contours on the surfaces of the BE8306B airfoil.

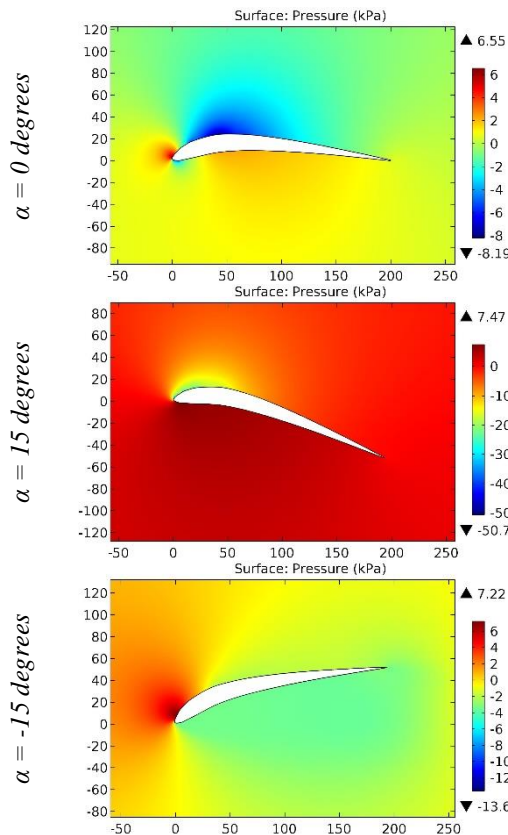


Figure 48. The pressure contours on the surfaces of the BE8308B airfoil.

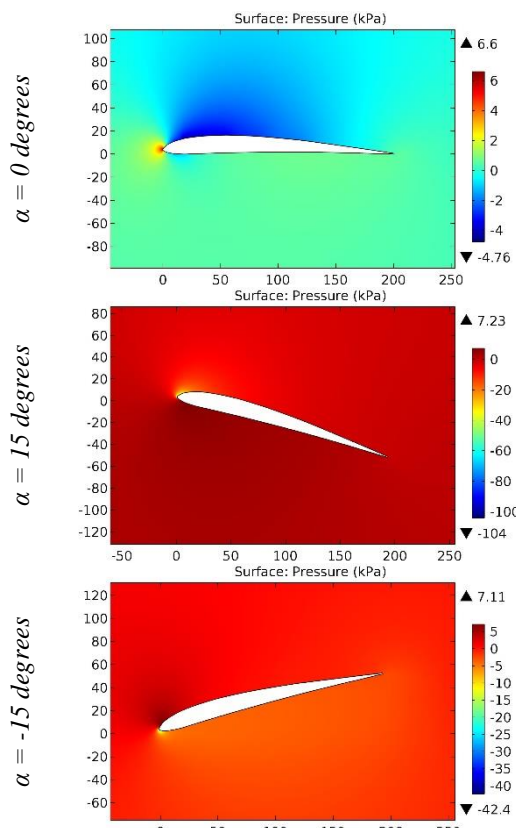


Figure 49. The pressure contours on the surfaces of the BE8353B airfoil.

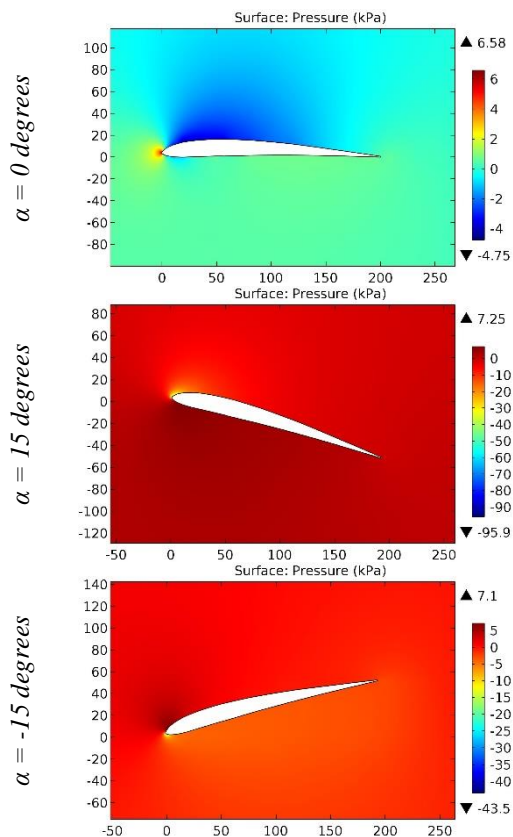


Figure 50. The pressure contours on the surfaces of the BE8353B2 airfoil.

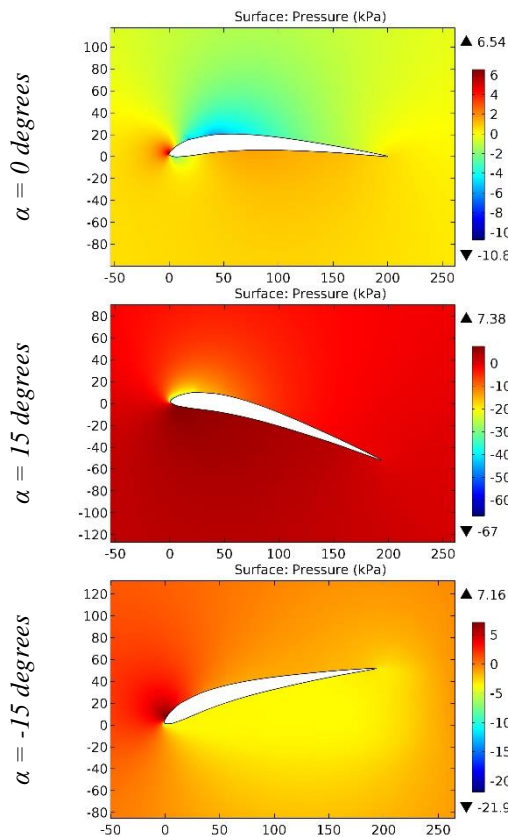


Figure 51. The pressure contours on the surfaces of the BE8356 airfoil.

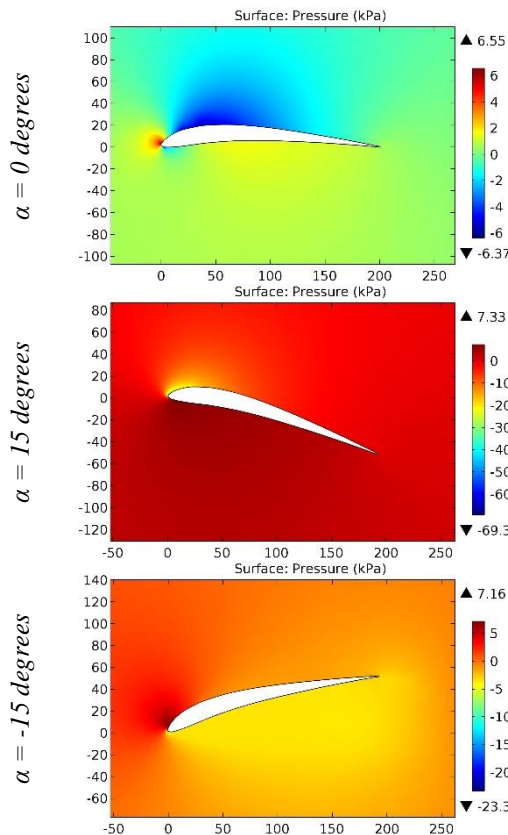


Figure 52. The pressure contours on the surfaces of the BE8356B airfoil.

Impact Factor:

ISRA (India)	= 6.317	SIS (USA)	= 0.912	ICV (Poland)	= 6.630
ISI (Dubai, UAE)	= 1.582	РИНЦ (Russia)	= 3.939	PIF (India)	= 1.940
GIF (Australia)	= 0.564	ESJI (KZ)	= 9.035	IBI (India)	= 4.260
JIF	= 1.500	SJIF (Morocco)	= 7.184	OAJI (USA)	= 0.350

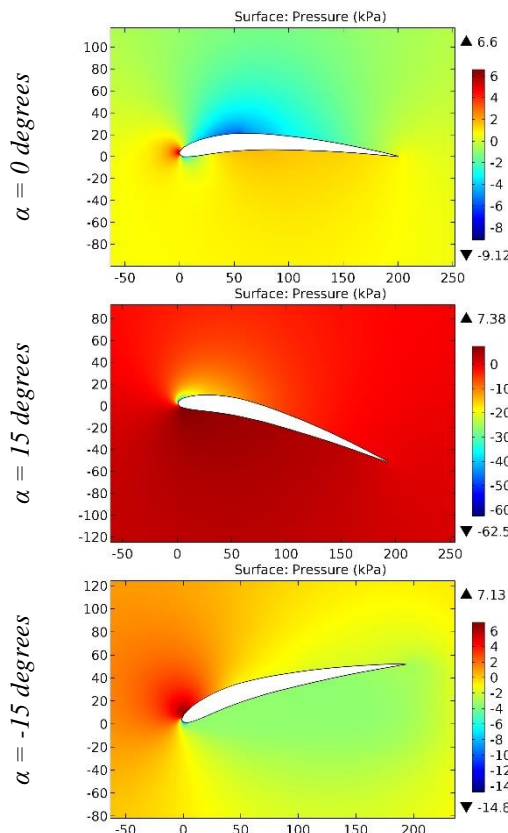


Figure 53. The pressure contours on the surfaces of the BE8356B2 airfoil.

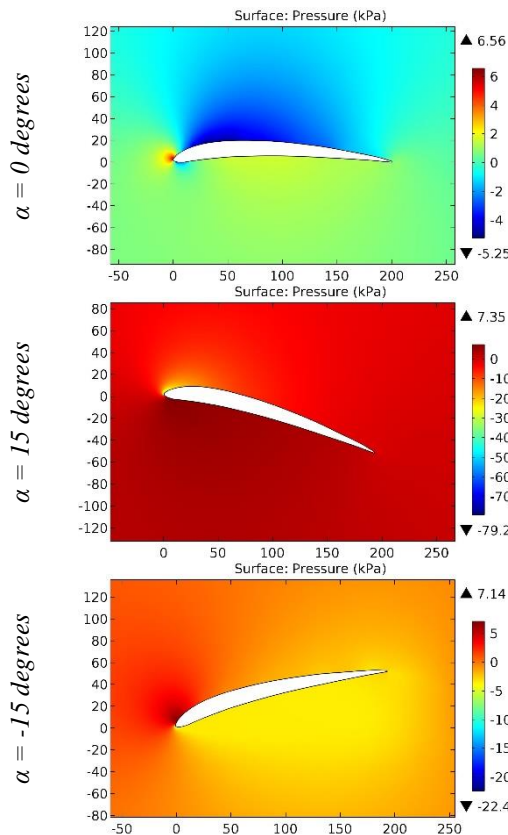


Figure 54. The pressure contours on the surfaces of the BE8356B3 airfoil.

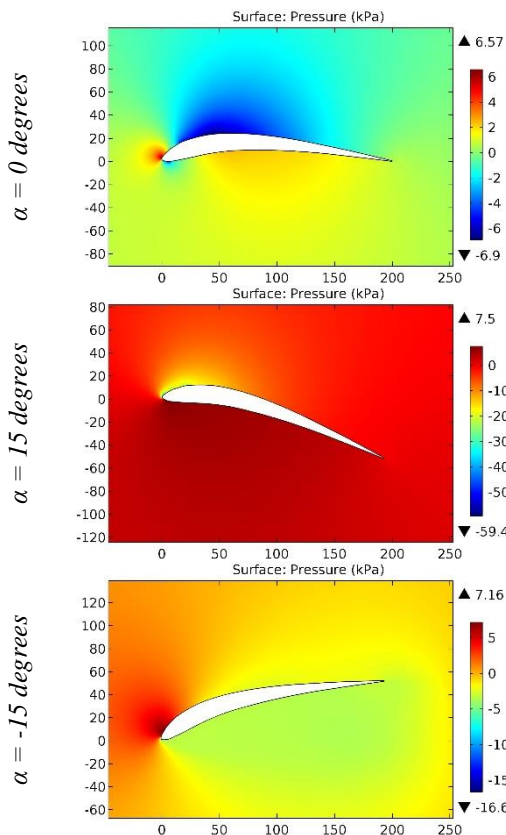


Figure 55. The pressure contours on the surfaces of the BE8358B airfoil.

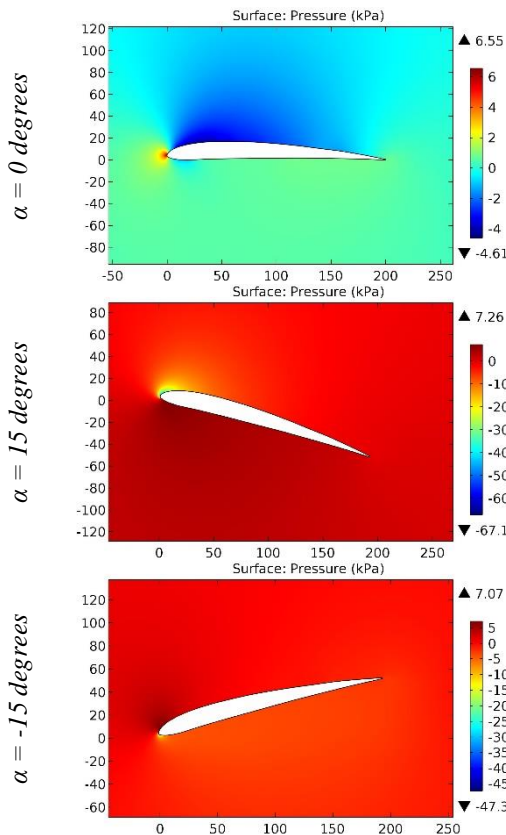


Figure 56. The pressure contours on the surfaces of the BE8403B airfoil.

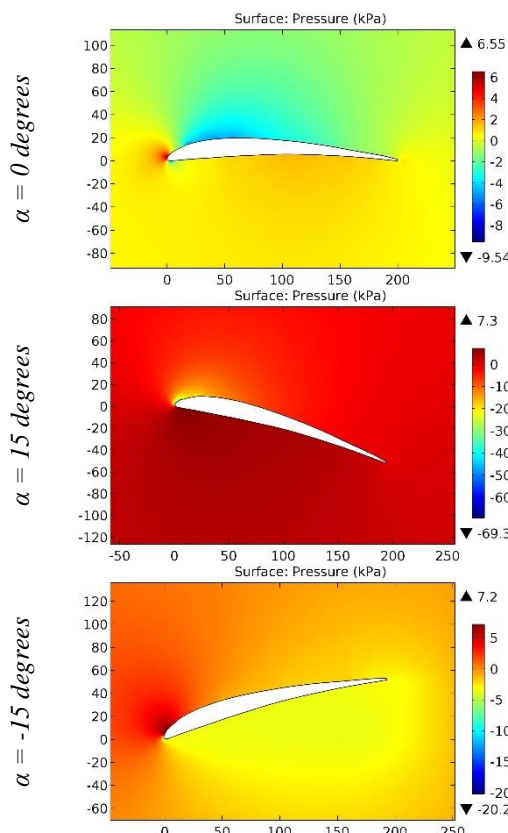


Figure 57. The pressure contours on the surfaces of the BE8405B airfoil.

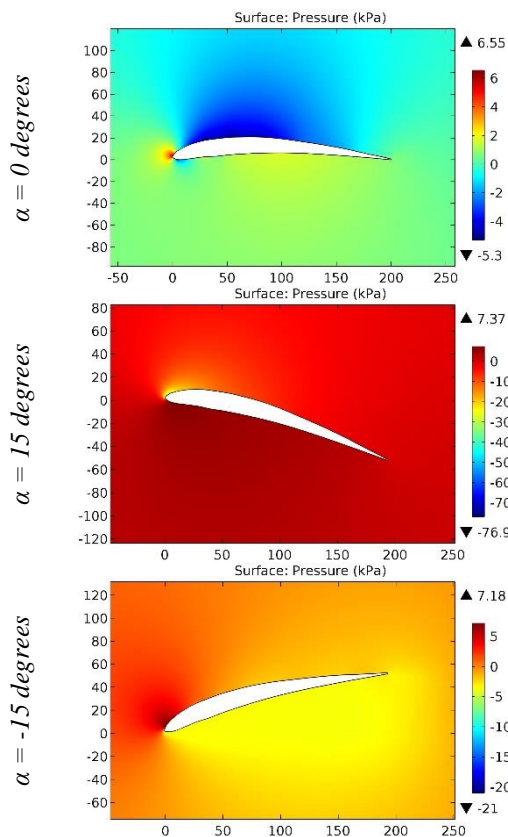


Figure 58. The pressure contours on the surfaces of the BE8406C airfoil.

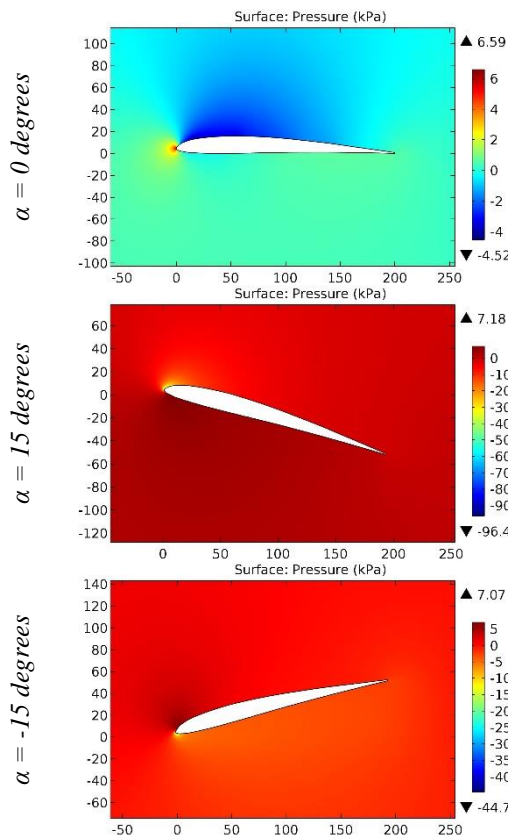


Figure 59. The pressure contours on the surfaces of the BE8452B airfoil.

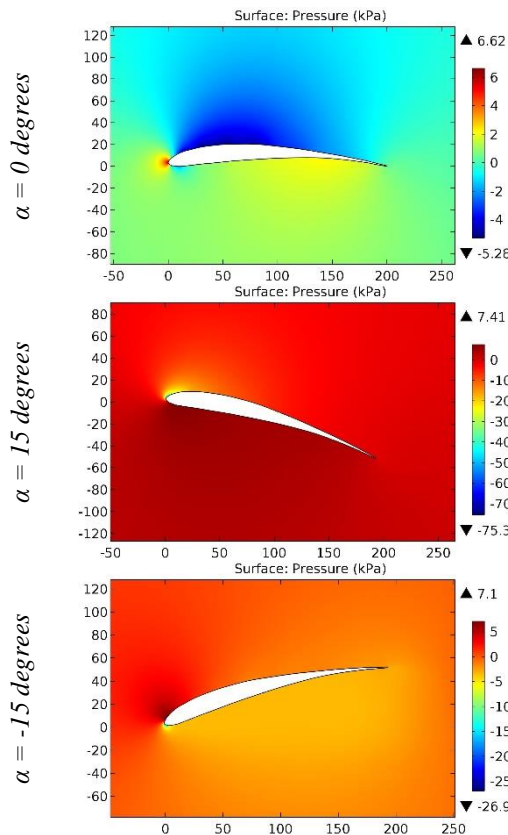


Figure 60. The pressure contours on the surfaces of the BE8456D airfoil.

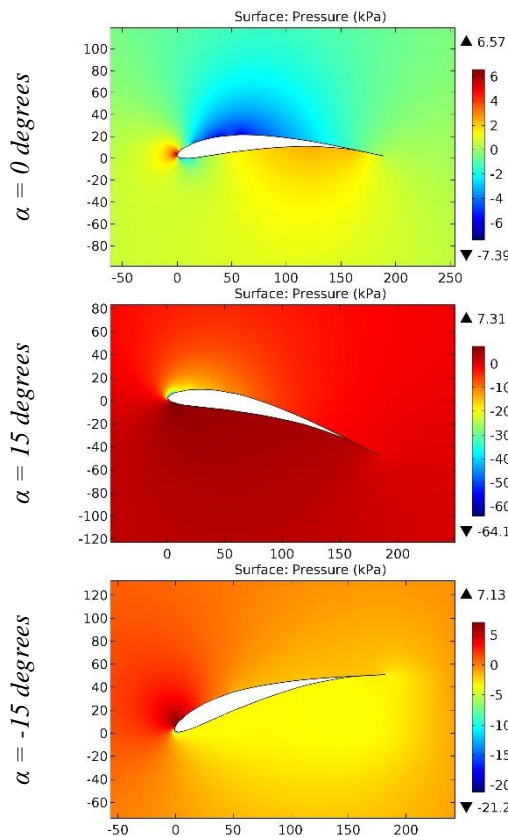


Figure 61. The pressure contours on the surfaces of the BE8457E airfoil.

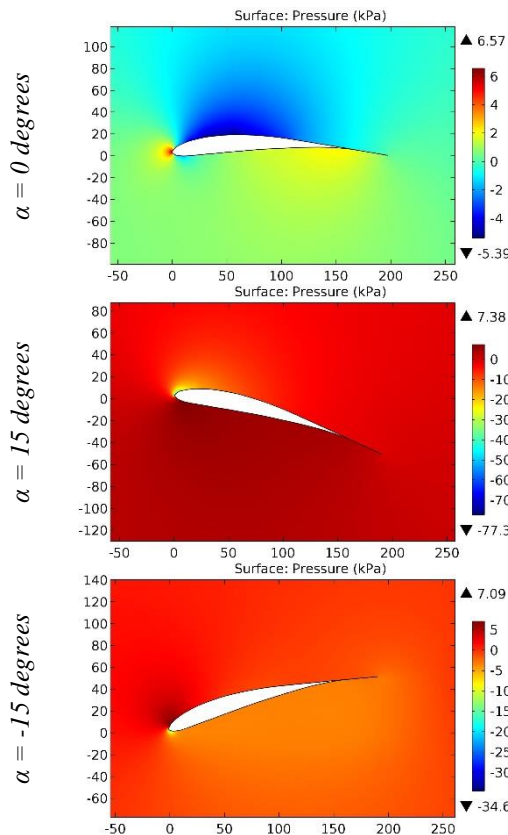


Figure 62. The pressure contours on the surfaces of the BE8505E airfoil.

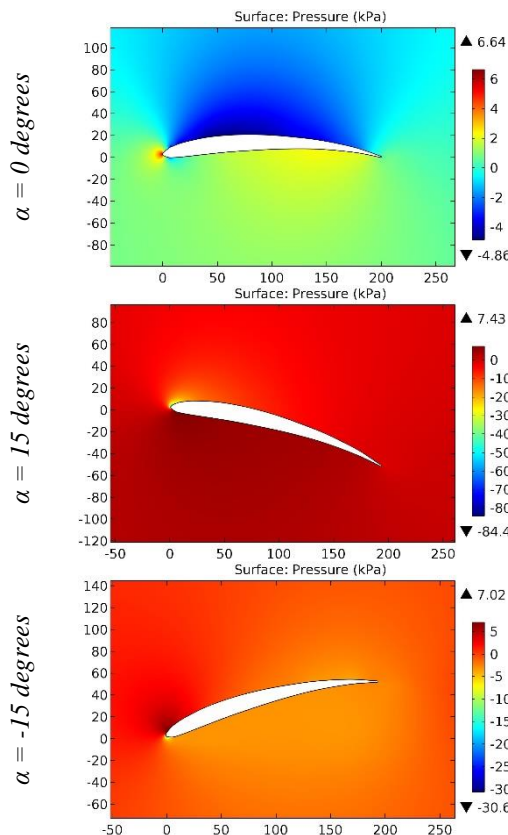


Figure 63. The pressure contours on the surfaces of the BE8556B airfoil.

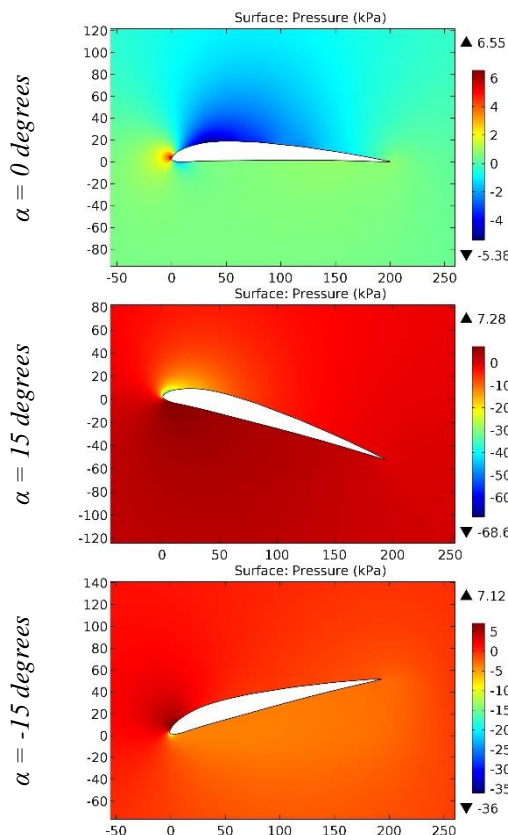


Figure 64. The pressure contours on the surfaces of the BE9304B airfoil.

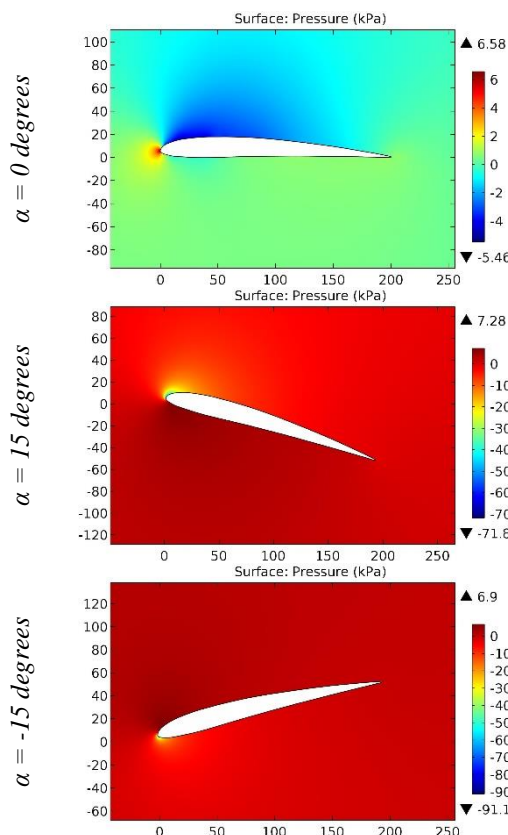


Figure 65. The pressure contours on the surfaces of the BE9403B airfoil.

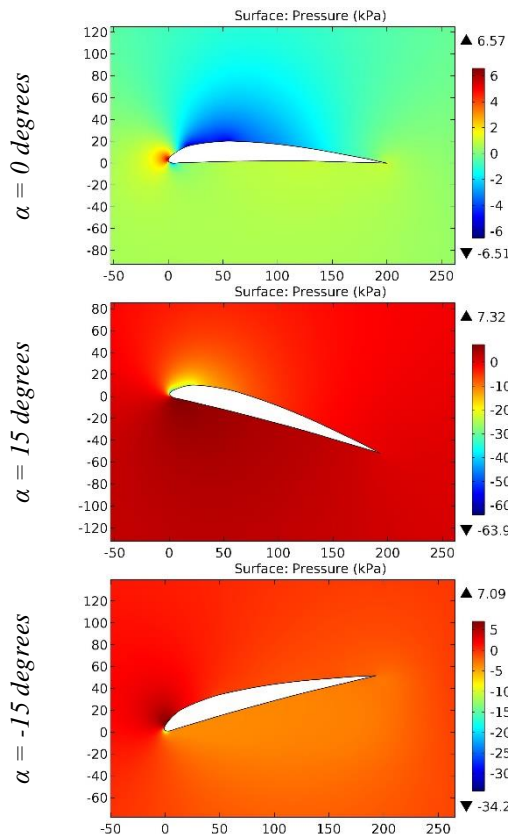


Figure 66. The pressure contours on the surfaces of the BE9404B airfoil.

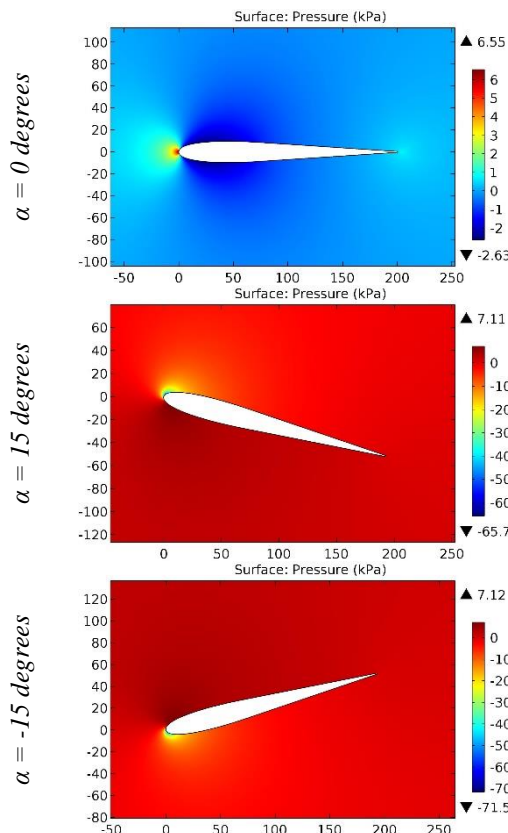


Figure 67. The pressure contours on the surfaces of the BELL 540 airfoil.

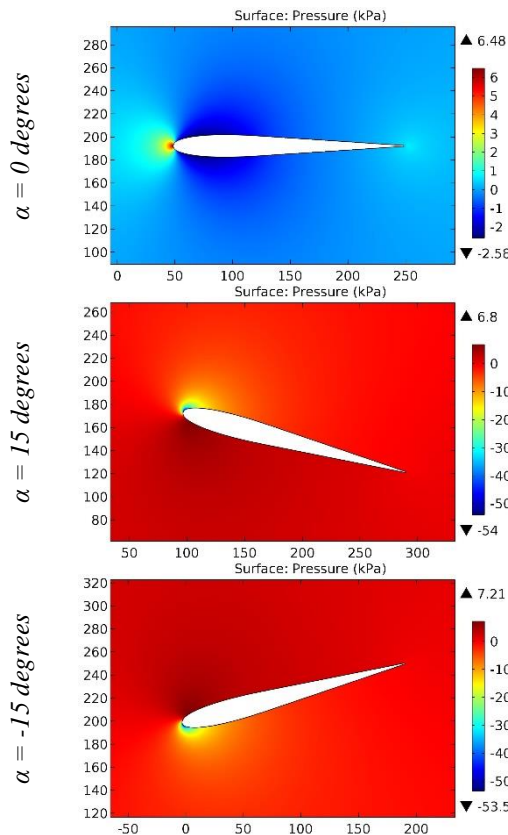


Figure 68. The pressure contours on the surfaces of the Bell AH-1 airfoil.

Impact Factor:

ISRA (India)	= 6.317	SIS (USA)	= 0.912	ICV (Poland)	= 6.630
ISI (Dubai, UAE)	= 1.582	РИНЦ (Russia)	= 3.939	PIF (India)	= 1.940
GIF (Australia)	= 0.564	ESJI (KZ)	= 9.035	IBI (India)	= 4.260
JIF	= 1.500	SJIF (Morocco)	= 7.184	OAJI (USA)	= 0.350

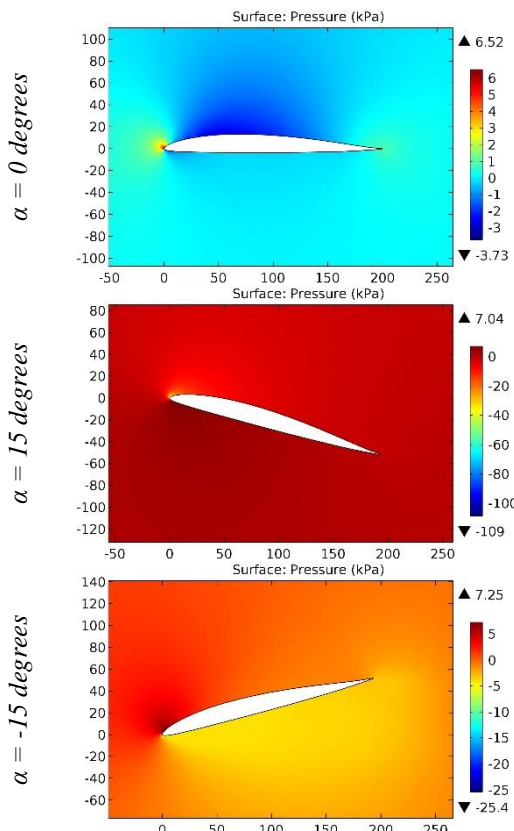


Figure 69. The pressure contours on the surfaces of the BELL-WORTMANN FX 69-H-083 airfoil.

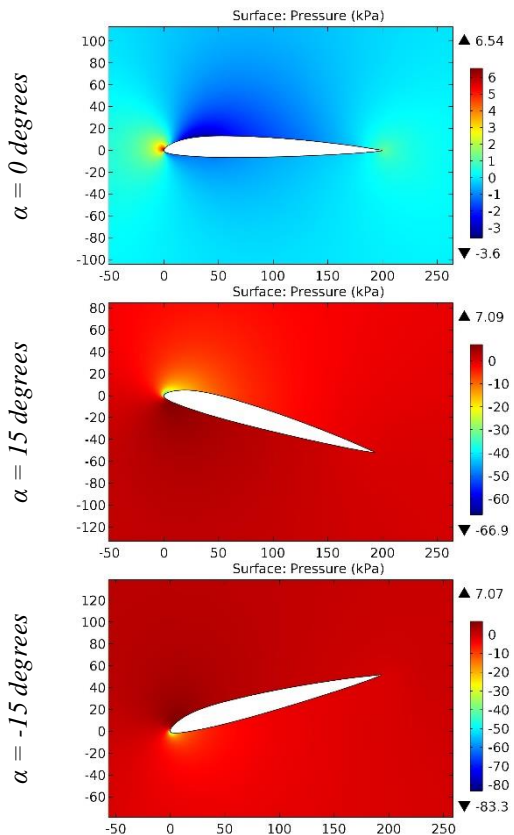


Figure 70. The pressure contours on the surfaces of the BELL-WORTMANN FX 69-H-098 airfoil.

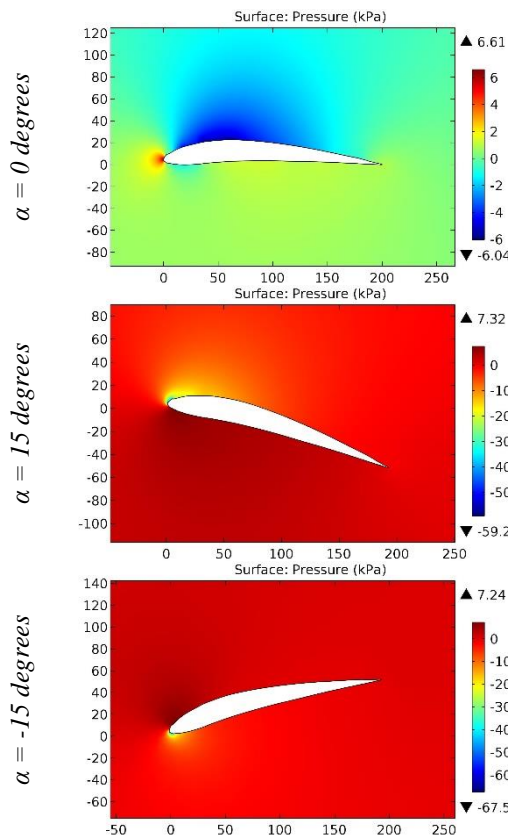


Figure 71. The pressure contours on the surfaces of the Benedek 10355 B airfoil.

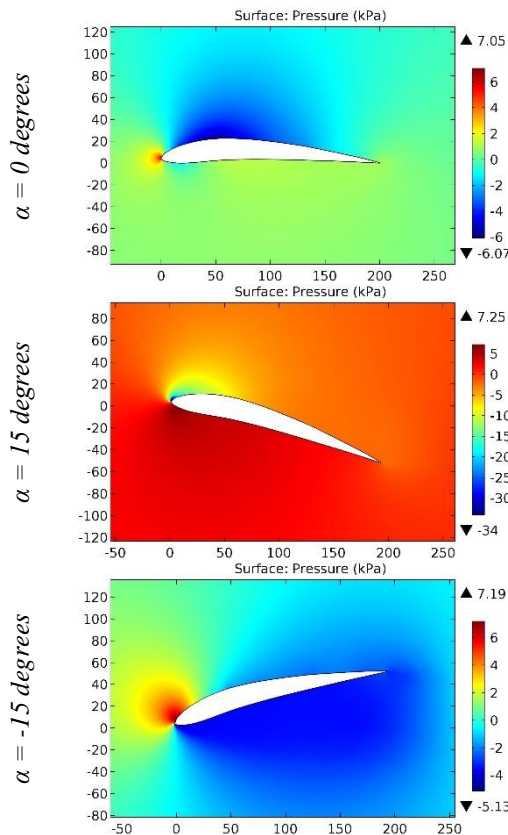


Figure 72. The pressure contours on the surfaces of the Benedek 1053 B airfoil.

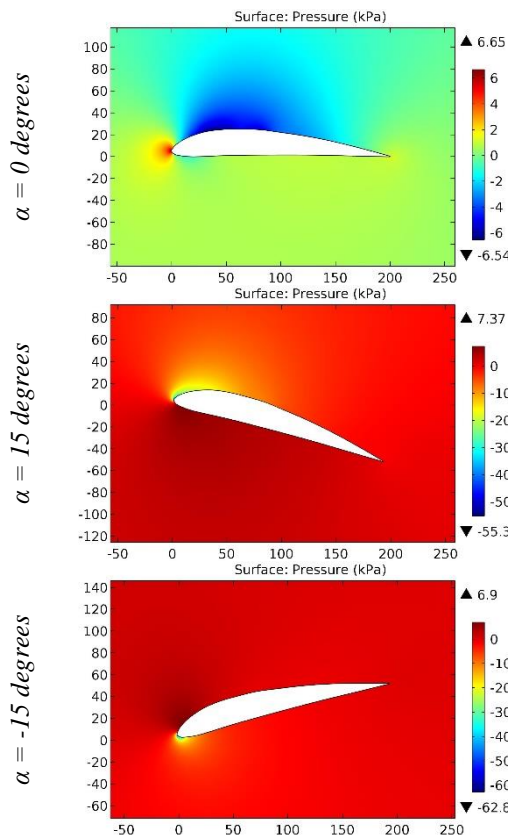


Figure 73. The pressure contours on the surfaces of the Benedek 12355 B airfoil.

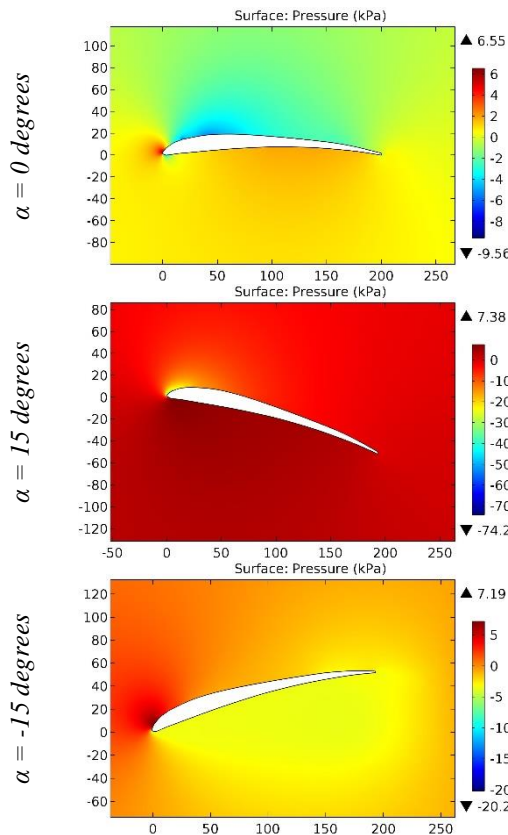


Figure 74. The pressure contours on the surfaces of the Benedek 7406 F airfoil.

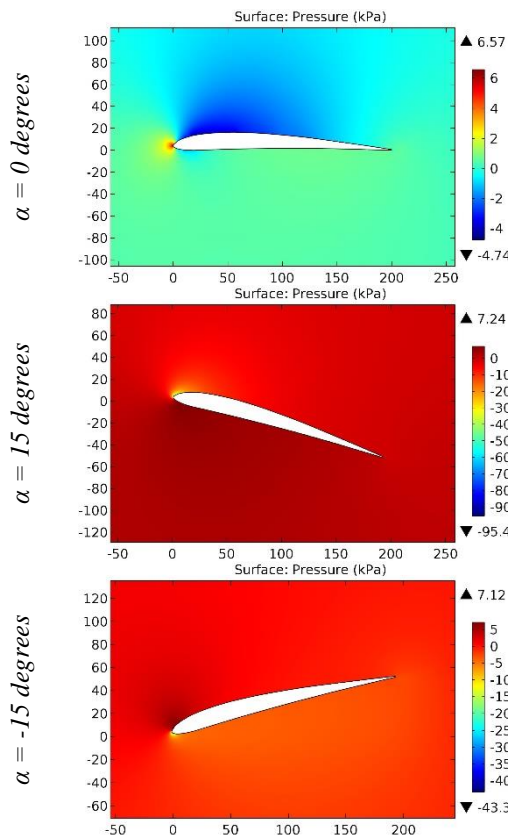


Figure 75. The pressure contours on the surfaces of the Benedek 8353 B-2 airfoil.

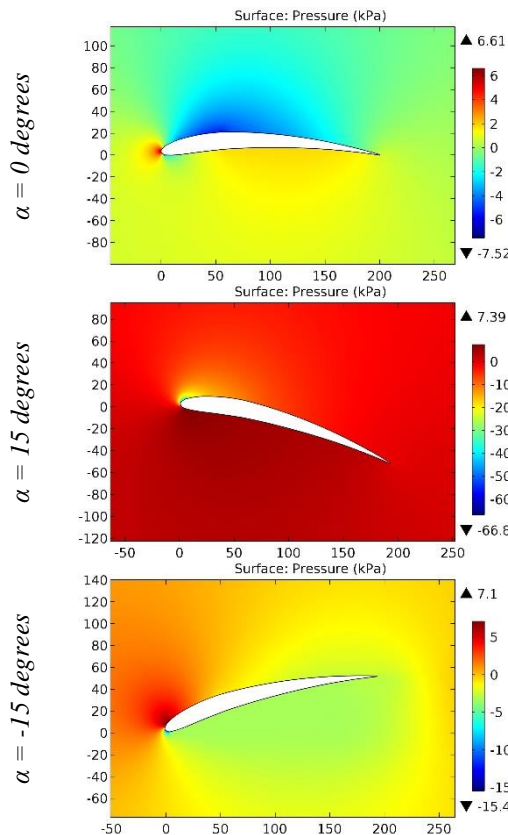


Figure 76. The pressure contours on the surfaces of the Benedek 8405 A airfoil.

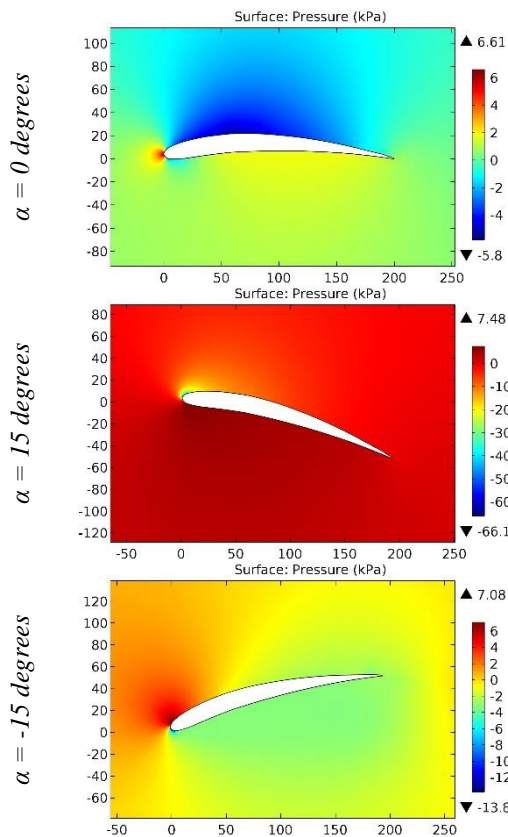


Figure 77. The pressure contours on the surfaces of the Benedek 8406 B airfoil.

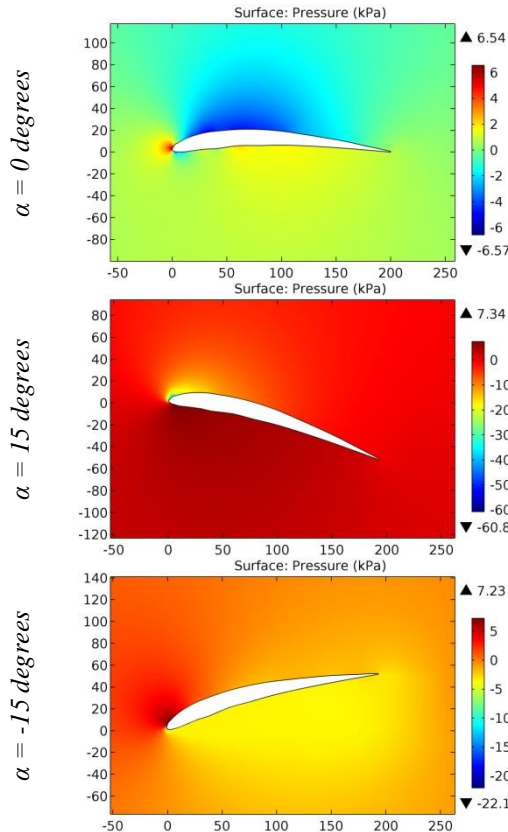


Figure 78. The pressure contours on the surfaces of the Benedek 8406 C airfoil.

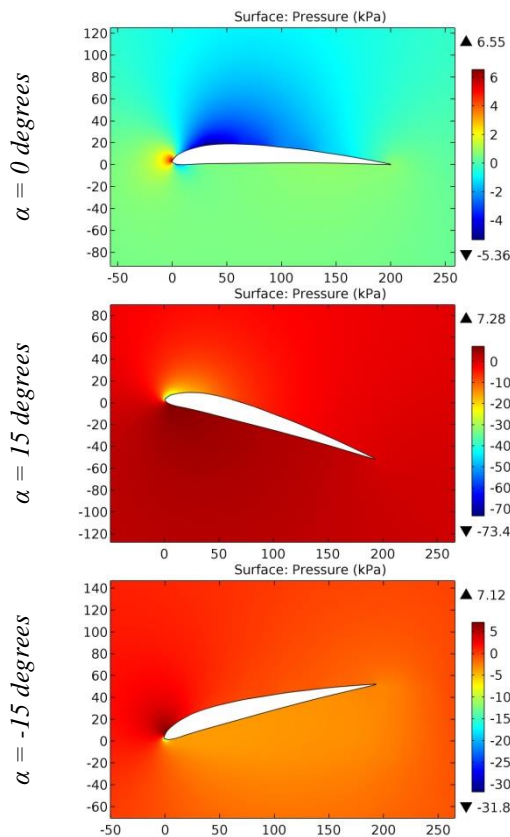


Figure 79. The pressure contours on the surfaces of the Benedek 9304 B airfoil.

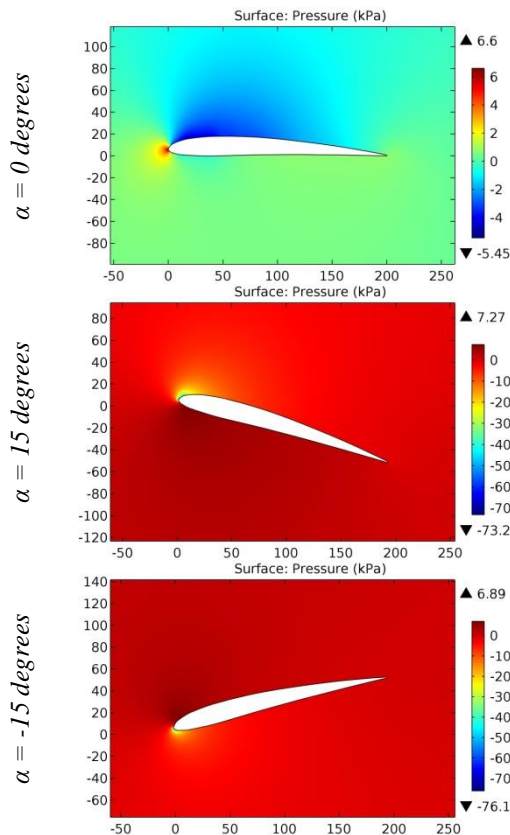


Figure 80. The pressure contours on the surfaces of the Benedek 9403 B airfoil.

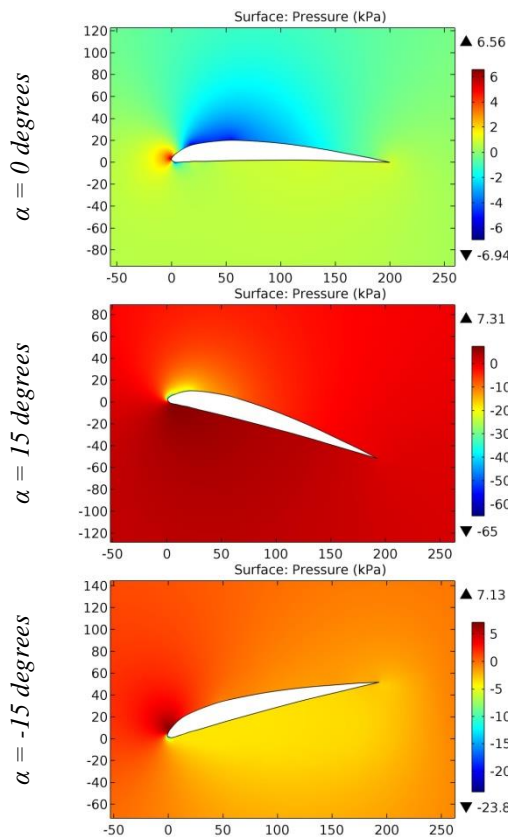


Figure 81. The pressure contours on the surfaces of the Benedek 9404 B airfoil.

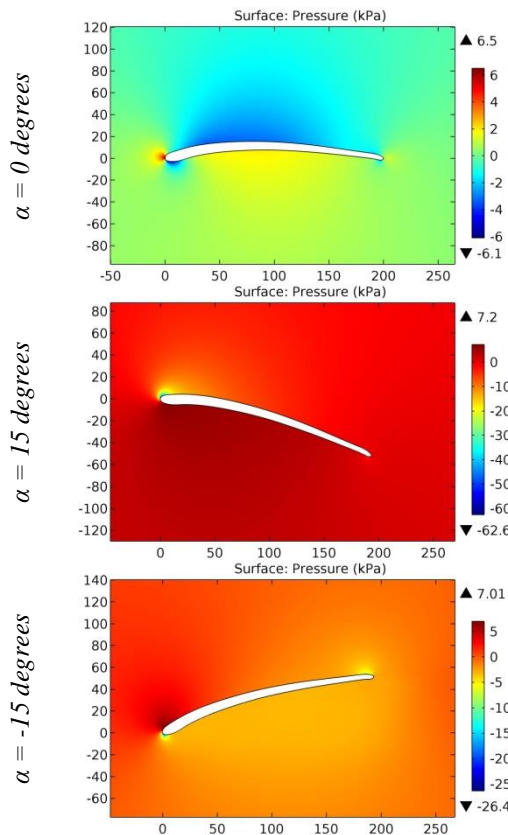


Figure 82. The pressure contours on the surfaces of the Bergey BW-3 (smoothed) airfoil.

Impact Factor:

ISRA (India)	= 6.317	SIS (USA)	= 0.912	ICV (Poland)	= 6.630
ISI (Dubai, UAE)	= 1.582	РИНЦ (Russia)	= 3.939	PIF (India)	= 1.940
GIF (Australia)	= 0.564	ESJI (KZ)	= 9.035	IBI (India)	= 4.260
JIF	= 1.500	SJIF (Morocco)	= 7.184	OAJI (USA)	= 0.350

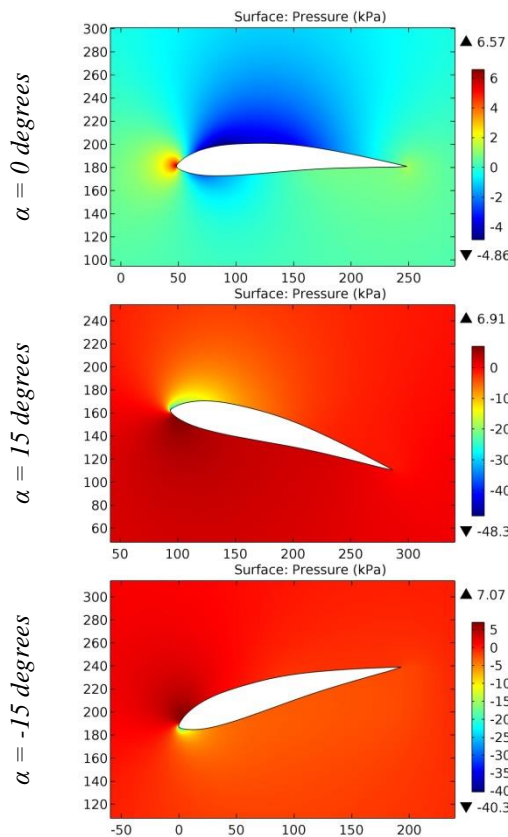


Figure 83. The pressure contours on the surfaces of the Blanchard WB135/35 airfoil.

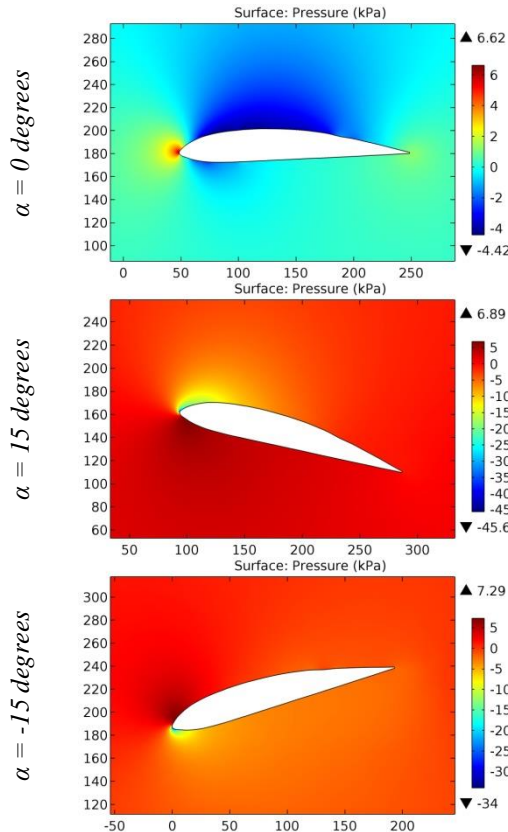


Figure 84. The pressure contours on the surfaces of the Blanchard WB140/35/FB airfoil.

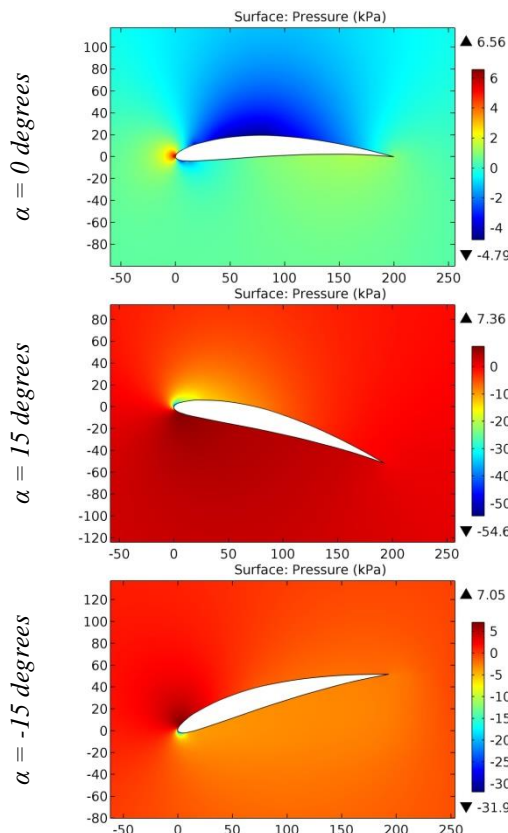


Figure 85. The pressure contours on the surfaces of the BO 545-310 airfoil.

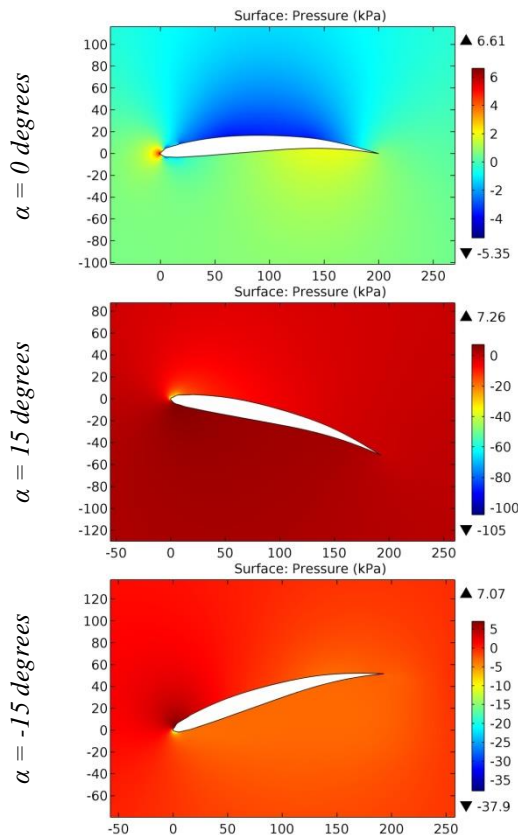


Figure 86. The pressure contours on the surfaces of the BO 560-38 airfoil.

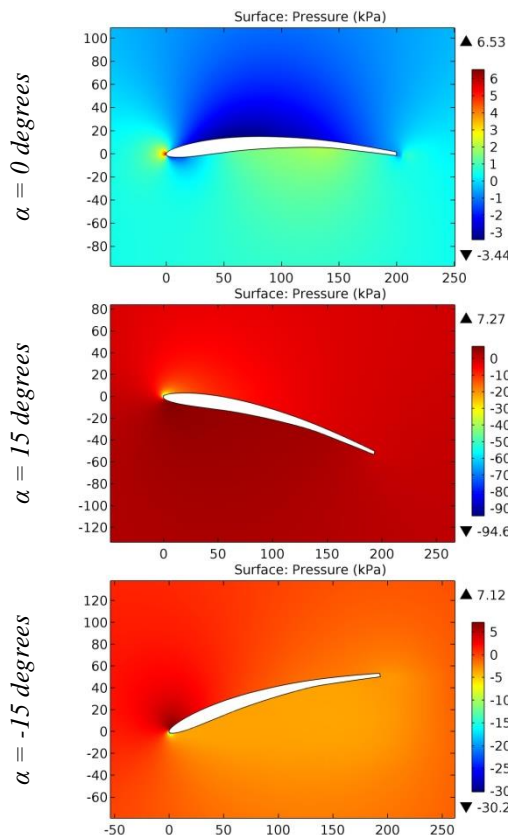


Figure 87. The pressure contours on the surfaces of the BOBWHITE airfoil.

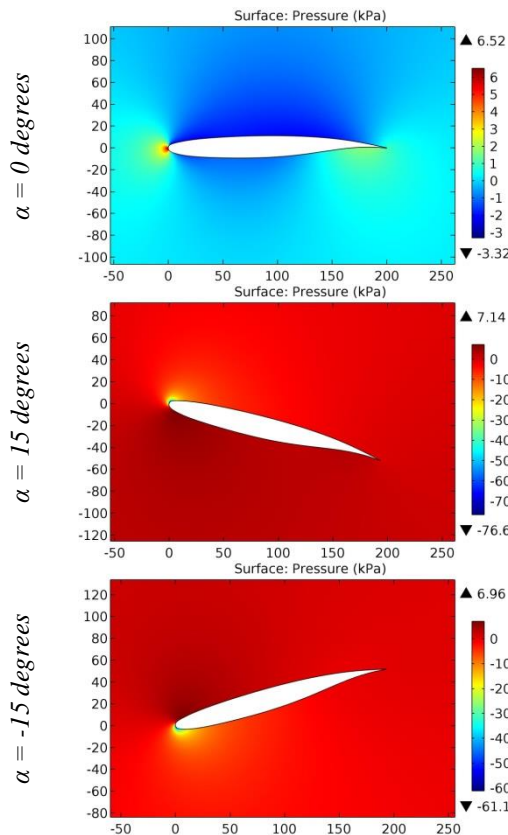


Figure 88. The pressure contours on the surfaces of the BOEING airfoil.

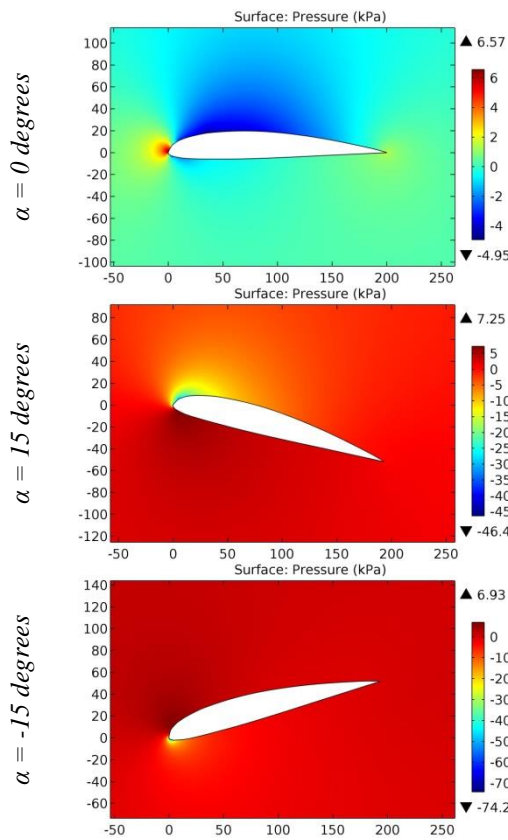


Figure 89. The pressure contours on the surfaces of the BOEING 103 airfoil.

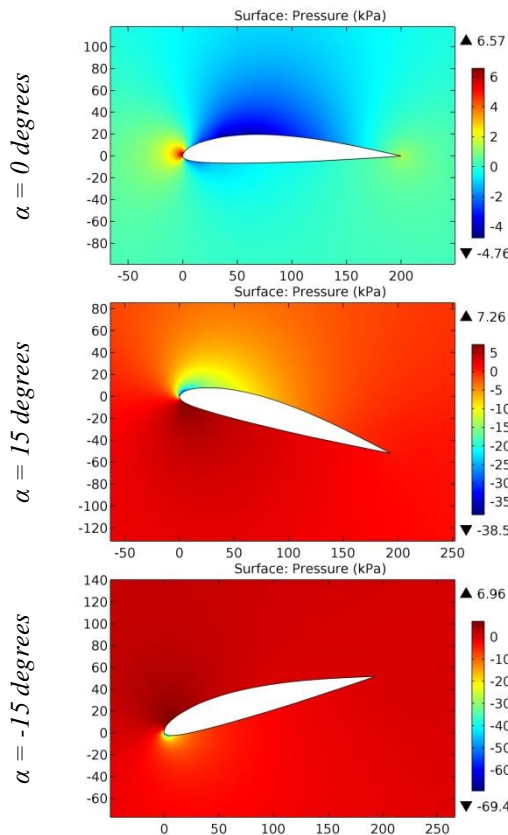


Figure 90. The pressure contours on the surfaces of the BOEING 106 airfoil.

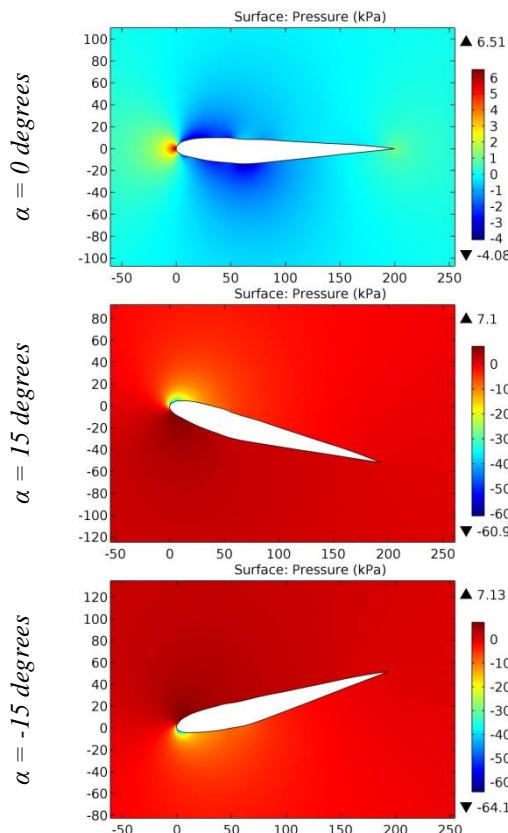


Figure 91. The pressure contours on the surfaces of the BOEING 707 ,08 SPAN airfoil.

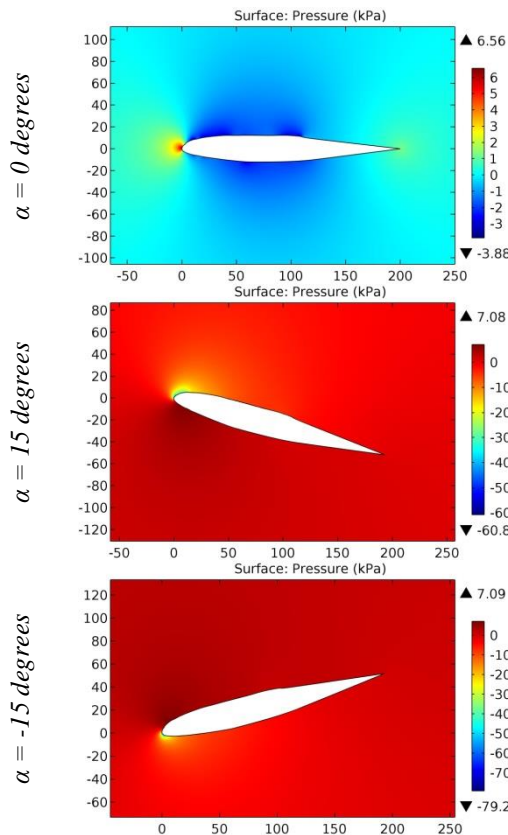


Figure 92. The pressure contours on the surfaces of the BOEING 707 ,19 SPAN airfoil.

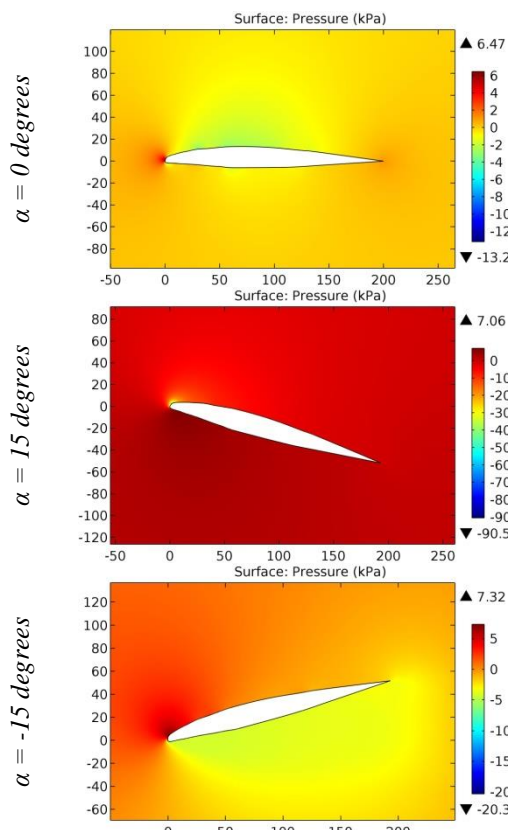


Figure 93. The pressure contours on the surfaces of the BOEING 707 ,40 SPAN airfoil.

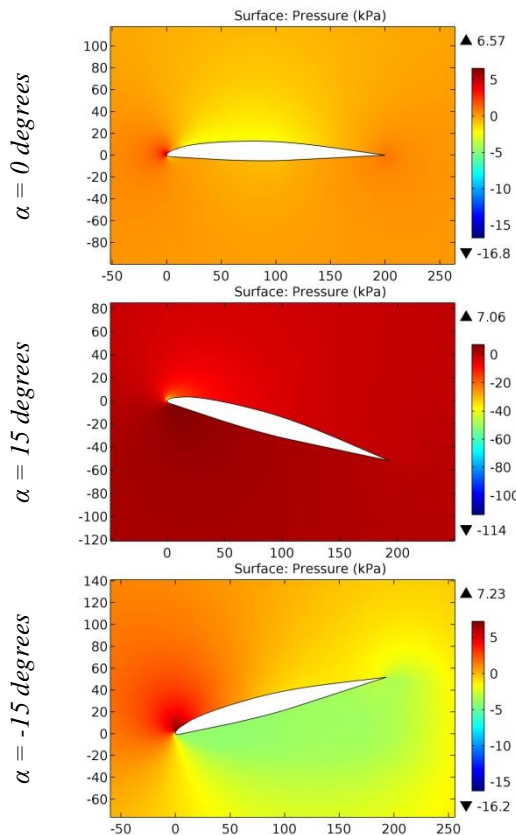


Figure 94. The pressure contours on the surfaces of the BOEING 707 ,54 SPAN airfoil.

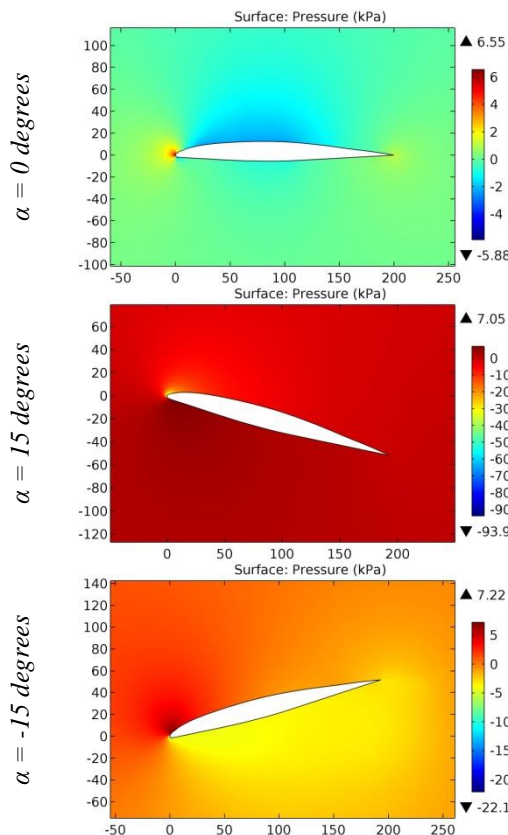


Figure 95. The pressure contours on the surfaces of the BOEING 707 .99 SPAN airfoil.

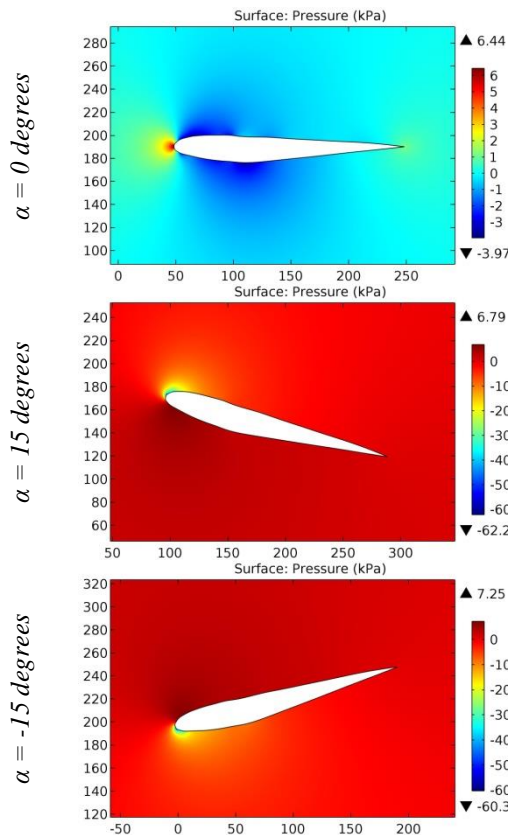


Figure 96. The pressure contours on the surfaces of the BOEING 707 .08 SPAN AIRFOIL.

ISRA (India) = 6.317	SIS (USA) = 0.912	ICV (Poland) = 6.630
ISI (Dubai, UAE) = 1.582	РИНЦ (Russia) = 3.939	PIF (India) = 1.940
GIF (Australia) = 0.564	ESJI (KZ) = 9.035	IBI (India) = 4.260
JIF = 1.500	SJIF (Morocco) = 7.184	OAJI (USA) = 0.350

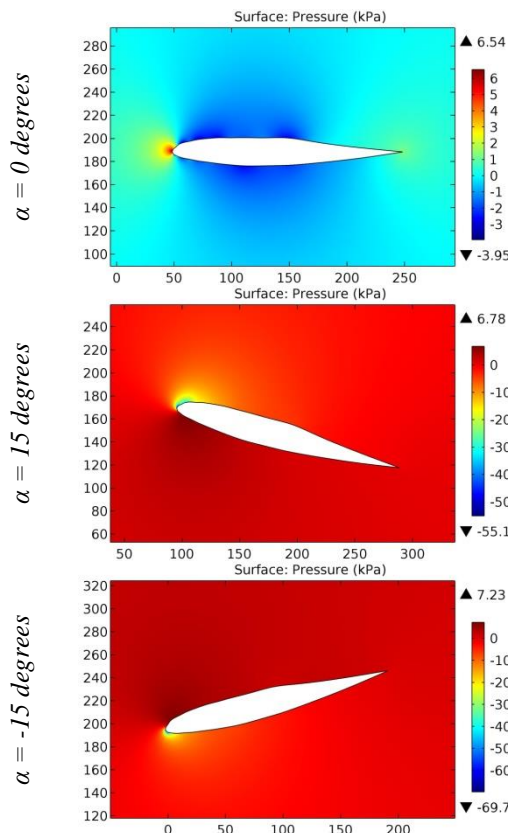


Figure 97. The pressure contours on the surfaces of the BOEING 707 .19 SPAN AIRFOIL.

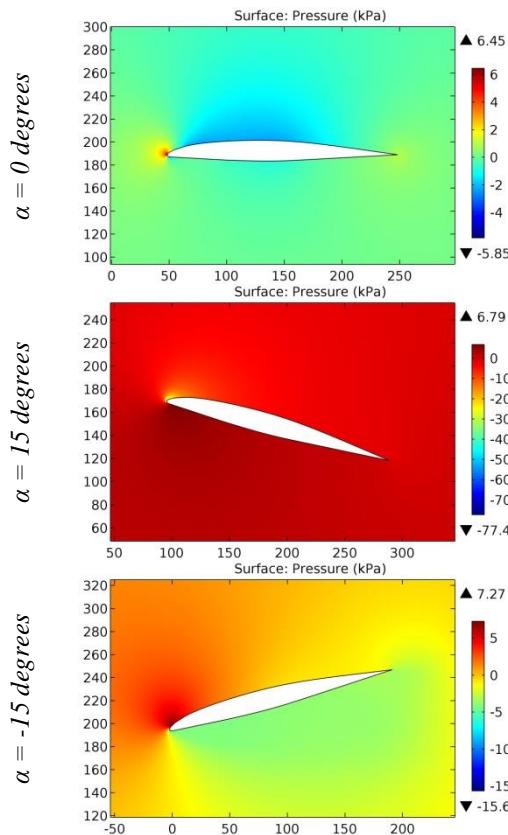


Figure 98. The pressure contours on the surfaces of the BOEING 707 .54 SPAN AIRFOIL.

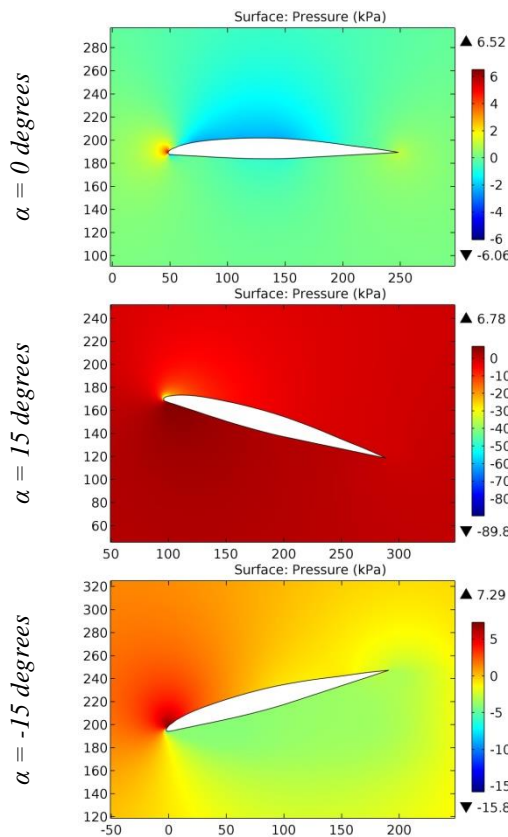


Figure 99. The pressure contours on the surfaces of the BOEING 707 .99 SPAN AIRFOIL.

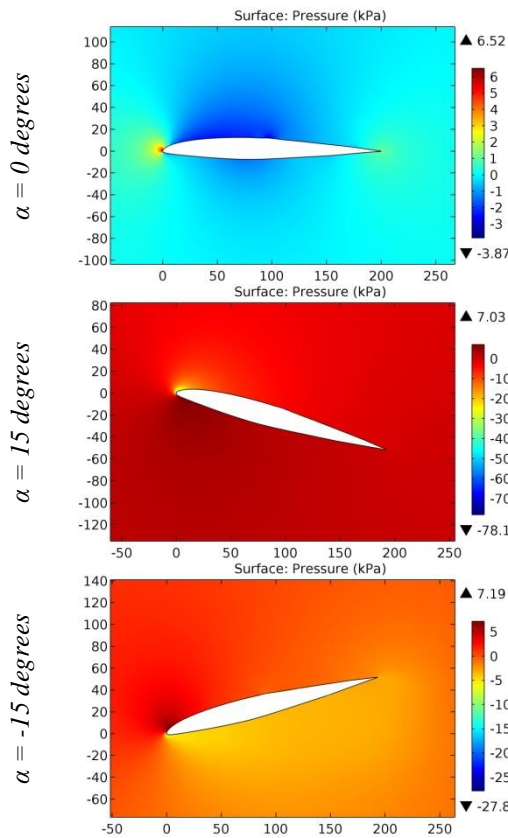


Figure 100. The pressure contours on the surfaces of the BOEING 737 MIDSPAN airfoil.

ISRA (India)	= 6.317	SIS (USA)	= 0.912	ICV (Poland)	= 6.630
ISI (Dubai, UAE)	= 1.582	РИНЦ (Russia)	= 3.939	PIF (India)	= 1.940
GIF (Australia)	= 0.564	ESJI (KZ)	= 9.035	IBI (India)	= 4.260
JIF	= 1.500	SJIF (Morocco)	= 7.184	OAJI (USA)	= 0.350

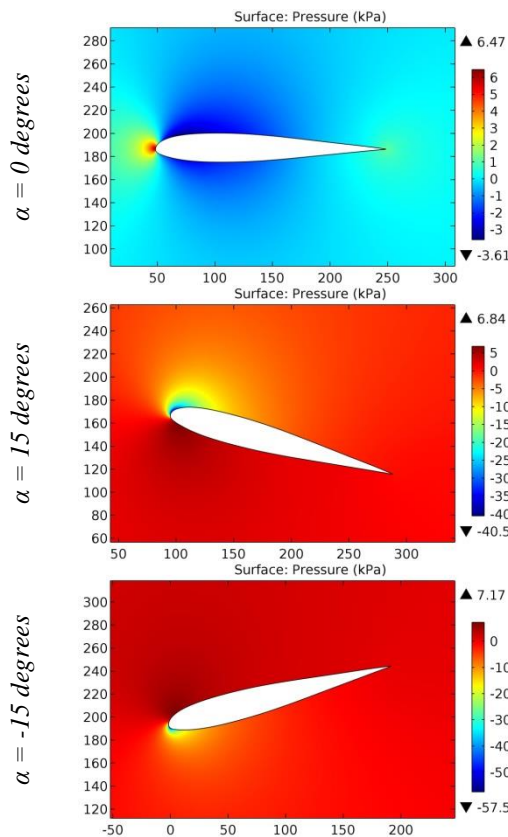


Figure 101. The pressure contours on the surfaces of the BOEING 737 MIDSPAN AIRFOIL.

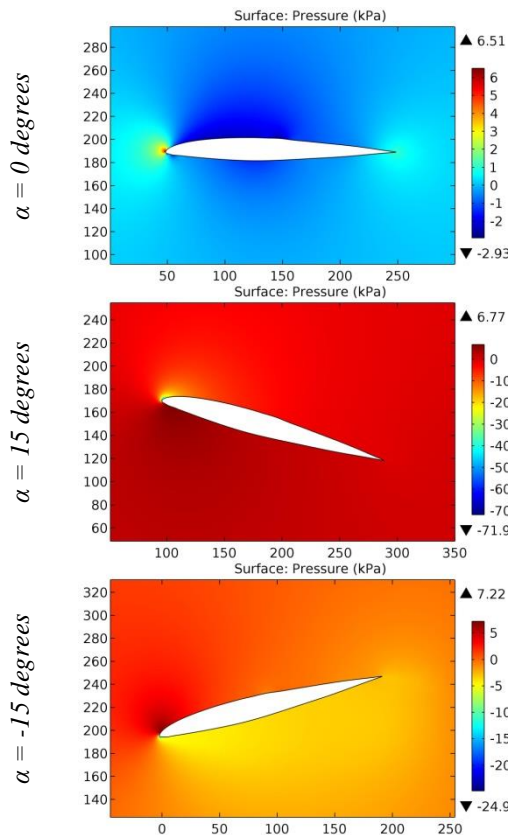


Figure 102. The pressure contours on the surfaces of the BOEING 737 MIDSPAN AIRFOIL-b.

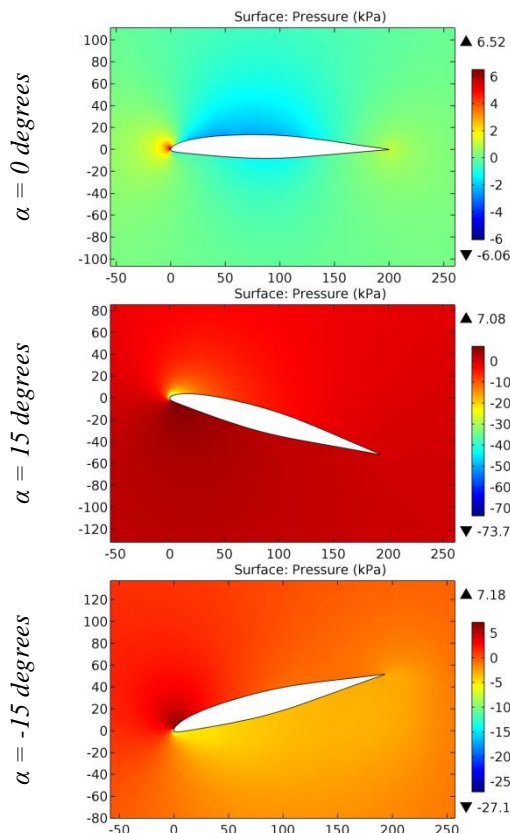


Figure 103. The pressure contours on the surfaces of the BOEING 737 OUTBOARD airfoil.

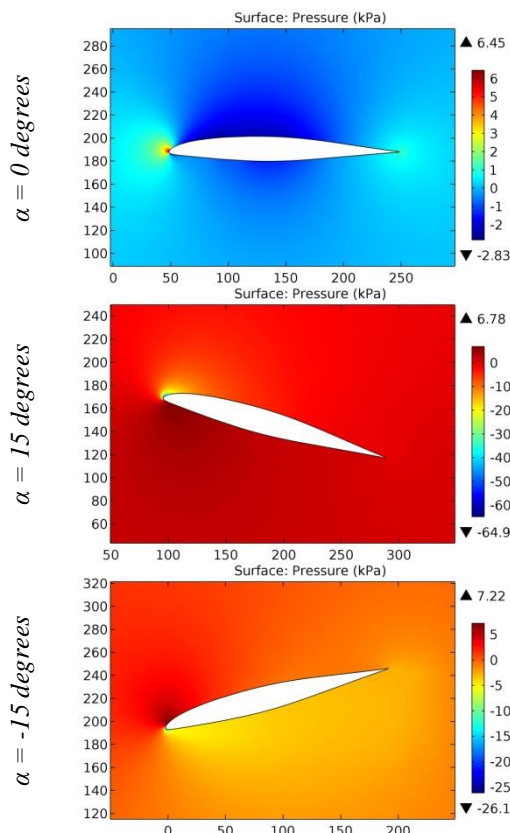


Figure 104. The pressure contours on the surfaces of the BOEING 737 OUTBOARD AIRFOIL.

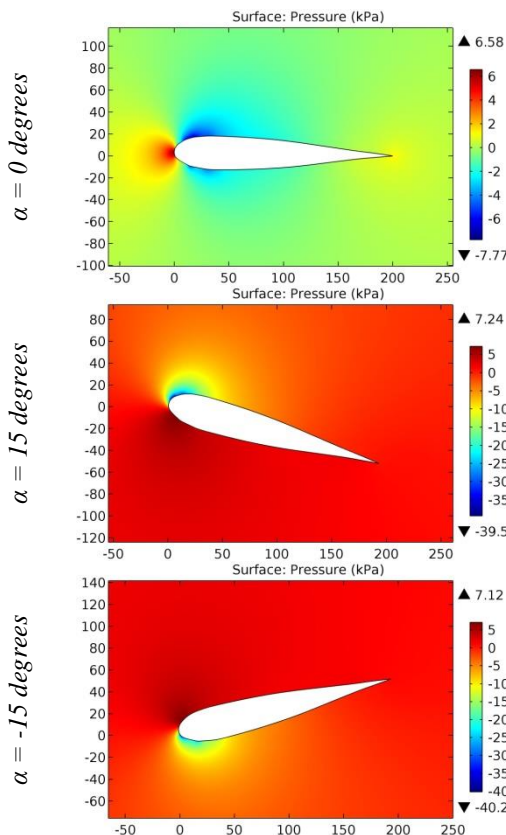


Figure 105. The pressure contours on the surfaces of the BOEING 737 ROOT airfoil.

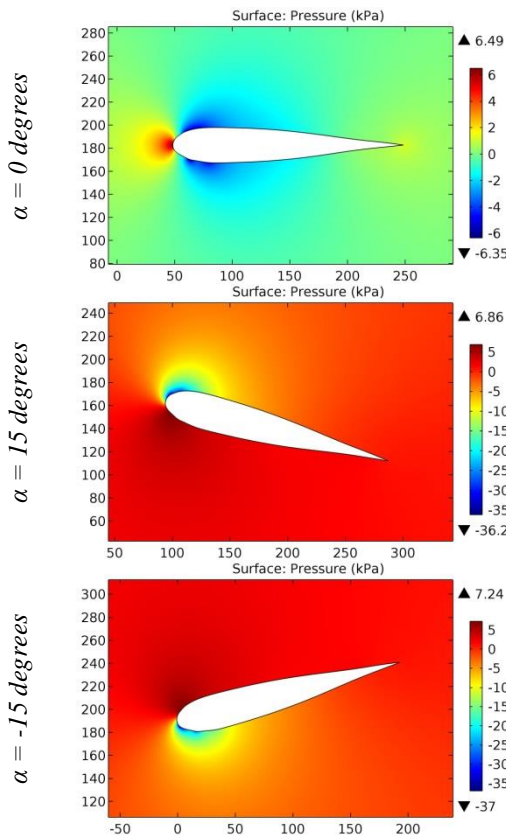


Figure 106. The pressure contours on the surfaces of the BOEING 737 AIRFOIL.

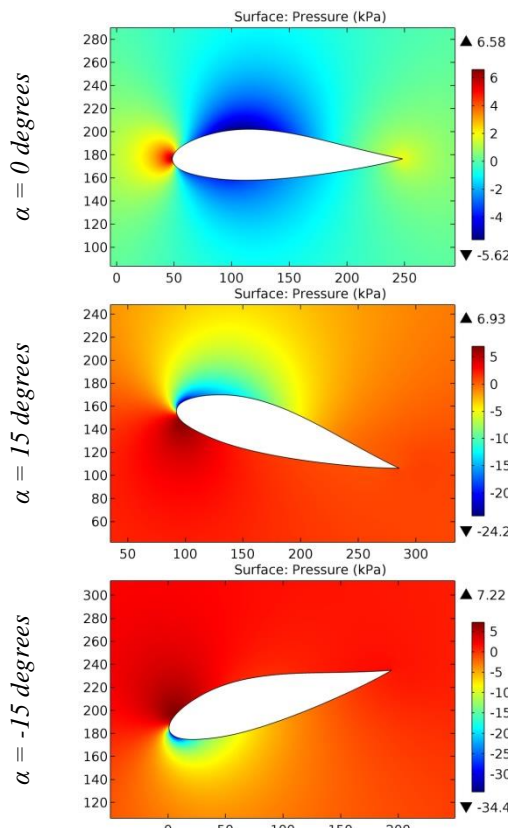


Figure 107. The pressure contours on the surfaces of the Boeing B-29 root airfoil.

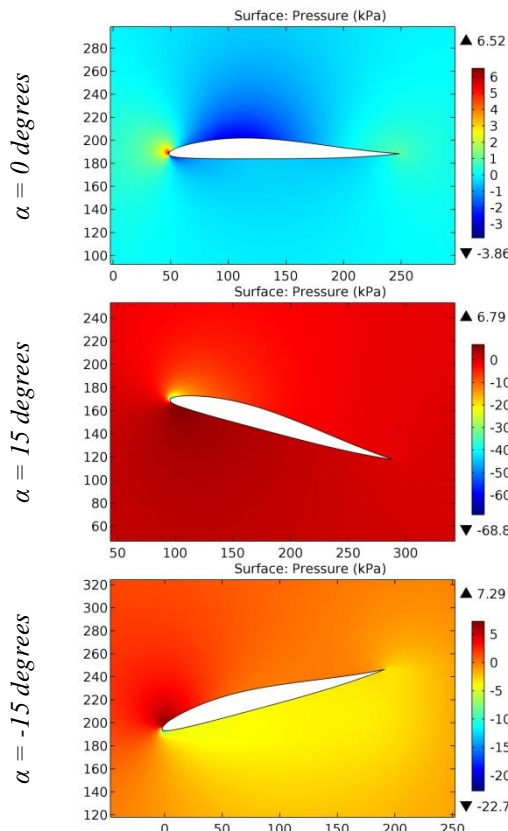


Figure 108. The pressure contours on the surfaces of the Boeing B-29 tip airfoil.

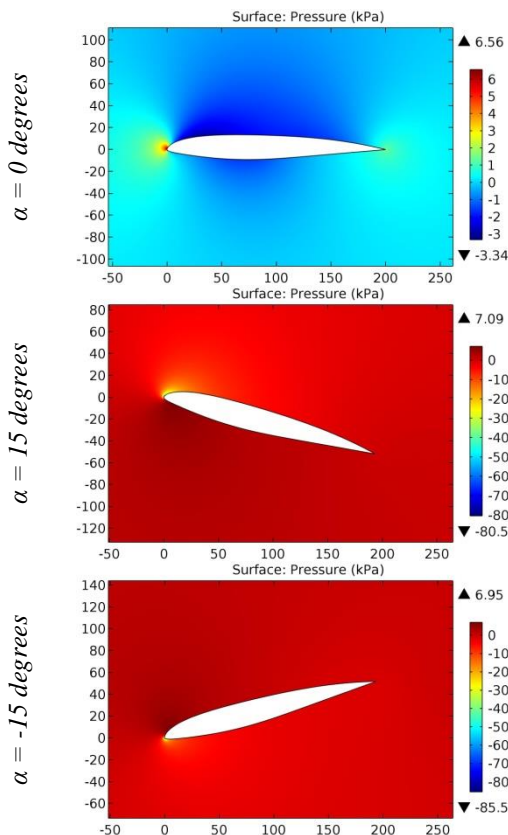


Figure 109. The pressure contours on the surfaces of the BOEING BACXXX airfoil.

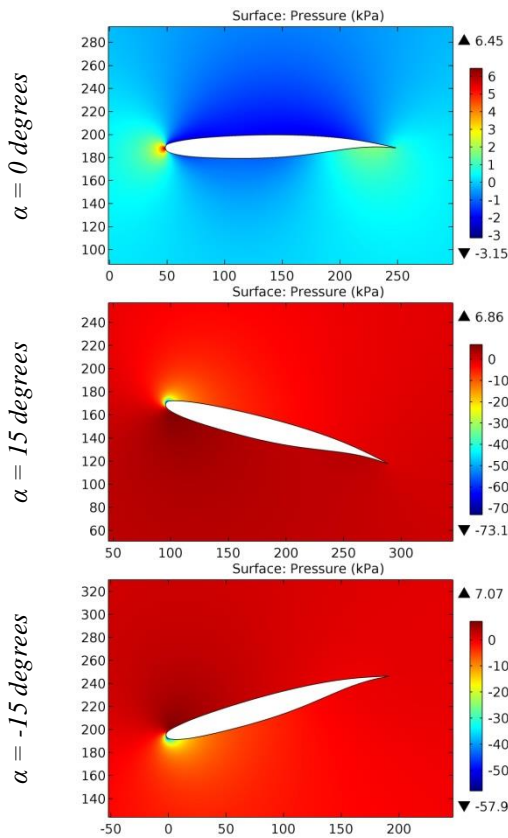


Figure 110. The pressure contours on the surfaces of the Boeing Commercial Airplane Company airfoil J.

ISRA (India) = 6.317	SIS (USA) = 0.912	ICV (Poland) = 6.630
ISI (Dubai, UAE) = 1.582	РИНЦ (Russia) = 3.939	PIF (India) = 1.940
GIF (Australia) = 0.564	ESJI (KZ) = 9.035	IBI (India) = 4.260
JIF = 1.500	SJIF (Morocco) = 7.184	OAJI (USA) = 0.350

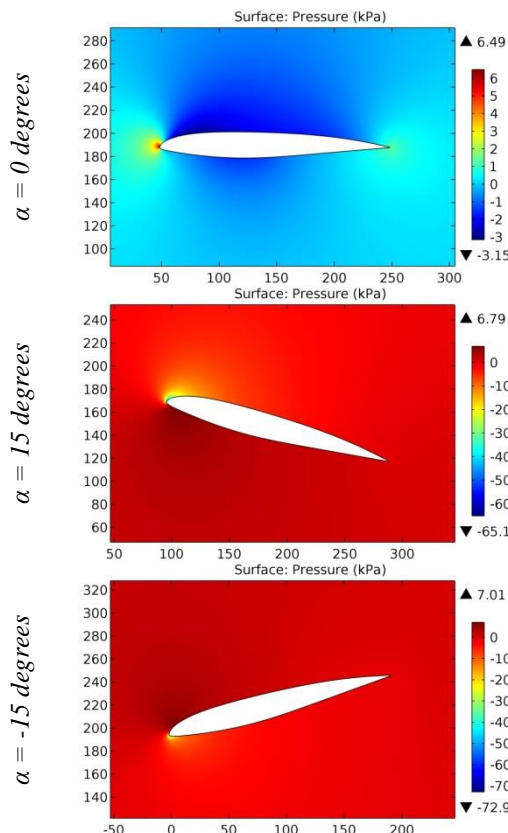


Figure 111. The pressure contours on the surfaces of the Boeing (Commercial Airplane) BACXXX airfoil.

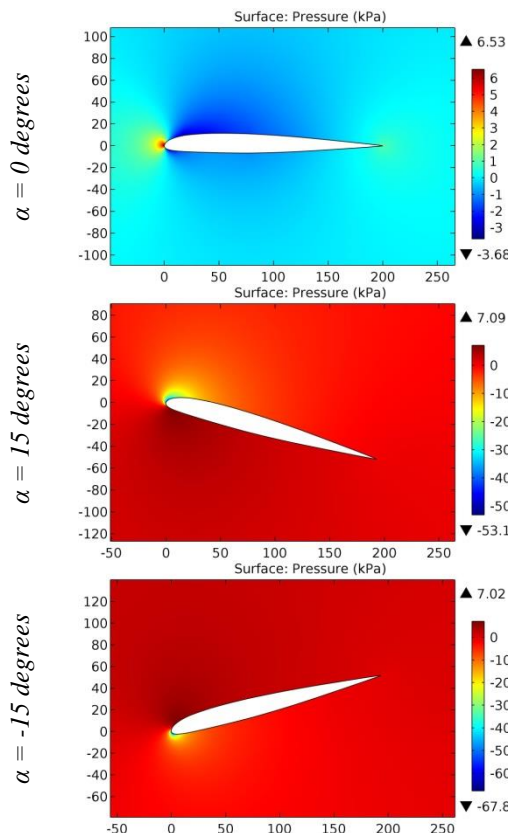


Figure 112. The pressure contours on the surfaces of the BOEING VERTOL V(1,95)3009-1,25 airfoil.

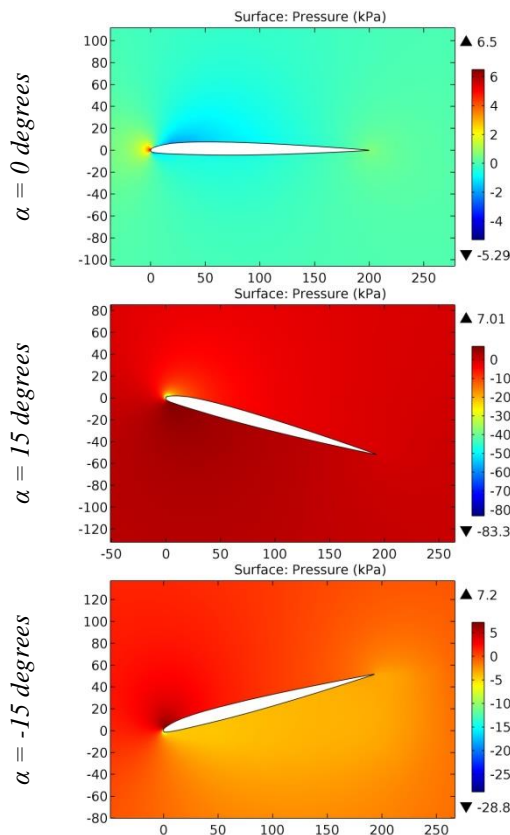


Figure 113. The pressure contours on the surfaces of the BOEING VERTOL V13006-7 airfoil.

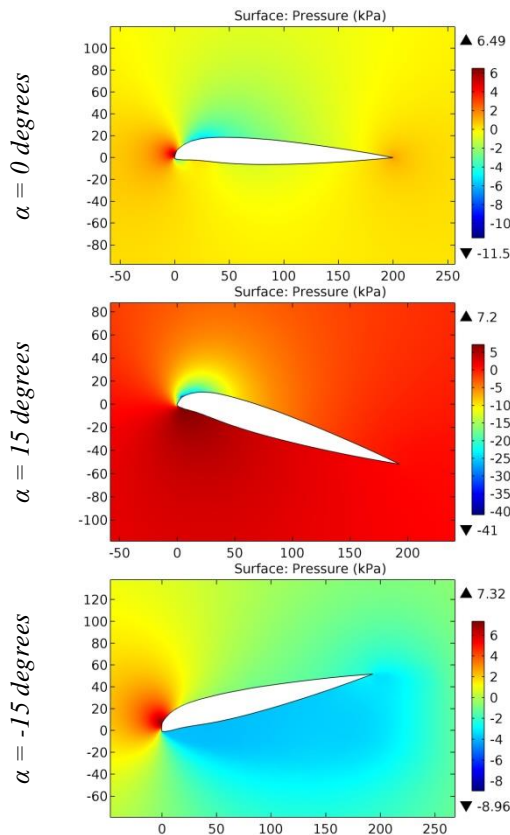


Figure 114. The pressure contours on the surfaces of the BOEING VERTOL V43012-1,58 airfoil.

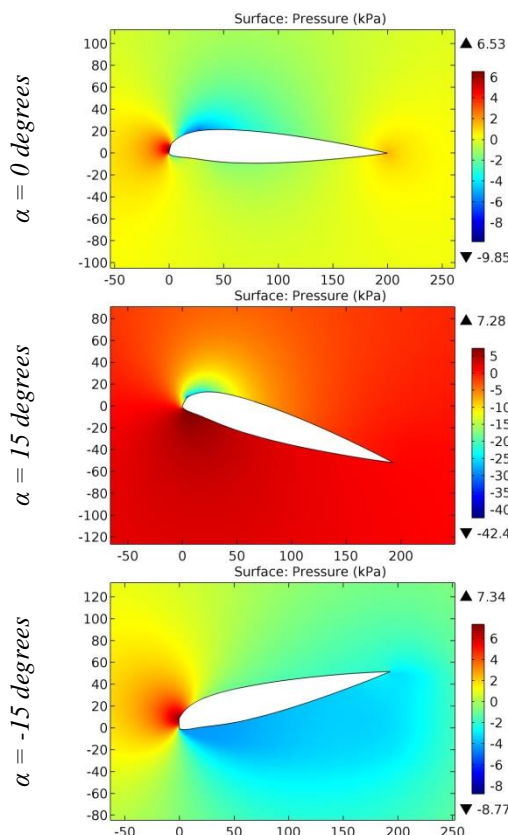


Figure 115. The pressure contours on the surfaces of the BOEING VERTOL V43015-2,48 airfoil.

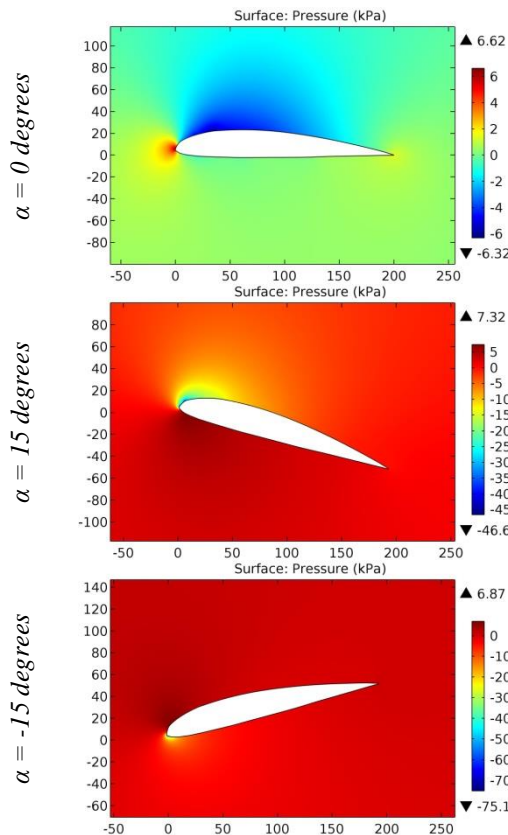


Figure 116. The pressure contours on the surfaces of the BOEING10 airfoil.

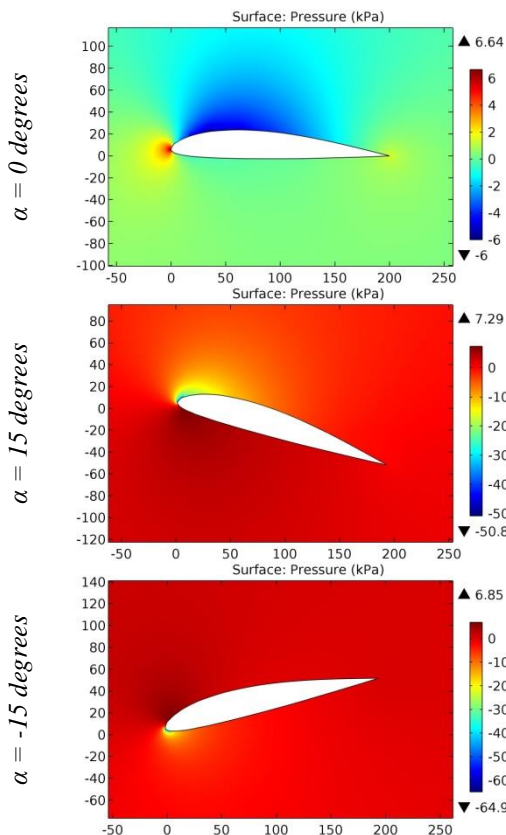


Figure 117. The pressure contours on the surfaces of the BOEING16 airfoil.

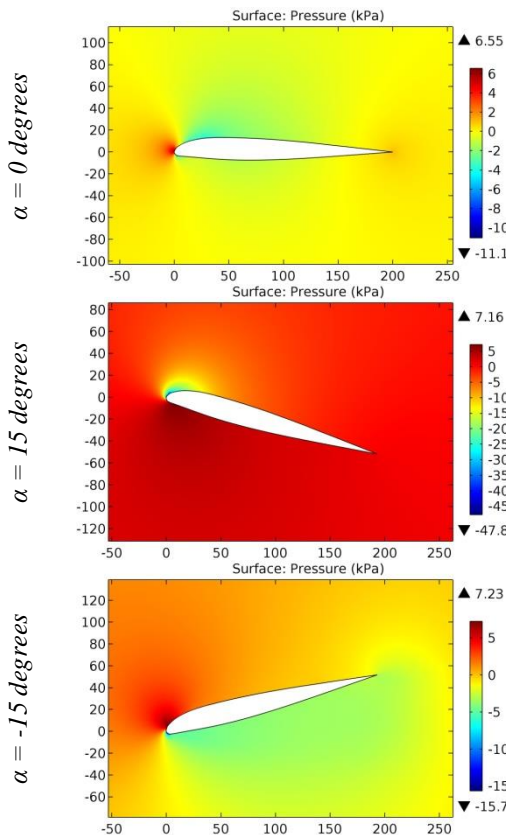


Figure 118. The pressure contours on the surfaces of the BOEING-VERTOL V23010-1,58 airfoil.

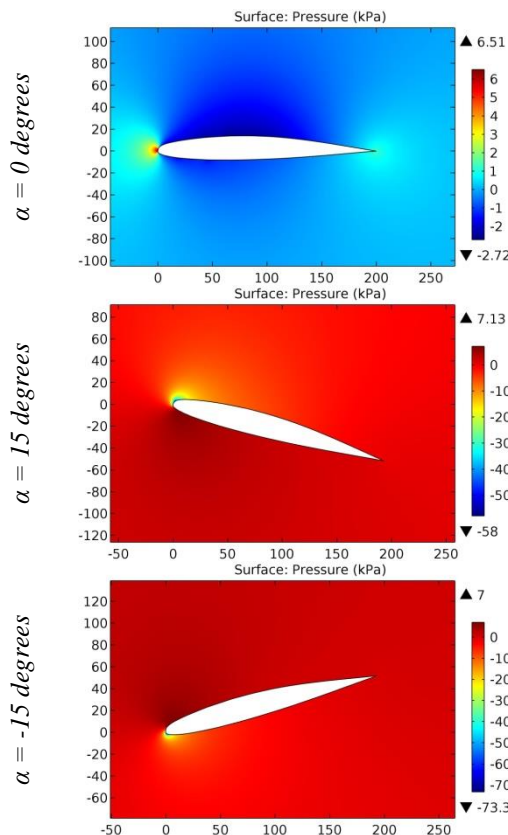


Figure 119. The pressure contours on the surfaces of the BOEING-VERTOL VR-1 airfoil.

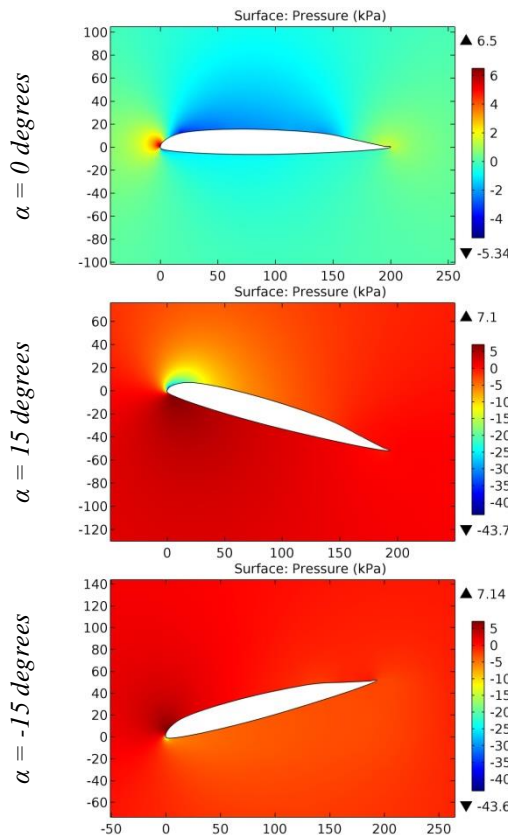


Figure 120. The pressure contours on the surfaces of the BOEING-VERTOL VR-11X airfoil.

ISRA (India) = 6.317	SIS (USA) = 0.912	ICV (Poland) = 6.630
ISI (Dubai, UAE) = 1.582	РИНЦ (Russia) = 3.939	PIF (India) = 1.940
GIF (Australia) = 0.564	ESJI (KZ) = 9.035	IBI (India) = 4.260
JIF = 1.500	SJIF (Morocco) = 7.184	OAJI (USA) = 0.350

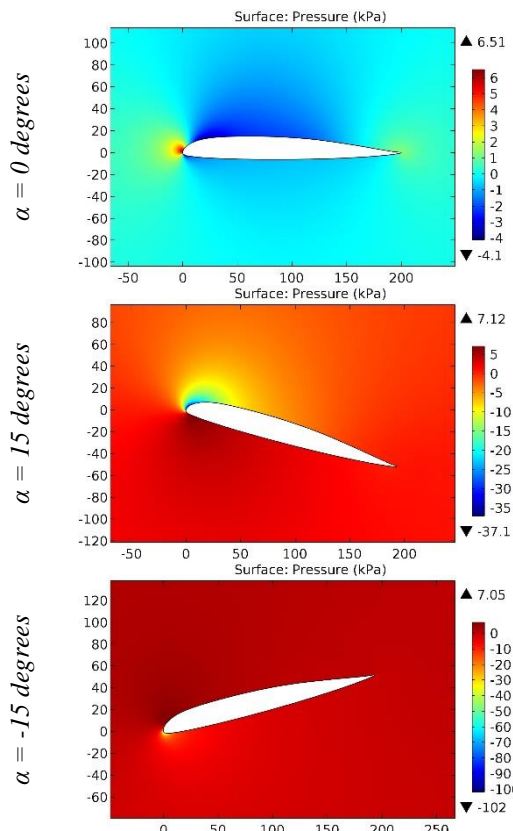


Figure 121. The pressure contours on the surfaces of the BOEING-VERTOL VR-12 airfoil.

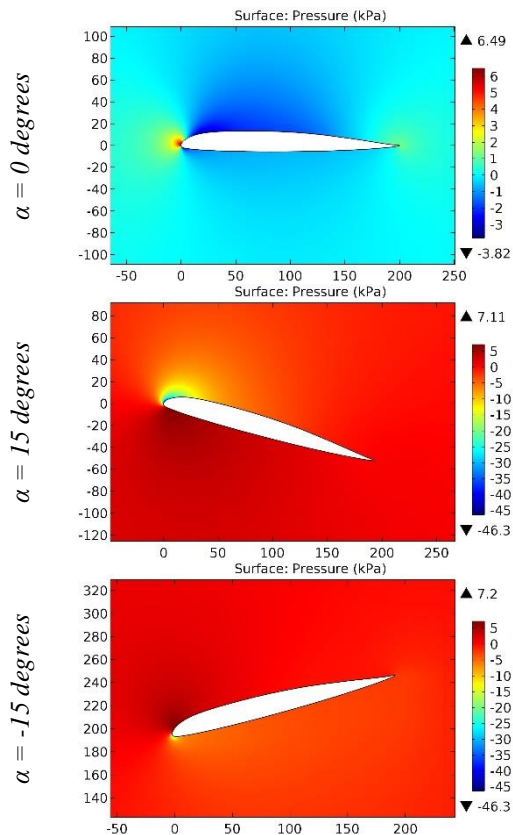


Figure 122. The pressure contours on the surfaces of the BOEING-VERTOL VR-13 airfoil.

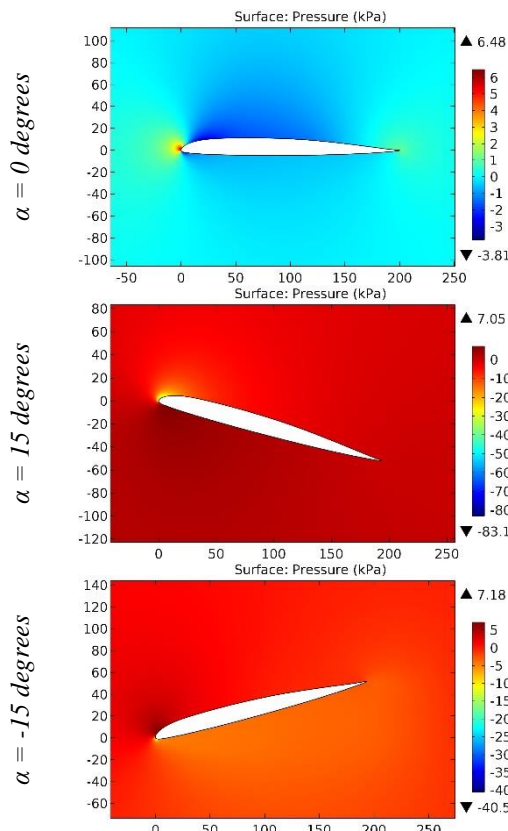


Figure 123. The pressure contours on the surfaces of the BOEING-VERTOL VR-14 airfoil.

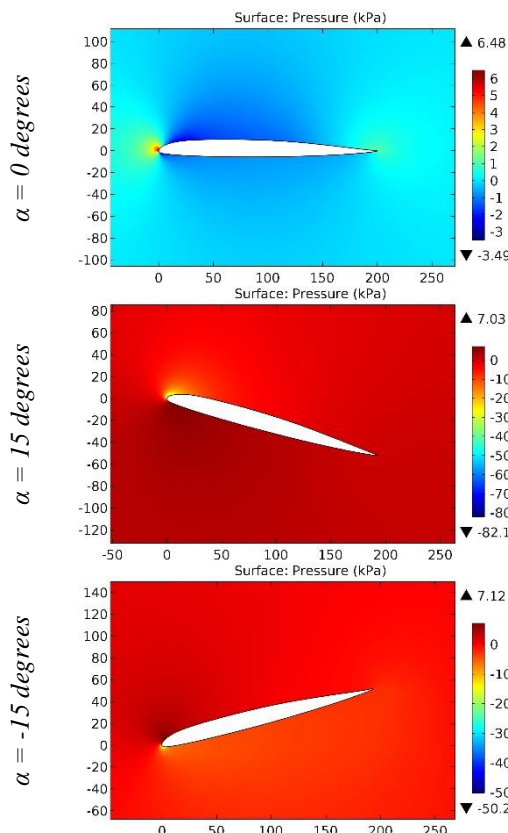


Figure 124. The pressure contours on the surfaces of the BOEING-VERTOL VR-15 airfoil.

ISRA (India)	= 6.317	SIS (USA)	= 0.912	ICV (Poland)	= 6.630
ISI (Dubai, UAE)	= 1.582	РИНЦ (Russia)	= 3.939	PIF (India)	= 1.940
GIF (Australia)	= 0.564	ESJI (KZ)	= 9.035	IBI (India)	= 4.260
JIF	= 1.500	SJIF (Morocco)	= 7.184	OAJI (USA)	= 0.350

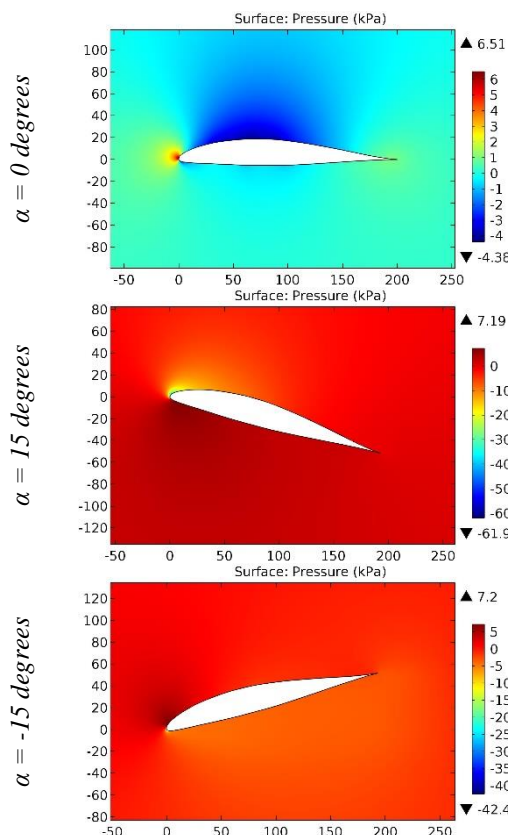


Figure 125. The pressure contours on the surfaces of the BOEING-VERTOL VR-5 airfoil.

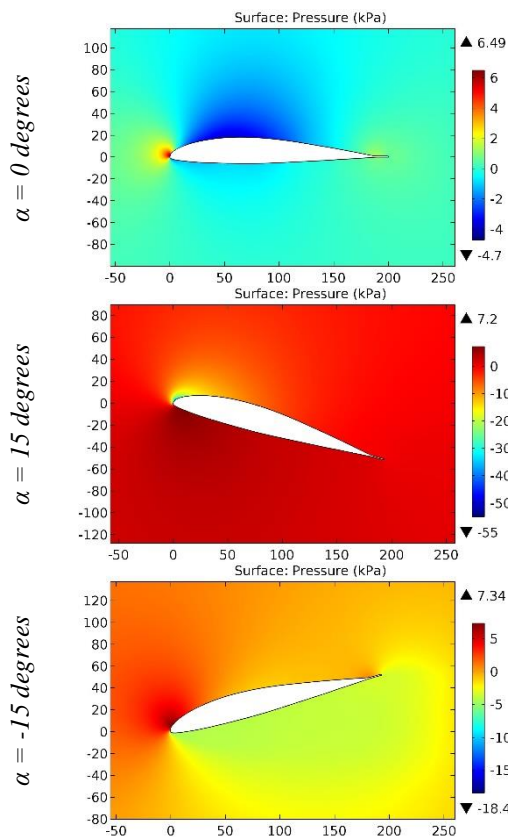


Figure 126. The pressure contours on the surfaces of the BOEING-VERTOL VR-7 airfoil.

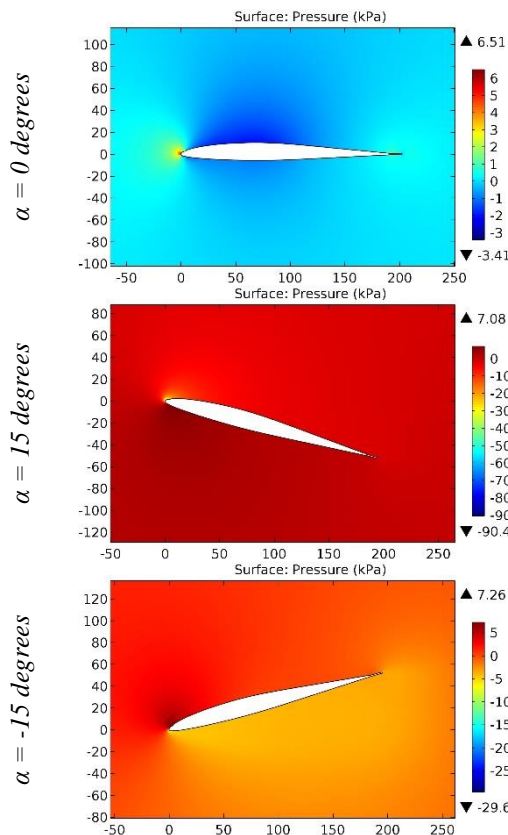


Figure 127. The pressure contours on the surfaces of the BOEING-VERTOL VR-8 airfoil.

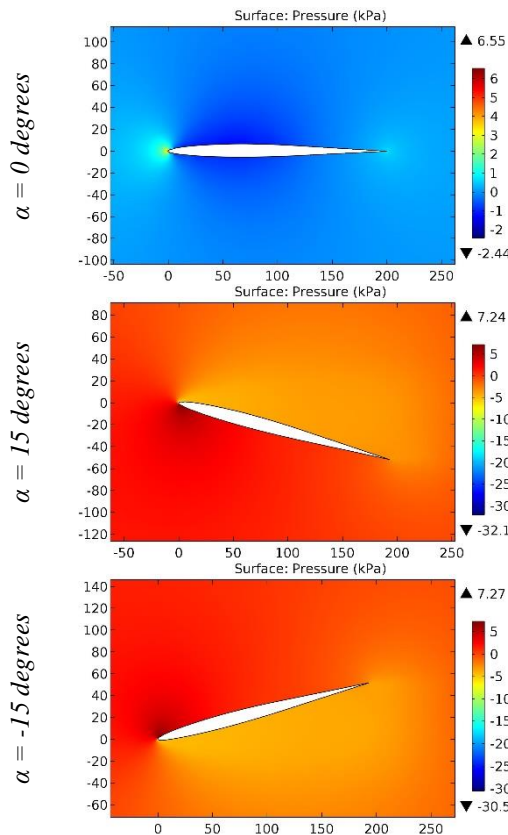


Figure 128. The pressure contours on the surfaces of the BOEING-VERTOL VR-9 airfoil.

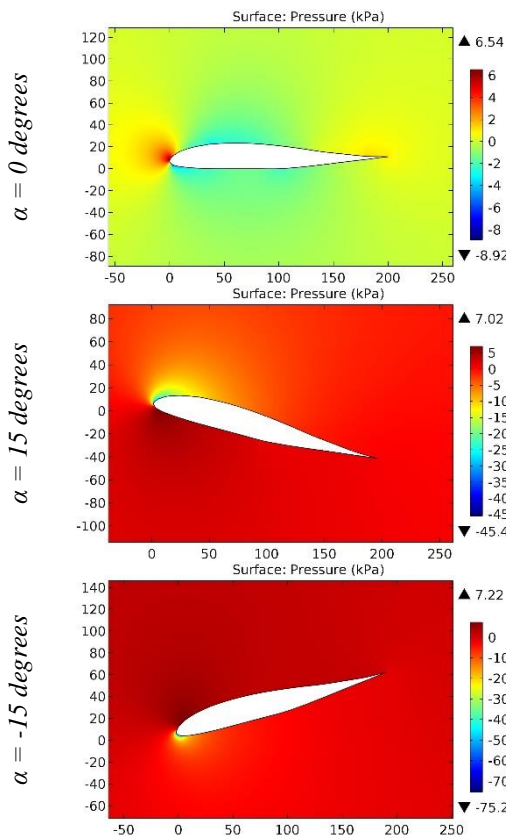


Figure 129. The pressure contours on the surfaces of the Borge' B3 airfoil.

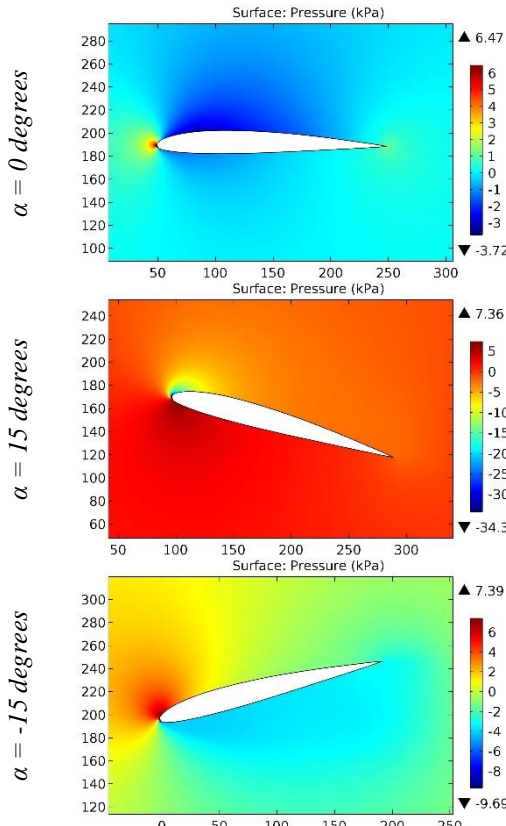


Figure 130. The pressure contours on the surfaces of the BP4D airfoil.

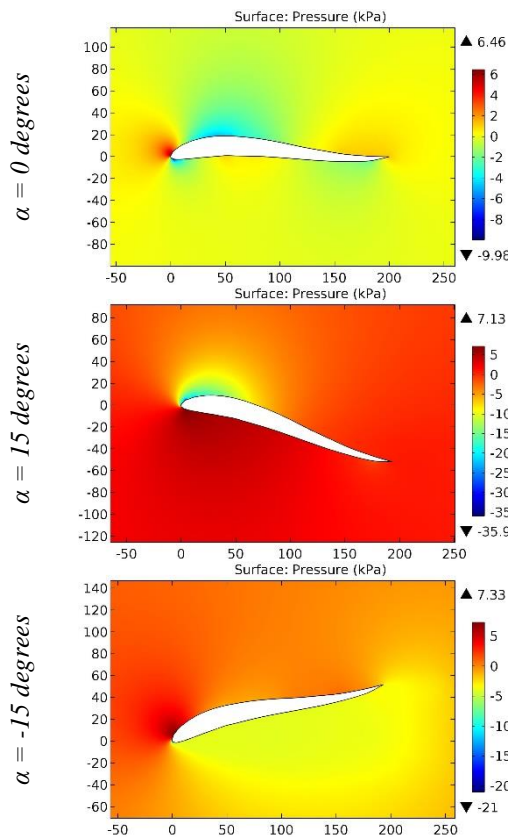


Figure 131. The pressure contours on the surfaces of the Broggini 55509 airfoil.

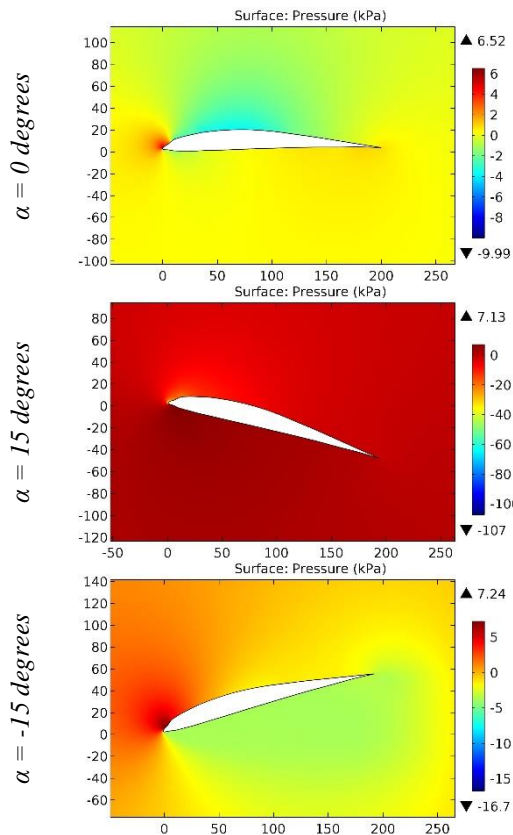


Figure 132. The pressure contours on the surfaces of the Brogely airfoil.

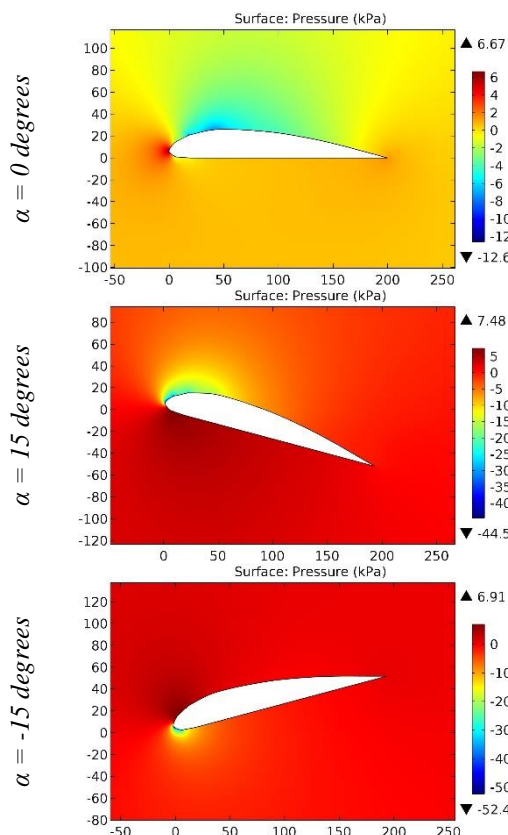


Figure 133. The pressure contours on the surfaces of the BRUXEL33 airfoil.

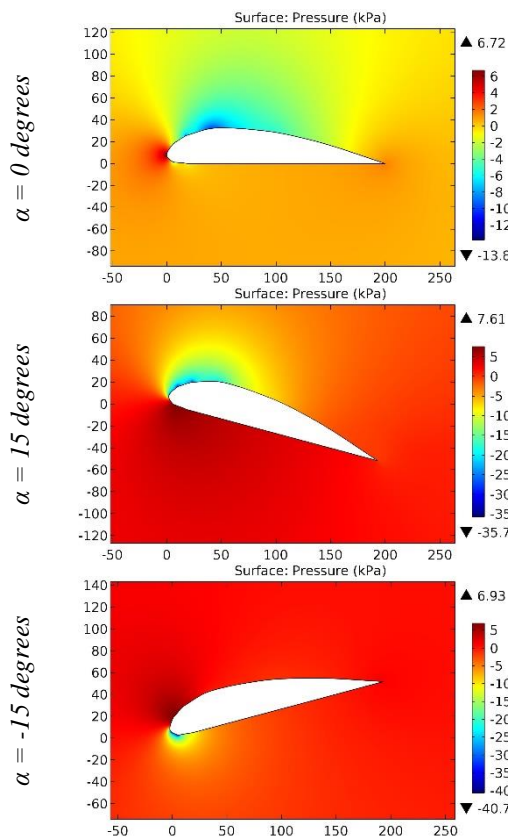


Figure 134. The pressure contours on the surfaces of the BRUXEL36 airfoil.

Impact Factor:

ISRA (India)	= 6.317	SIS (USA)	= 0.912	ICV (Poland)	= 6.630
ISI (Dubai, UAE)	= 1.582	РИНЦ (Russia)	= 3.939	PIF (India)	= 1.940
GIF (Australia)	= 0.564	ESJI (KZ)	= 9.035	IBI (India)	= 4.260
JIF	= 1.500	SJIF (Morocco)	= 7.184	OAJI (USA)	= 0.350

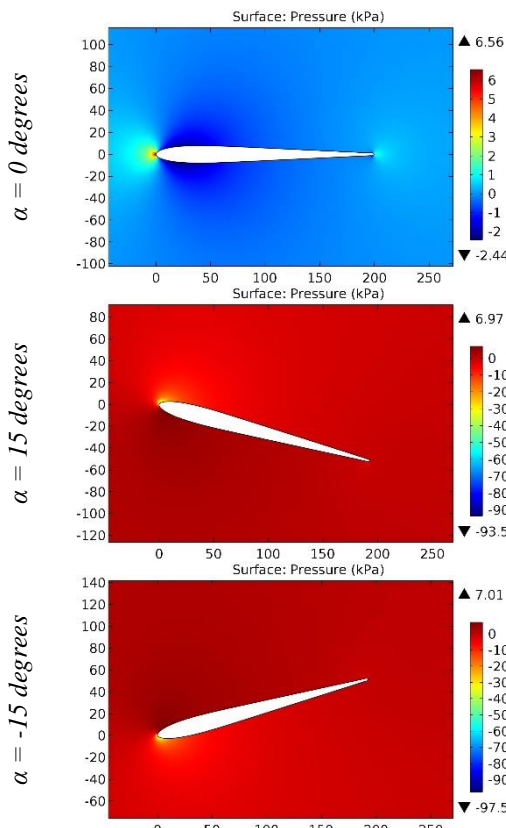


Figure 135. The pressure contours on the surfaces of the BTP8 airfoil.

The BE airfoils series is characterized mainly by an increase in pressure on the surfaces during the take-off maneuver of the airplane and a decrease in pressure during the landing maneuver of the airplane due to the thickness of the airfoil (thin and medium thickness). With an increase in the thickness of the airfoil (for example, the BOEING, B-29, BA, Blanchard, Bruxel airfoils series), the nature of pressure distribution on the surfaces changes inversely. The most advantageous geometry was determined for the Benedek 1053 B airfoil. The minimum magnitudes of the gradients of positive and negative pressures on the upper and lower surfaces and the leading edge of this airfoil were calculated at 15 and -15 degrees.

In the least favorable conditions, flight of the airplane having the wing with the large curvature in the cross section is carried out. For example, at the leading edge of the BE3307B airfoil, maximum drag occurs when air flows around at the angle of attack of 0 and 15 degrees. However, with the negative angle of attack, pressure on the surfaces of the airfoil is significantly reduced to the calculated magnitudes of pressure that occurs with the similar angle of attack of the biconvex symmetrical airfoils.

Maximum increase in negative pressure on the leading edge occurs at the angle of attack of -15 degrees for some airfoils (B-29 ROOT, BA 19, BE12305B, BE12355D, BE 9403B, BELL 540,

BELL-WORTMANN FX 69-H-098, Benedek 10355 B, Benedek 12355 B, Benedek 9403 B, BOEING 103, BOEING 106, BOEING 707 ,08 SPAN, BOEING 707 ,19 SPAN, BOEING 707 .19 SPAN AIRFOIL, BOEING 737 MIDSPAN AIRFOIL, BOEING 737 ROOT, BOEING 737 ROOT AIRFOIL, Boeing B-29 root airfoil, BOEING BACXXX, Boeing Commercial Airplane Company BACXXX, BOEING VERTOL V(1,95)3009-1,25, BOEING10, BOEING16, BOEING-VERTOL VR-1, BOEING-VERTOL VR-12, Borge' B3, BRUXEL33, BRUXEL36, BTP8). The BOEING-VERTOL VR-13 airfoil is subjected to the same positive and negative pressures under conditions of changing the angle of attack by 15 and -15 degrees. Maximum increase in negative pressure on the leading edge occurs at the angle of attack of 15 degrees for the remaining airfoils.

Conclusion

The airfoils of the wings of the first airplanes (BE3259B, BE3307B, BE309B, BE3357B, BE3359B) were imperfect. Analysis of the results of computer calculations revealed the occurrence of the large drag on the leading edge of these airfoils in conditions of horizontal flight and climb of the airplane. Good aerodynamic properties are shown by the S-shaped airfoils and the airfoils with the thickness of more than 12%.

Impact Factor:

ISRA (India) = 6.317	SIS (USA) = 0.912	ICV (Poland) = 6.630
ISI (Dubai, UAE) = 1.582	РИНЦ (Russia) = 3.939	PIF (India) = 1.940
GIF (Australia) = 0.564	ESJI (KZ) = 9.035	IBI (India) = 4.260
JIF = 1.500	SJIF (Morocco) = 7.184	OAJI (USA) = 0.350

References:

1. Anderson, J. D. (2010). Fundamentals of Aerodynamics. *McGraw-Hill, Fifth edition.*
2. Shevell, R. S. (1989). Fundamentals of Flight. *Prentice Hall, Second edition.*
3. Houghton, E. L., & Carpenter, P. W. (2003). Aerodynamics for Engineering Students. *Fifth edition, Elsevier.*
4. Lan, E. C. T., & Roskam, J. (2003). Airplane Aerodynamics and Performance. *DAR Corp.*
5. Sadraey, M. (2009). Aircraft Performance Analysis. *VDM Verlag Dr. Müller.*
6. Anderson, J. D. (1999). Aircraft Performance and Design. *McGraw-Hill.*
7. Roskam, J. (2007). Airplane Flight Dynamics and Automatic Flight Control, Part I. *DAR Corp.*
8. Etkin, B., & Reid, L. D. (1996). Dynamics of Flight, Stability and Control. *Third Edition, Wiley.*
9. Stevens, B. L., & Lewis, F. L. (2003). Aircraft Control and Simulation. *Second Edition, Wiley.*
10. Chemezov, D., et al. (2021). Pressure distribution on the surfaces of the NACA 0012 airfoil under conditions of changing the angle of attack. *ISJ Theoretical & Applied Science, 09* (101), 601-606.
11. Chemezov, D., et al. (2021). Stressed state of surfaces of the NACA 0012 airfoil at high angles of attack. *ISJ Theoretical & Applied Science, 10* (102), 601-604.
12. Chemezov, D., et al. (2021). Reference data of pressure distribution on the surfaces of airfoils having the names beginning with the letter A (the first part). *ISJ Theoretical & Applied Science, 10* (102), 943-958.